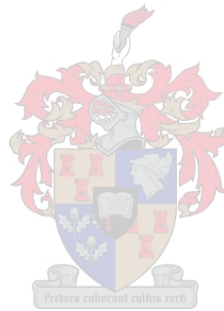


**EFFECTS OF MELATONIN ON THE HISTOMORPHOMETRY OF THE  
PANCREAS, LIVER AND KIDNEY OF RATS ON ANTIRETROVIRAL  
TREATMENT**

by

Danéille Truter

Thesis presented in fulfilment of the requirements for the degree of Master of Science the  
Faculty of Health Sciences at Stellenbosch University.



The financial assistance of the National Research Foundation (NRF) towards this research is hereby acknowledged. Opinions expressed, and conclusions arrived at, are of the author and are not necessarily to be attributed to the NRF.

Supervisor: Prof. S.H. Kotzé

Co-supervisor: Dr. N. Chellan

December 2017

## **DECLARATION**

By submitting this assignment electronically, I declare that the entirety of the work contained therein is my own, original work, that I am the sole author thereof (save to the extent explicitly otherwise stated), that reproduction and publication thereof by Stellenbosch University will not infringe any third-party rights and that I have not previously in its entirety or in part submitted it for obtaining any qualification.

Date: December 2017

## ABSTRACT

The administration of combination antiretroviral therapy (cART) in HIV positive patients has shown to cause side histologically observable effects in the pancreas, liver and kidneys. These conditions include acute pancreatitis, cellular injury, oxidative stress, hepatotoxicity and nephrotoxicity, which presents as inflammation and cellular injury. Melatonin has been successful in the prevention and reduction of inflammatory markers, oxidative stress and cellular damage, and has been observed as a treatment option in various conditions. The aim of this study was to evaluate the observable morphometric changes caused by cART as well as the potential therapeutic effects of melatonin on the pancreas, liver and kidney of the control (C/ART-), cART (C/ART+), melatonin (C/M+) and cART and melatonin (ART+/M+) groups in the absence of HIV in a rat model.

Tissue samples (N=40) of the ventral part of the pancreas, the median lobe of the liver and the right kidney male Wistar rats were collected. The blood samples (n=37) were collected from the abdominal aorta after euthanasia. Samples of the pancreas, liver and kidney were stained with haematoxylin and eosin (H&E) and evaluated for histopathology. The pancreas was labelled with anti-insulin and anti-glucagon to determine  $\alpha$ - and  $\beta$ -cell areas in the pancreatic islets. Blood samples were collected for liver enzyme tests to evaluate hepatotoxicity. The kidneys were stained with periodic acid Schiff (PAS) and the area, perimeter, diameter and radius of 30 renal corpuscles, with their associated glomeruli and 90 proximal convoluted tubules (PCTs) were measured per rat.

The pancreas, liver and kidney showed no significant histologically observable changes in histology. The mean islets per  $\text{mm}^2$  in the pancreas was significantly higher in the C/M- group than in the C/ART- and ART+/M+ groups. Melatonin stimulated the abundance of pancreatic islets and thus indirectly the availability of  $\alpha$ -cells. The haemoglobin value in the C/ART+ group was significantly higher than in the C/ART- group, which indicates that the mechanism in which cART increases serum haemoglobin is possibly still active in the absence of immune compromise. The C/M+ group showed a decrease in serum lipaemia compared to the C/ART- group, due to melatonin's its inhibitory effect on peroxidation of cellular lipids by free radicals.

In the kidneys, all parameters of the renal corpuscle were significantly lower in the C/ART+ and C/M+ groups compared to the C/ART- group. In the glomeruli, some parameters were significantly lower in the C/ART+ group compared to the C/ART-, C/M+ and ART+/M+ groups. The renal space was significantly decreased in the C/ART+, C/M+ and ART+/M+ groups. All parameters of the PCTs were significantly decreased in the C/ART+ group compared to the C/ART- group. All the components of the nephron were affected by cART, which may have caused tubular dysfunction, cellular damage and a decreased estimated glomerular filtration rate (eGFR). In conclusion, cART and melatonin each affected the histomorphometry of the pancreas, liver and kidney in a rat model without immune compromise. This should be considered when medication is prescribed to patients with HIV, specifically in patients with susceptibility to renal injury.

## OPSOMMING

Kombinasie antiretrovirale middels (kART) veroorsaak waarneembare veranderinge in die histologie van die pankreas, lewer en niere van menslike immuniteitsgebreksvirus (MIV)-positiewe pasiënte. Hierdie toestande sluit akute pankreatitis, oksidatiewe stres, hepatotoksisiteit en toksisiteit van die niere in, wat as inflammasie en sellulêre skade voorkom. Melatonien voorkom en verminder inflammatoriese merkers, oksidatiewe stres en sellulêre skade en word vir verskeie toestande as behandelingsopsie oorweeg. Hierdie studie het ten doel gehad om die waarneembare morfometriese veranderinge in die pankreas, lewer of niere wat veroorsaak word deur kART of melatonien te vergelyk tussen 'n kontrole (K/ART-) groep, kART (K/ART+) groep, melatonien (K/M+) groep en 'n kART en melatonien (ART+/M+) groep in die afwesigheid van MIV in 'n rotmodel.

Weefselmonsters (N=40) vanaf die ventrale deel van die pankreas, die mediane lob van die lewer en die regter nier en bloedmonsters (n=37) vanaf die abdominale aorta is geneem van manlike Wistar rotte. Die pankreas-, lewer- en nierweefsels is deur hematoksilien en eosien (H&E) gekleur vir die evaluering van histopatologie. Die pankreas is ook gemerk deur anti-glukagon en anti-insulien om die  $\alpha$ - and  $\beta$ -selle, onderskeidelik, in die pankreatiese eilande te identifiseer. Toksisiteit van die lewer is getoets deur die lewerensieme te evalueer. Die niere is gekleur deur periodieke suur en Schiff (PAS) om die area, omtrek, deursnee en radius van 30 renale liggampies en hul glomeruli, asook 90 proksimale kronkelbuisse per rot te meet.

Geen beduidende verskille is waargeneem in die histologie van die pankreas, lewer en nier in enige van die vier groepe nie. Die gemiddelde pankreatiese eilandjies per  $\text{mm}^2$  was beduidend hoër in die K/M+ groep in vergelyking met die K/ART- en ART+/M+ groepe. Melatonien het die hoeveelheid eilandjies vermeerder en dus indirek die beskikbaarheid van  $\alpha$ -selle in die pankreas. Hemoglobien in die K/ART+ groep was beduidend hoër as die K/ART- groep, wat moontlik aandui dat die meganisme waarmee kART hemoglobien in MIV-positiewe individue vermeerder, steeds aktief is in die afwesigheid van immuniteitsgebrek. Die lipiedinhoud in die bloed van die K/M+ groep was beduidend laer as in die K/ART+ groep, wat kan aandui dat melatonien lipiedafbraak, wat deur vrye radikale gestimuleer word, onderdruk.

Al die komponente van die renale liggampies was beduidebd laer in die K/ART- en K/M+ groepe in vergelyking met die K/ART- groep. In die glomeruli, is verskeie komponente

beduidend verlaag in die K/ART+ groep in vergelyking met die K/ART-, K/M+ en ART+/M+ groepe. Die renale spasie was ook beduidend kleiner in die K/ART+, K/M+ en ART+/M+ groepe in vergelyking met die K/ART- groep. Al die komponente van die proksimale kronkelbuis was beduidend laer in die K/ART+ groep in vergelyking met die C/ART- groep. Al die komponente van die nefron is deur kART beïnvloed, hetsy deur tubulêre disfunksie of sellulêre skade, wat kan lei tot 'n verminderde beraamde glomerulêre filtrasietyempo (bGFT). Ten slotte het cART en melatonien elk die histomorfometrie van die pankreas, lewer en nier in 'n rotmodel sonder immuniteitsgebrek verander. Dit moet in ag geneem word wanneer medikasie voorgeskryf word aan pasiënte met MIV, spesifiek in pasiënte wat sensitief is vir nierbesering.

## AKNOWLEDGEMENTS

I would firstly like to thank Prof S.H. Kotzé and Dr N. Chellan for their invaluable contribution throughout the writing of this thesis. I also appreciate the assistance received from Dr E. Geldenhuys, Mr R. P. Williams and the staff and colleagues of the Division of Anatomy and Histology, as well as the staff at the South African Medical Research Council.

Thank you to Prof M. Kidd for the statistical analysis of the data. I am also extremely grateful to Pieter Venter for his programming expertise, technical assistance with data handling, endless patience and moral support.

Thank you to my parents for their amazing, continuous, support; emotionally and financially. Without you, this would not have been possible.

Lastly, thank you to my Heavenly Father, who has given me opportunities where I thought it impossible. Zephaniah 3:7- “The Lord your God is with you, the Mighty Warrior who saves. He will take great delight in you; in his love, he will no longer rebuke you, but will rejoice over you with singing.”

## CONTENTS

Chapter 1 INTRODUCTION.....	1
1.1 Background.....	1
1.2 Justification.....	2
1.3 Research Question.....	3
1.4 Research Problem.....	3
1.5 Hypotheses.....	3
1.6 Aim.....	3
1.7 Objectives.....	4
1.8 Key Terminology.....	4
Chapter 2 LITERATURE REVIEW.....	5
2.1 Human Immunodeficiency Virus (HIV).....	5
2.2 Antiretroviral treatment (ART).....	6
2.2.1 Odimmune <sup>TM</sup> /Atripla®.....	6
2.2.2 Side Effects of cART on the Pancreas.....	8
2.2.3 Side Effects of cART on the Liver.....	8
2.2.4 Side Effects of cART on the Kidneys.....	10
2.3 Melatonin.....	11
2.3.1 Protective action of melatonin.....	13
2.3.2 Influence of melatonin on the pancreas.....	15
2.3.3 Influence of melatonin on the liver.....	16
2.3.4 Influence of melatonin on the kidneys.....	16
2.4 Histology of the Pancreas.....	17
2.5 Histology of the Liver.....	20
2.6 Histology of the Kidneys.....	21
2.7 Different Fixation and Staining Methods.....	24
2.7.1 Common fixatives.....	24
2.7.2 Haematoxylin and Eosin (H&E).....	25
2.7.3 Periodic acid and Schiff (PAS).....	25
2.7.4 Immunohistochemistry.....	25
Chapter 3 MATERIALS AND METHODS.....	26



3.1 Tissue sample collection .....	27
3.2 Tissue processing .....	28
3.2.1 Fixation .....	28
3.2.2 Tissue processing .....	28
3.2.3 Embedding .....	29
3.2.4 Sectioning .....	30
3.2.5 Heating .....	30
3.2.6 Staining .....	30
3.3 Analyses of pancreata, livers and kidneys .....	32
3.3.1 Pancreas .....	33
3.3.2 Liver analyses .....	35
3.3.3 Kidney analyses .....	36
3.3.4 Statistical analyses .....	40
Chapter 4 RESULTS.....	41
4.1 Body Mass .....	41
4.2 Pancreas .....	42
4.2.1 Histopathology of the pancreas.....	42
4.2.2 Other findings .....	43
4.2.3 Analysis of the pancreatic islets.....	45
4.3 Liver.....	50
4.3.1 Histopathology of the liver .....	50
4.3.2 Liver enzyme analysis.....	56
4.4 Kidney.....	59
4.4.1 Histopathology of the kidney.....	59
4.4.2 Analysis of renal corpuscles with accompanying proximal convoluted tubules ....	62
Chapter 5 DISCUSSION .....	72
Chapter 6 CONCLUSION .....	81
6.1 Concluding Remarks.....	81
6.2 Limitations of the Study and Prospective Research .....	82
REFERENCES .....	83

## FIGURES

Figure 2.1 Percentages of individuals infected with HIV in 2016 in each province of South Africa. ....	5
Figure 2.2 Chemical diagram of a tryptophan and melatonin molecule.....	12
Figure 2.3 Cellular effects of low, intermediate and high doses of reactive oxygen species. .	14
Figure 2.4 Diagram showing duodenal, splenic and gastric lobes of the rat pancreas .....	17
Figure 2.5 Rat pancreas showing acinar cells, pancreatic islet with capillaries and pancreatic duct (D) stained with H&E. ....	18
Figure 2.6 Arrangement of endocrine cells in islets of Langerhans of A) mice and B) humans. ....	19
Figure 2.7 Histology of the liver parenchyma with the portal triad stained with H&E.....	20
Figure 2.8 Diagram of a part of the liver lobule illustrating the different zones .....	21
Figure 2.9 Histology of the kidney stained with H&E. Arrows indicate renal corpuscles in cortex.....	22
Figure 2.10 A) Schematic diagram of the renal corpuscle, B) Histology of the renal corpuscle stained with H&E.....	23
Figure 3.1 Design of the experiment consists of four groups; C/ART-, C/ART+, C/M+ and ART+/M+. ....	26
Figure 3.2 Diagram showing how the kidney was cut before processing. ....	29
Figure 3.3 Summary of stains and tests for the pancreas, liver and kidney.....	32
Figure 3.4 Examples of measurements of the pancreas in a control rat, including the total islet area, $\alpha$ -cell area and the $\beta$ -cell area.....	34
Figure 3.5 Composite image of the kidney showing the superior, middle and inferior part. ..	36

Figure 3.6 Examples of measurements of the kidney of a control rat, including the renal corpuscle, glomerulus, PCTs and lumen of the PCTs .....	38
Figure 4.1 Body mass of the rats did not differ significantly between the four treatment groups. ....	41
Figure 4.2 Proteinaceous material outside of ducts as indicated by the arrows in a rat from the C/ART+ group .....	42
Figure 4.3 Proteinaceous material in ducts of all four groups of the pancreas as indicated by the arrows.....	43
Figure 4.4 Included lymph tissue of ART+/M+ group appears mildly active.....	44
Figure 4.5 The area of the $\alpha$ - and $\beta$ -cells did not differ between the four treatment groups. .	46
Figure 4.6 Examples of the islet area and $\alpha$ - and $\beta$ -cell area of the four treatment groups showed no significant differences. The C/M+ group had more islets per $\text{mm}^2$ than the other groups.. ....	48
Figure 4.7 The number of pancreatic islets per $\text{mm}^2$ differed significantly between the treatment groups.....	49
Figure 4.8 Percentages of the histopathology seen in the liver in the total of four treatment groups.....	51
Figure 4.9 The percentages of the granular appearance of hepatocytes did not differ significantly between the four treatment groups.....	52
Figure 4.10 Granular appearance and vacuolation of hepatocytes. ....	53
Figure 4.11 The percentages of the mild vacuolation of hepatocytes did not differ significantly between the four treatment groups.....	54
Figure 4.12 Lymphocyte infiltration in various areas around the central veins of a C/M+ liver. ....	55

Figure 4.13 Serum haemoglobin value differed significantly between the C/ART- group and C/ART+ group. ....	57
Figure 4.14 Serum lipaemia value differed significantly between the C/ART- group and C/M+ group. ....	58
Figure 4.15 Percentage of A) swelling and B) vacuolation seen in the kidneys in the total of four treatment groups. ....	59
Figure 4.16 Percentage of mild swelling seen in the kidneys did not differ significantly between the four treatment groups. ....	60
Figure 4.17 Percentage of mild and moderate vacuolation seen in the kidneys did not differ significantly between the four treatment groups. ....	61
Figure 4.18 Serial sections of slides stained with H&E and PAS. PAS distinguishes between the DCTs and PCTs. ....	62
Figure 4.19 The area, diameter, perimeter and radius of the renal corpuscle differed significantly between the four treatment groups. ....	64
Figure 4.20 The area, diameter, perimeter and radius of the glomerulus differed significantly between the four treatment groups. ....	66
Figure 4.21 The area, diameter, perimeter and radius of the renal corpuscle differed significantly between the four treatment groups. ....	68
Figure 4.22 Proximal tubule area differed significantly between the four treatment groups. ....	69
Figure 4.23 The renal space differed significantly between the four treatment groups. ....	71
P-values for Figure 7.1: The area of the $\alpha$ - and $\beta$ -cells did not differ between the four treatment groups. ....	109
P-values for Figure 7.2: The area of the $\alpha$ - and $\beta$ -cells did not differ between the four treatment groups. ....	109

P-values for Figure 7.3: Serum haemoglobin value differed significantly between the C/ART- group and C/ART+ group. ....	113
P-values for Figure 7.4: Serum lipaemia value differed significantly between the C/ART- group and C/M+ group. ....	113
P-values for Figure 7.5: The area, diameter, perimeter and radius of the renal corpuscle differed significantly between the four treatment groups. ....	114
P-values for Figure 7.6: The area, diameter, perimeter and radius of the renal corpuscle differed significantly between the four treatment groups. ....	114
P-values for Figure 7.7: The area, diameter, perimeter and radius of the renal corpuscle differed significantly between the four treatment groups. ....	115
P-values for Figure 7.8: The area, diameter, perimeter and radius of the renal corpuscle differed significantly between the four treatment groups. ....	115
P-values for Figure 7.9: The area, diameter, and radius of the glomerulus differed significantly between the four treatment groups. ....	116
P-values for Figure 7.10: The area, diameter and radius of the glomerulus differed significantly between the four treatment groups. ....	116
P-values for Figure 7.11: The area, diameter and radius of the glomerulus differed significantly between the four treatment groups. ....	117
P-values for Figure 7.12: The area, diameter and radius of the glomerulus differed significantly between the four treatment groups. ....	117
P-values for Figure 7.13: The area, diameter, perimeter and radius of the LPCT differed significantly between the four treatment groups. ....	118
P-values for Figure 7.14: The area, diameter, perimeter and radius of the LPCT differed significantly between the four treatment groups. ....	118

P-values for Figure 7.15: The area, diameter, perimeter and radius of the LPCT differed significantly between the four treatment groups.....	119
P-values for Figure 7.16: The area, diameter, perimeter and radius of the LPCT differed significantly between the four treatment groups.....	119
P-values for Figure 7.17: Proximal tubule area differed significantly between the four treatment groups.....	120
P-values for Figure 7.18: The renal space differed significantly between the four treatment groups.....	120

## TABLES

Table 2-1 Summary of common side effects caused by ART and their features .....	7
Table 2-2 Normal values and causes of bilirubin, haemoglobin and serum lipid interference in AST and ALT levels in rats .....	9
Table 2-3 Protective effects of melatonin .....	13
Table 4-1 Summary of the measurements on the pancreatic islets in the pancreas labelled with anti-insulin and anti-glucagon $\pm$ SD of the four treatment groups .....	45
Table 4-2 Percentage of $\alpha$ -cell area and $\beta$ -cell area in the pancreatic islets $\pm$ SD of the four treatment groups.....	47
Table 4-3 Summary of the values from liver function tests $\pm$ SD of the four treatment groups .....	56
Table 4-4 Summary of the measurements of the renal corpuscle of the four treatment groups $\pm$ SD .....	63
Table 4-5 Summary of the measurements of the glomeruli of the four treatment groups $\pm$ SD .....	65
Table 4-6 Summary of the measurements of the LPCT and the PCT of the four treatment groups $\pm$ SD .....	67
Table 4-7 Summary of the measurements of the renal space of the four treatment groups $\pm$ SD .....	70

## EQUATIONS

Equation 1 Calculation of melatonin needed for two days of stock .....	27
Equation 2 Hormone fraction.....	35



## APPENDICES

APPENDIX 1 Haematoxylin and eosin protocol.....	101
APPENDIX 2 Immunolabeling for anti-glucagon and anti-insulin protocol .....	102
APPENDIX 3 Periodic acid Schiff protocol.....	105
APPENDIX 4 Liver enzyme tests.....	106
APPENDIX 5 p-values obtained from pancreas measurements.....	109
APPENDIX 6 p-values obtained from body weight and liver enzyme tests .....	111
APPENDIX 7 p-values obtained from kidney measurements.....	113
APPENDIX 8 Pathology observed in the pancreas .....	120
APPENDIX 9 Pathology observed in the liver.....	122
APPENDIX 10 Pathology observed in the kidney .....	124

## ABBREVIATIONS

%	percentage
°C	degree Celsius
µl	microliter
µm	micrometre
µm <sup>2</sup>	cubic micrometre
•OH	hydroxyl radical
AA-NAT	arylalkylamino-N- acetyl-serotonin-transferase
AIDS	acquired immune deficiency syndrome
ALT	alanine aminotransferase
ANOVA	analysis of variance
ART	antiretroviral therapy/treatment
ART+/M+	antiretroviral treatment and melatonin
AST	aspartate aminotransferase
BD	Becton Dickinson
BD	biliary duct
C/ART-	control
C/ART+	antiretroviral treatment
C/M+	melatonin
cART	combination antiretroviral treatment
CAT	catalase
CD4	cluster of differentiation four
CLD	chronic liver disease
cm	centimetre
CV	central vein
D	pancreatic duct
DAB	3'3-diaminobenzidine
DCT	distal convoluted tubules
DI	diabetes insipidus
DPX	distyrene/plasticizer/xylene
EFV	Efavirenz
eGFR	estimated glomerular filtration rate

FDC	fixed dose combination
FTC	Emtricitabine
g	gram
g/dl	gram per decilitre
GALT	gut-associated lymphoid tissue
GSH	glutathione
GSH-Px	glutathione peroxidase
H&E	haematoxylin and eosin
H <sub>2</sub> O <sub>2</sub>	hydrogen peroxide
HAART	highly active antiretroviral treatment
HCC	hepatocellular carcinoma
HDL	high density lipoprotein
HFD	high fat diet
HIOMT	hydroxyindolo-O-methyl-transferase
HIV	human immunodeficiency virus
HSP	heat shock protein
IgG	immunoglobulin G
IHC	immunohistochemistry
INSTIs	integrase strand transfer inhibitors
JG	juxtaglomerular complex
kg	kilogram
L	lymphatic vessels
LDL	low density lipoprotein
LPCT	proximal convoluted tubule area with lumen
mg	milligram
mg/dl	milligram per decilitre
ml	millilitre
mm	millimetre
MT	melatonin receptor
NASH	non-alcoholic steatohepatitis
NBF	neutral buffered formalin
NGS	normal goat serum
NHLS	National Health Laboratory Service
NHS	normal horse serum

NNRTIs	non-nucleoside analogue reverse transcriptase inhibitors
NO·	nitric oxide
NRTIs	nucleoside analogue reverse transcriptase inhibitors
O <sub>2</sub>	superoxide anion
PAS	periodic acid Schiff
PBS	phosphate buffered saline
PCT	proximal convoluted tubules
PFA	paraformaldehyde
pH	potential of hydrogen
PIs	protease inhibitors
PP	pancreatic polypeptide
RBCs	red blood cells
RCT	randomised control study
RNS	reactive nitrogen species
ROS	reactive oxygen species
SA	South Africa
SD	standard deviation
SEM	standard error of the mean
TBS	tris buffered saline
TDF	tenofovir disoproxil fumarate
U/L	units per litre
VLDL	very low-density lipoprotein
α	alpha
β	beta
δ	delta

## CHAPTER 1 INTRODUCTION

### 1.1 BACKGROUND

Antiretroviral therapy (ART) has proven to be effective in reducing mortality and morbidity in individuals positive for human immunodeficiency virus (HIV) (Max and Sherer, 2000; Sulkowski, 2004; Mouly *et al.*, 2006; Brown *et al.*, 2010). Viral suppression and a decrease in opportunistic infections are associated with the use of ART (Kim and Rutstein, 2010; Kabbara and Ramadan, 2015). Combination ART (cART) regimens has improved medication adherence among HIV positive individuals due to the simplified single-tablet design (Bobek *et al.*, 2010; Deeks and Perry, 2010; Casado *et al.*, 2015). Odimmune<sup>TM</sup> (the generic version of Atripla®), which is used in South Africa (SA), is one of the latest examples of the latter and consists of Tenofovir Disoproxil Fumarate (TDF), Efavirenz (EFV) and Emtricitabine (FTC) (Kabbara and Ramadan, 2015).

Despite the continuous development of medication to improve adherence, patients are reluctant to adhere to treatment regimens because of the severe side effects that accompanies ART use (Max and Sherer, 2000). Metabolic alterations observed with the use of cART includes weight gain leading to obesity, increase insulin secretion and glucose uptake in cells causing insulin resistance and diabetes (Guzik *et al.*, 2006; Barbosa *et al.*, 2013). Additional histological side effects of cART in the pancreas includes pancreatic toxicity, which may include pancreatitis, steatosis, islet hypertrophy, and alpha- ( $\alpha$ ) and beta- ( $\beta$ ) cell dysfunction, therefore causing diabetes (Radogna *et al.*, 2010; Ferreira *et al.*, 2015). The administration of melatonin may prevent the necrosis of  $\beta$ -cells and reduce the excessive production of free radicals that is associated with diabetes and inflammatory conditions such as acute pancreatitis (Radogna *et al.*, 2010; Jaworek *et al.*, 2012).

Hepatotoxicity, hepatitis, hepatic fibrosis and steatosis, are common conditions caused by various regimens of cART. Hepatotoxicity is commonly measured by evaluating liver enzymes such as alanine aminotransferase (ALT) and aspartate aminotransferase (AST) (Sulkowski, 2004; Chang & Schiano, 2007). Melatonin protects against oxidative and inflammatory damage in the liver and has been shown to inhibit proliferation and induce apoptosis of fibroblasts (Hu *et al.*, 2015).

Similarly, cART causes various side effects in the kidneys of HIV positive individuals. Nephrotoxicity expressed as degeneration of tubules, loss of brush borders, luminal ectasia, thickening of the tubular basement membrane, simplification and dropout of tubular epithelial cells and acute renal failure may also occur. Conversely, melatonin prevents the accumulation of leukocytes in injured renal tissue. Melatonin reduces lipid peroxidation and protein oxidation in the kidneys. The anti-inflammatory properties of melatonin also protect the kidneys against fibrosis (Ersoz *et al.*, 2009; Jao & Wyatt, 2010; Hu *et al.*, 2015).

In summary, it is evident that cART causes multiple disruptions in the histology of the pancreas, liver and kidneys. As melatonin is proven to eradicate similar disruptions due to its anti-inflammatory and antioxidant qualities, it is proposed that melatonin might be a therapeutic option for HIV positive patients receiving cART.

## **1.2 JUSTIFICATION**

The prevalence of individuals living with HIV in South Africa is estimated at 6.19 million for 2015. This is equal to 11.2% of the total population, of which 18.99% and 16.59% is infected women and children, respectively (Statistics South Africa, 2014). This substantial number of patients puts great strain on South Africa's health services.

Melatonin is a hormone available in tablet form and is easily accessible as it is both cost effective and available without a medical prescription. If proven that melatonin can eradicate or improve the majority of side effects caused by ART, it can be administered to improve adherence of ART medication and improve the quality of life of HIV positive individuals. Ultimately, medication adherence will lead to higher life expectancy, fewer unemployment due to medical incompetency and a lower HIV prevalence in SA. By lowering unemployment due to medical reasons, unemployment compensation will also be lowered. It will ultimately lessen the strain on the health care system in South Africa and create a platform of socio-economic growth.

### **1.3 RESEARCH QUESTION**

The primary research question was whether cART induces observable morphometric changes on the histology of the pancreas, liver and kidneys in a male Wistar rat model and if so, does melatonin reduce or eradicate these effects?

### **1.4 RESEARCH PROBLEM**

Melatonin reduces the possible morphometric changes of cART as induced in the pancreas, liver and kidneys of the male Wistar rat, due to its scavenging and antioxidant properties.

### **1.5 HYPOTHESES**

Null hypothesis: Neither cART nor melatonin will cause histological observable changes in the pancreas, liver and kidney between four male Wistar rat groups: 1) a control group (C/ART-), 2) a group subjected to antiretroviral treatment (C/ART+), 3) rats that received melatonin treatment (C/M+) and lastly, 4) a group that received melatonin and has been subjected to ART (ART+/M+).

Alternative hypotheses:

- a) Histological observable changes will be observed in the pancreas, liver or kidney due to cART between the four rat groups.
- b) Histological observable changes will be observed in the pancreas, liver or kidney due to melatonin between the four rat groups.

### **1.6 AIM**

This randomised control study (RCS) aimed to evaluate the observable morphometric changes of melatonin and cART on the pancreas, liver and kidney of the C/ART-, C/ART+, C/M+ and ART+/M+ groups. In addition to morphometric measurements, the general structure of the pancreas, liver and kidney was evaluated for histopathology whilst evaluating melatonin as treatment option.

## 1.7 OBJECTIVES

- To compare the area and number of pancreatic islets per surface area between the fore mentioned treatment groups using morphometric measurements.
- To compare the area of  $\alpha$ -cells that labelled positive with anti-glucagon between the fore mentioned treatment groups using morphometric measurements.
- To compare the area of  $\beta$ -cells that labelled positive with anti-insulin between the fore mentioned treatment groups using morphometric measurements.
- To classify observable histopathology in the pancreas, liver and kidney as possibly induced by cART using semi-quantitative scaling methods.
- To classify observable cellular changes in the pancreas, liver and kidney as possibly induced by melatonin using semi-quantitative scaling methods.
- To determine hepatotoxicity by liver enzyme tests, specifically AST and ALT, on 1 ml blood serum samples.

## 1.8 KEY TERMINOLOGY

cART: The use of cART in the study will refer to Odimune<sup>TM</sup> as used in South Africa as treatment for HIV positive patients receiving combination therapy.

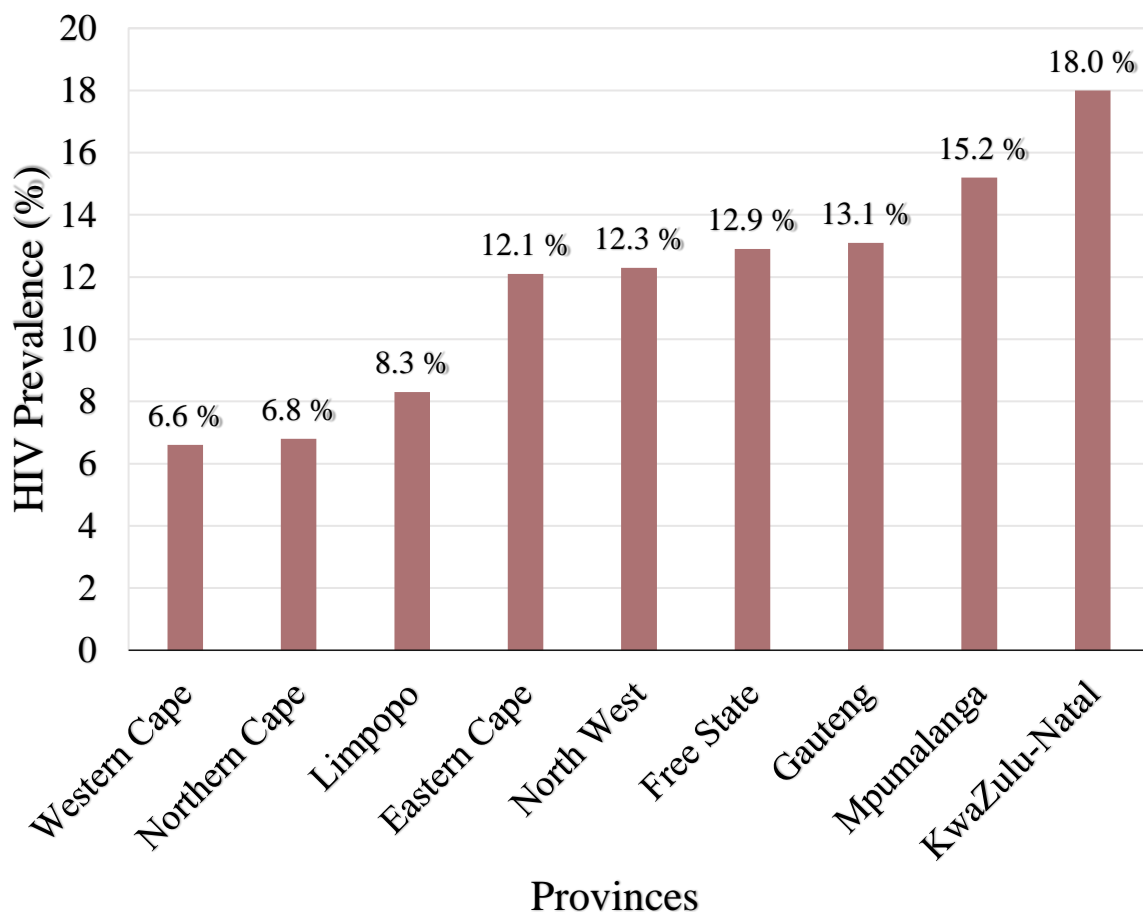
Pancreatic islets: The islets of Langerhans will be termed pancreatic islets.



## CHAPTER 2 LITERATURE REVIEW

### 2.1 HUMAN IMMUNODEFICIENCY VIRUS (HIV)

Globally, 36.7 million individuals are living with human immunodeficiency virus (HIV) as estimated in 2016, with an incidence of 1.8 million. An estimated 25.5 million (69%) of these individuals reside in sub-Saharan Africa (UNAIDS, 2016). In South Africa (SA), the Western Cape has the lowest percentage of HIV positive individuals (6.6%), whereas Kwazulu Natal has the highest (18.0%), as seen in Figure 2.1. Less than 10% of the population in the Western Cape, Northern Cape and Limpopo have a HIV, whereas the Eastern Cape, North West, Free State, Gauteng, Mpumalanga and Kwazulu Natal have a HIV prevalence above 12%.



Adapted from UNAIDS (2016)

**Figure 2.1 Percentages of individuals infected with HIV in 2016 in each province of South Africa.**

In 2016, 19.5 million HIV positive individuals had access to ART (UNAIDS, 2016). However, HIV treatment remains a prominent health priority worldwide, and especially in SA.

## **2.2 ANTIRETROVIRAL TREATMENT (ART)**

Undetectable levels of HIV can be achieved by the effective use of ART. Although the virus is still present in the body, replication can be suppressed by targeting HIV reverse transcriptase and HIV protease (Di Mascio *et al.*, 2009; Deeks & Perry, 2010). By repressing the virus and restoring immune function, opportunistic infections are less likely to manifest in the body (Fisher *et al.*, 2006).

Antiretroviral therapy can be classified into five groups: 1) nucleoside analogue reverse transcriptase inhibitors (NRTIs), 2) non-nucleoside analogue reverse transcriptase inhibitors (NNRTIs), 3) protease inhibitors (PIs), entry inhibitors and integrase strand transfer inhibitors (INSTIs). When three of these medications are combined it is classified as highly active antiretroviral treatment (HAART) or combination ART (cART) (Deeks and Perry, 2010; Tseng *et al.*, 2015). Dual NRTI combinations in cART regimens have shown to react positively in terms of drug related interactions, patient adherence, toxicity and costs (Manfredi *et al.*, 2001).

### **2.2.1 Odimune<sup>TM</sup>/Atripla<sup>®</sup>**

Odimune<sup>TM</sup> (the generic version of Atripla<sup>®</sup>), manufactured by Cipla, is the cART regimen commonly used in South Africa and consists of two NRTIs namely Tenofovir Disoproxil Fumarate (TDF) and Emtricitabine (FTC) and one NNRTI namely Efavirenz (EFV). (Amorosa *et al.*, 2005). Atripla<sup>®</sup> is a single tablet that contains 600mg EFV, 200mg FTC and 300 mg TDF. The combined dosage proves beneficial in regards to treatment adherence and convenience (Deeks and Perry, 2010). These treatments, however, are associated with severe side effects (Table 2.1), which may hinder adherence to the medication (Max and Sherer, 2000).

**Table 2-1 Summary of common side effects caused by ART and their features**

<b>Condition caused by ART</b>	<b>Features</b>	<b>Source</b>
Acute pancreatitis	Haemorrhage	(Muñoz-Casares <i>et al.</i> , 2006)
	Lymphocyte infiltrate	(Barbosa <i>et al.</i> , 2013)
	Necrosis	
	Oedema	
Cell injury	Apoptosis	(Muñoz-Casares <i>et al.</i> , 2006)
	Necrosis	(Barbosa <i>et al.</i> , 2013)
Oxidative stress	Catalase	(Muñoz-Casares <i>et al.</i> , 2006)
	Glutathione peroxidase	(Apostolova <i>et al.</i> , 2010)
	Lipoperoxides	(van Vonderen <i>et al.</i> , 2010)
	Reduced glutathione	(Dossou-Yovo <i>et al.</i> , 2014)
	Superoxide dismutase	
Hepatotoxicity	Elevated transaminases	(Sulkowski, 2004)
	Lactic acidosis with hepatic steatosis	(Núñez, 2010)
	Nodular regenerative hyperplasia	
	Portal hypertension	
	Steatohepatitis	
Tubular dysfunction in kidneys	Dilation of proximal tubules	(Labarga <i>et al.</i> , 2009)
	Glycosuria	(Lebrecht <i>et al.</i> , 2009)
	Hyperaminoaciduria	
Nephrotoxicity	Degenerative changes in tubular epithelial cells	(Van Rompay <i>et al.</i> , 2004)
	Fibrosis	
	Loss of brush border	
	Luminal ectasia	
	Tubular basement membrane thickening	
Glomerulonephritis	Endothelial proliferation	(Adjene <i>et al.</i> , 2011)
	Mesangial proliferation	(Young and O'Dowd, 2014)
	Thickening of basement membrane	

This study focussed on the effects of cART of the pancreas, liver and kidneys as listed in Table 2.1.

### **2.2.2 Side Effects of cART on the Pancreas**

Evidence of metabolic alteration is associated with the use of ART. This metabolic change may lead to increased insulin secretion and glucose uptake of somatic cells, ultimately causing diabetes (Barbosa *et al.*, 2013). Side effects of HAART observed in the pancreas include acute pancreatitis, pancreatic atrophy, parenchymal steatosis and apoptosis in patients who died of acquired immune deficiency syndrome (AIDS). Furthermore, an increase in the number, volume and dysplasia of nuclei is associated with the use of cART (Barbosa *et al.*, 2013; Oliveira *et al.*, 2014).

As concluded by Jaworek *et al.* (2005) the extent of pancreatic damage in cases of acute pancreatitis (Table 2.1) depends on factors involved in inflammation. Reactive oxygen species (ROS) are an active component of inflammatory conditions. In addition, inflammation can be associated with multiple aspects of the use of ART, including the prevalence of HIV (Brown *et al.*, 2010). Brown *et al.* (2010) postulated that inflammatory markers are still expressed in HIV positive individuals, despite the use of ART. Furthermore, an increase in inflammatory markers was noted after 48 weeks of ART in diabetic patients (Brown *et al.*, 2010).

### **2.2.3 Side Effects of cART on the Liver**

Hepatitis, hepatic fibrosis, lactic acidosis with hepatic steatosis, portal hypertension and nodular regenerative hyperplasia are common conditions caused by various regimens of cART (Sulkowski, 2004; Chang & Schiano, 2007; Núñez, 2010; Neuman *et al.*, 2013). Furthermore, Gallien *et al.* (2015) found that the specific combination of TDF/EFV/FTC caused hepatitis in 3% of HIV positive patients. Hepatitis C in HIV positive patients markedly increases the liver injury induced by cART (Bonacini, 2004).

Combination ART also causes progressive liver damage, which includes portal hypertension and nodular regenerative hyperplasia and non-alcoholic steatohepatitis (Núñez, 2010). The latter, which can lead to inflammation and fibrosis, occurs via altered lipid and carbohydrate

metabolism (Rector *et al.*, 2008; Ingiliz *et al.*, 2009). Efavirenz, specifically, contributes greatly to hypercholesterolemia and may cause hyperlipidaemia in patients with HIV (Fisher *et al.*, 2006; Oliveira *et al.*, 2014).

The prevalence of hepatotoxicity in HIV positive patients on cART is 3-18% (Nunez and Soriano, 2005). Clinically, hepatotoxicity is commonly measured by evaluating liver enzymes such as aspartate aminotransferase (AST) and alanine aminotransferase (ALT) (Sulkowski 2004; Chang & Schiano 2007). Efavirenz, specifically, has shown to elevate AST and ALT levels in HIV positive patients (Max and Sherer, 2000).

Bilirubin, haemoglobin and serum lipid tests may interfere with AST or ALT values, if elevated. If either of these components are elevated, it can indicate haemolysis of the red blood cells (RBCs) (Glick *et al.*, 1986; Thapa and Walia, 2007). Table 2.2 shows the normal values for bilirubin, haemoglobin and serum lipids, as conducted in conjunction with AST and ALT tests, and what abnormal values may indicate.

**Table 2-2 Normal values and causes of bilirubin, haemoglobin and serum lipid interference in AST and ALT levels in rats**

Test	Normal value	Clinical cause of elevation	Cause of interference
Bilirubin	0-1 mg/dl	Mild elevation: liver disease Moderate elevation: Viral hepatitis Necrosis	Haemolysis Ineffective erythropoiesis
Haemoglobin	13.7-16.8 g/dl	Necrosis	Haemolysis
Serum lipids	16-18 mg/dl	Accumulation of lipoproteins	Elevated AST & ALT
AST	74-143 U/L	Liver injury	Oral gavage
ALT	18-45 U/L	Hepatocyte necrosis, fatty change, cirrhosis	Oral gavage
AST/ALT ratio	1:1	Ratio > 2: Chronic liver disease Ratio > 1: Acute hepatitis or injury	

Adapted from Glick *et al.* (1986); Kannappan *et al.* (2006); Thapa and Walia (2007); Giknis and Clifford (2008)

Elevation of bilirubin levels in the blood may be indicative of liver disease or viral hepatitis, whereas an elevation in haemoglobin may be caused by necrosis of RBCs. Specifically, an increase in ALT indicates hepatocellular membrane injury for example hypoxia, fatty change, cirrhosis and necrosis (Thapa and Walia, 2007; Haschek *et al.*, 2009b), whereas an increase in AST may indicate liver injury. The latter may increase hours after injury, but ALT can be normal for several days after necrosis occurs (Haschek *et al.*, 2009b). Changes in AST are not liver specific, due to its high activity in muscle, whereas changes in ALT are considered liver specific in rodents, dogs and non-human primates (Haschek *et al.*, 2009b).

An increase in lipoproteins (lipaemia) may also interfere with liver enzyme tests. Lipoproteins include chylomicrons, high density lipoproteins (HDL) and low density lipoproteins (LDL). (Nikolac, 2014). Tenofovir has shown to decrease cholesterol and triglyceride levels, whereas didanosine, stavudine, and zidovudine increase triglycerides in HIV positive patients (Souza *et al.*, 2013). An increase in HDL and hypertriglyceridemia have been associated with lipodystrophy in HIV positive patients on cART. Lipodystrophy causes fat relocation in the body of patients on cART (Roubenoff *et al.*, 2002). Shikuma *et al.* (2004) found that HIV positive patients who have received cART for 16 weeks have higher body weights than patients who have not initiated cART.

#### **2.2.4 Side Effects of cART on the Kidneys**

Similar to the pancreas and liver, cART causes various side effects in the kidneys of HIV positive individuals. Various NRTIs may aggravate renal complications already experienced by HIV positive patients, as they are excreted by the kidneys (Max and Sherer, 2000). Nephrotoxicity in the form of urolithiasis, acute renal failure, Fanconi syndrome, nephrogenic diabetes insipidus (DI) and hypophosphatemia osteomalacia may be experienced in patients on cART (Karras *et al.*, 2003; Jao and Wyatt, 2010).

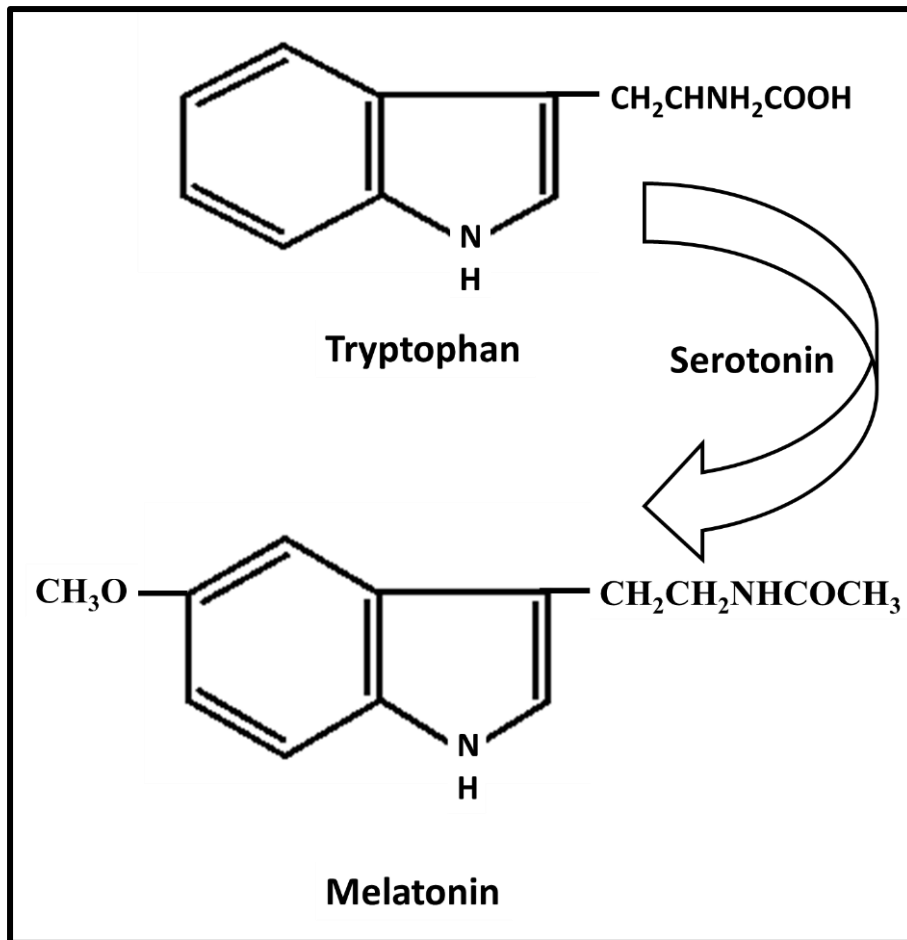
Adjene *et al.*, (2011) found that chronic administration of 600 mg/70 kg efavirenz decreased kidney weight and impaired the cellular structure of the renal cortex of Wistar rats after 30 days. In this study specifically, loss of cell architecture, glomerulonephritis and congested, dilated renal spaces were observed. Nephrotoxicity can be observed histologically as degeneration of tubules, loss of brush borders, luminal ectasia, thickening of the tubular

basement membrane, simplification and dropout of tubular epithelial cells. As tenofovir is directly eliminated through the proximal convoluted tubules (PCTs) and glomerular filtration, an increase in tenofovir may cause cell injury in the proximal tubules (Jao and Wyatt, 2010; Ryom *et al.*, 2012). However, according to Izzedine *et al.* (2005) normal glomeruli was observed in HIV positive patients on cART, whereas the PCTs were damaged due to tenofovir-induced nephrotoxicity in patients.

Furthermore, the estimated glomerular filtration rate (eGFR) in patients who are already exposed to Odimune<sup>TM</sup> was found to be significantly lower than in HIV positive patients who have not started treatment. However, after six months the eGFR of both groups were similar (Squillace *et al.*, 2017). It is suspected that TDF causes the decrease in eGFR due to its effects on the tubular function (Post *et al.*, 2010; Squillace *et al.*, 2017). According to Post *et al.* (2010) proteinuria was elevated in HIV positive patients on a combination of FTC and TDF, which is indicative of altered PCT function. It was postulated that this result was an effect associated with altered tubular function, but not injury (Post *et al.*, 2010).

### **2.3 MELATONIN**

Melatonin (*N*-acetyl-5-methoxytryptamine) is mainly produced by the pineal gland and is responsible for the regulation of circadian rhythms in the body. Pinealocytes synthesize melatonin from tryptophan in darkness and secrete it immediately. Melatonin synthesis decreases with exposure to light or  $\beta$ -adrenergic blockers (Radogna *et al.*, 2010; Acuña-Castroviejo *et al.*, 2014).



Adapted from Tan *et al.* (2007)

**Figure 2.2 Chemical diagram of a tryptophan and melatonin molecule.**

After tryptophan is converted to melatonin (Figure 2.2) through serotonin, it acts on the hypothalamus and hypophysis and induces sleep (Radogna *et al.*, 2010; Acuña-Castroviejo *et al.*, 2014). A review by Jaworek *et al.* (2012) suggests that the enzymes arylalkylamino-N-acetyl-serotonin-transferase (AA-NAT) and hydroxyindolo-O-methyl-transferase (HIOMT) regulates melatonin synthesis.

Various studies have proven that melatonin is synthesized by tissues other than the pineal gland (Radogna *et al.*, 2010; Acuña-Castroviejo *et al.*, 2014). These tissues include the retina, liver, kidneys, Harderian gland of the rat, cerebellum, skin, digestive tract and leukocytes. Extrapineal melatonin maintains cell homeostasis and is considered to be involved in regulatory mechanisms, whereas pineal melatonin is responsible for biological rhythms, anti-inflammatory and antioxidant properties (Radogna *et al.*, 2010; Acuña-Castroviejo *et al.*, 2014).



### 2.3.1 Protective action of melatonin

Melatonin has protective and restorative qualities in tissues damaged by renal ischemia-reperfusion injury, free radical damage in burn patients, major depression, sleep disorders, irritable bowel syndrome and migraine (Dolberg *et al.*, 1998; Maldonado *et al.*, 2007; Baykara *et al.*, 2009; Hickie and Rogers, 2011; Wilhelmsen *et al.*, 2011). The positive effect of melatonin on these conditions are due to the pleiotropic nature of this molecule, as it affects multiple systems in the body (Diger Hardeland *et al.*, 2010; Radogna *et al.*, 2010). Not only does melatonin regulate circadian rhythms, it is also an antioxidant, anti-inflammatory, analgesic, radical scavenger and anxiolytic (Nava *et al.*, 2003; Maldonado *et al.*, 2007; Baykara *et al.*, 2009; Yousaf *et al.*, 2010). Table 2.3 outlines some mechanisms in which melatonin influences antioxidant action, immune defence, apoptosis and heat shock protein (HSP).

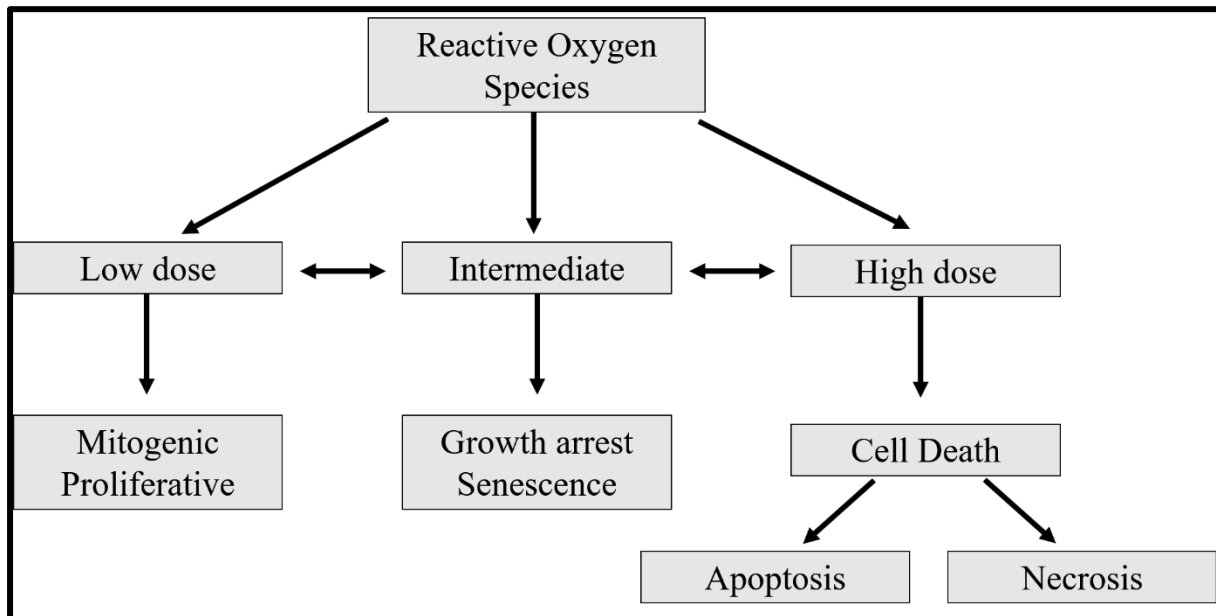
**Table 2-3 Protective effects of melatonin**

Protective effect	Mechanism
Antioxidant properties	Scavenge free radicals Activates antioxidant enzymes
Influences immune system	Strengthens immune defence Inhibits neutrophil infiltration Decrease myeloperoxidase (MPO) activity Activates/reduces proinflammatory cytokine production
Controls apoptosis	Reduce apoptosis and necrosis of healthy cells Induce apoptosis and necrosis of tumour cells
Stimulates heat shock protein (HSP)	Stimulates HSP, which protects cells in response to increased temperature, oxidative stress and inflammation

Adapted from Baydas *et al.* (2002); Jaworek *et al.* (2002); Muñoz-Casares *et al.* (2006); Joly *et al.* (2010); Leja-Szpak *et al.* (2010)

As mentioned above (Table 2.3), melatonin scavenges free radicals including reactive oxygen species (ROS) and reactive nitrogen species (RNS). At normal physiological levels, ROS

causes proliferative and mitogenic activity (Figure 2.3). These low doses of ROS are inactivated by antioxidants (such as melatonin) as it is generated. However, in higher doses, ROS accumulates, and cells cease division and growth. Ultimately, cell death occurs in the form of apoptosis or necrosis (Bergamini *et al.*, 2004).



Adapted from Bergamini *et al.* (2004)

**Figure 2.3 Cellular effects of low, intermediate and high doses of reactive oxygen species.**

Melatonin and its second and tertiary metabolites scavenges ROS and RNS (Table 2.3) such as hydroxyl radical ( $\bullet\text{OH}$ ), superoxide anion ( $\text{O}_2^-$ ), hydrogen peroxide ( $\text{H}_2\text{O}_2$ ) and nitric oxide ( $\text{NO}\cdot$ ) (Allegra *et al.*, 2003; Reiter *et al.*, 2007; Tan *et al.*, 2015). Melatonin possesses an electron-rich aromatic indole ring, which functions as an electron donor, thereby reducing and repairing radicals with unpaired electrons (Allegra *et al.*, 2003; Tan *et al.*, 2007).

The anti-inflammatory properties of melatonin vary depending on the stage of inflammation that is experienced. In the early phase of inflammation melatonin activates pro-inflammatory mediators, whereas melatonin has the opposite effect during chronic inflammation (Table 2.3). In addition, the antioxidant characteristics of melatonin acts in the chronic stage of inflammation. Melatonin also induces apoptosis with de-regulation of inflammation. This hormone thus controls inflammatory markers and mediators to allow it to act specific to the conditions in the body as needed for either healing or inflammatory disturbances (Radogna *et*

*al.*, 2010) Specifically, the present study focussed on the effects of melatonin on the pancreas, liver and kidney.

### **2.3.2 Influence of melatonin on the pancreas**

Melatonin is thought to affect carbohydrate metabolism, but the mechanism is still unclear. Various authors suggest that melatonin causes a reaction similar to insulin and is associated with hypoglycaemia and a higher glucose tolerance. Others postulate that melatonin increases blood glucose levels and plasma insulin levels (John *et al.*, 1990; Shima *et al.*, 1997; Peschke *et al.*, 2006; Cuesta *et al.*, 2013). Peschke *et al.* (2006) discovered that the  $\beta$ -cells in the pancreas have the melatonin receptor (MT) 1, which opposes insulin secretion. Insulin secretion is thus decreased at night, when melatonin levels are high and increased in the day, when melatonin levels are low (Peschke and Peschke, 1998).

Conversely, Cipolla-Neto *et al.* (2014) postulated that a decrease in melatonin levels has been proven to induce insulin resistance, as insulin secretion is dependent on the circadian rhythm of various mammals (Peschke, 2008). Furthermore, ingestion of food causes an increase in melatonin in the GIT, which may stimulate the secretion of pancreatic enzymes. This mechanism is important in the postprandial function of the exocrine pancreas (Jaworek *et al.*, 2007).

Although the effect of melatonin on the pancreas is mainly unknown, evidence suggests that the administration of melatonin may prevent necrosis of beta cells (Picinato *et al.*, 2002a) and reduce free radicals as produced by diabetes and inflammatory conditions (Baydas *et al.*, 2002; Radogna *et al.*, 2010). Furthermore, pancreatic regeneration following acute pancreatitis is stimulated by melatonin (Sidhu *et al.*, 2009). Melatonin significantly reduces oedema, leukocyte infiltration and cell oedema, which are characteristic of acute pancreatitis. It also decreases ROS by reducing the products of lipid peroxidation by restoring catalase (CAT) and glutathione peroxidase (GSH-Px) (Muñoz-Casares *et al.*, 2006).

### 2.3.3 Influence of melatonin on the liver

Melatonin is thought to increase glycogen levels in the liver and decrease plasma free fatty acids. These changes suggest that melatonin affects glycogen storage by altering carbohydrate and lipid utilization (Mazepa *et al.*, 1999). Conversely, Fabis *et al.* (2002) found that high doses of melatonin caused an increase in high density lipoproteins (HDL) cholesterol, which suggests that there is a fixed effect of melatonin on lipid parameters. An elevation in AST, ALT and LDL were measured in rats with hepatotoxic injury. Melatonin decreased these liver enzymes and LDL levels significantly (Sigala *et al.*, 2006)

Sigala *et al.* (2006) discussed the therapeutic value of melatonin in liver injury due to oxidative stress. Melatonin inhibits lipid peroxidation in acute liver necrosis by restoring glutathione (GSH). In addition, melatonin protects against oxidative and inflammatory damage in the liver (Cuesta *et al.*, 2010; Bekyarova and Tzaneva, 2015). Melatonin has been shown to inhibit proliferation and induce apoptosis of hepatocellular carcinoma (HCC) cells. This is of importance in the present study as cART induces cellular injury (Barbosa *et al.*, 2013). In addition, HCC is induced by cirrhosis and steatohepatitis, which are also suspected side effects of cART (Carbajo-Pescador *et al.*, 2009; Oliveira *et al.*, 2014).

### 2.3.4 Influence of melatonin on the kidneys

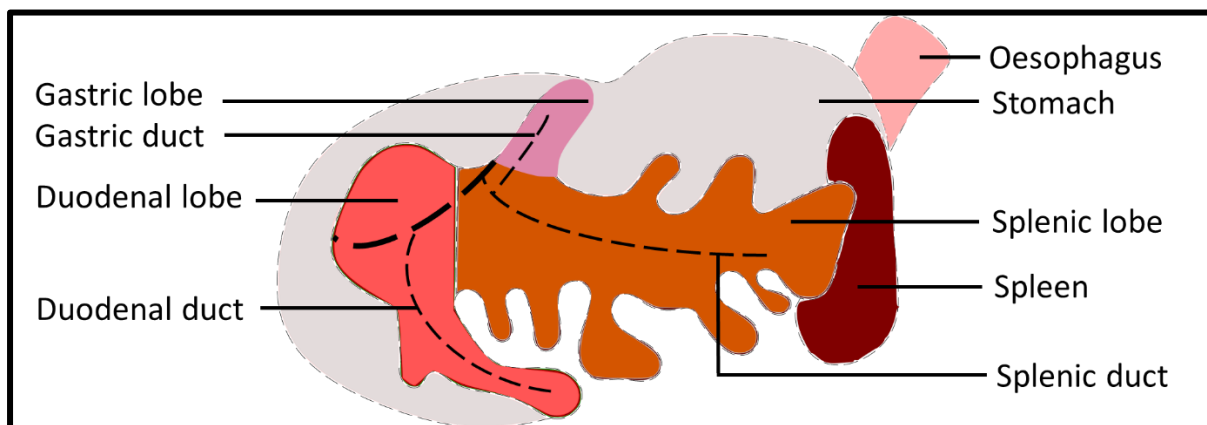
Melatonin plays a cytoprotective role in the kidneys; preventing accumulation of neutrophils in damaged renal tissue (Sener *et al.*, 2002). Melatonin reduces lipid peroxidation and protein oxidation in the kidneys which have been exposed to drug-induced nephrotoxicity (Hara *et al.*, 2001; Sener *et al.*, 2002). Similarly, melatonin protects the kidneys against fibrosis due to its anti-inflammatory properties (Ersoz *et al.*, 2009; Hu *et al.*, 2015).

Nava *et al.* (2003) found that melatonin reduced tubulo-interstitial infiltration of macrophages and lymphocytes which presented in hypertensive rats. These immune cells infiltrate the kidney when salt-dependant hypertension occurs, whereas melatonin potentially prevents damage to the renal tissue by the reduction of ROS and inflammatory markers (Nava *et al.*, 2003). Similarly, the antioxidant properties of melatonin were found to ameliorate tubular necrosis and nephrotoxicity in rats exposed to high levels of uranium (Bellés *et al.*, 2007).

For the purposes of this study, the morphometric characteristics of changes to the pancreas, liver and kidney following cART was determined, as this is not well described in the literature. Although various semi-quantitative evaluations have been conducted, limited morphometric measurements on the changes of the histology of these organs have been reported. Similarly, the literature on the biochemical and antioxidant actions of melatonin has been thoroughly discussed, but the morphometric changes of melatonin in tissue is lacking.

## 2.4 HISTOLOGY OF THE PANCREAS

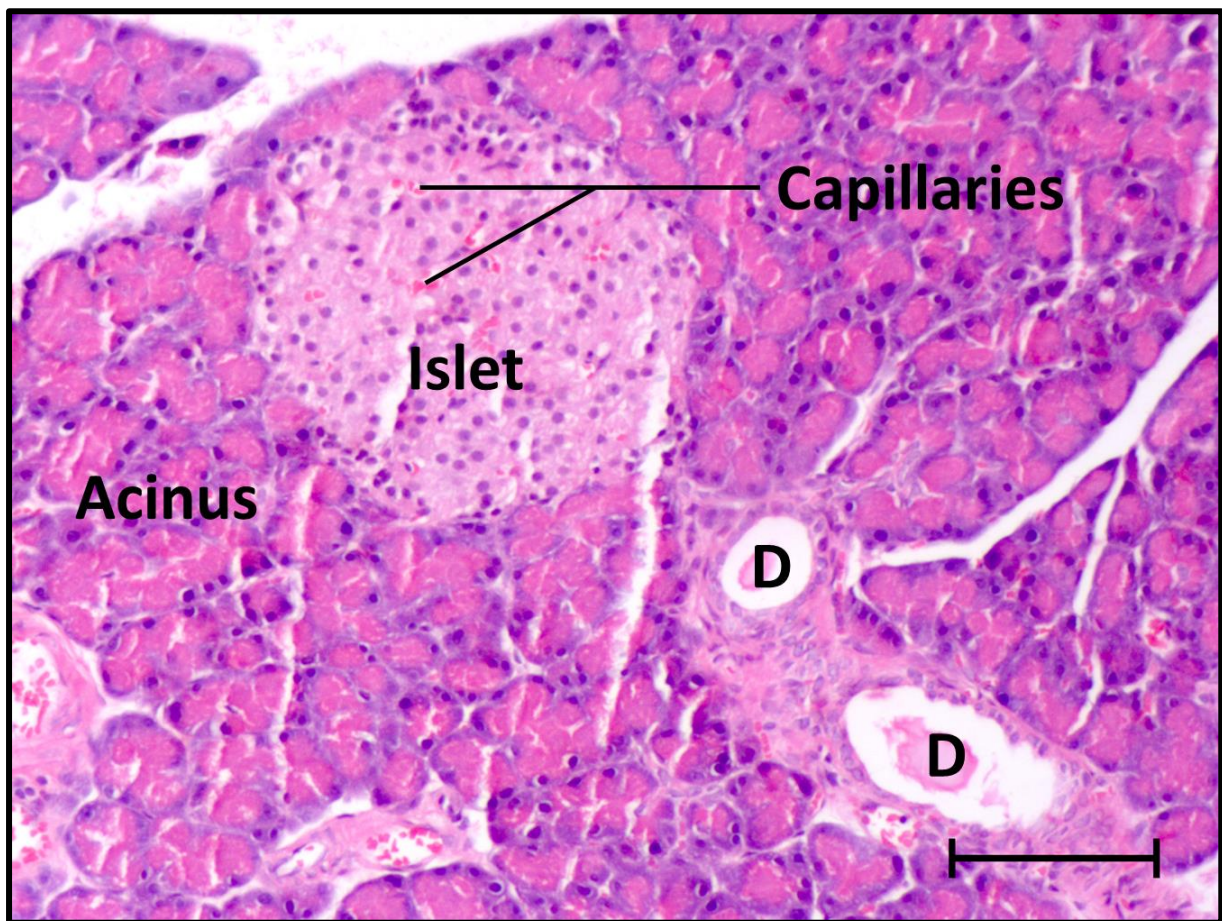
The pancreas is a retroperitoneal accessory digestive gland and is divided into an exocrine and an endocrine part. The exocrine portion, which is classified as a branched tubuloacinar gland, is responsible for the secretion of digestive enzymes into the duodenum and represents about 98% of the pancreas in humans (Motta *et al.* 1997; Johnson, 1991; Kierszenbaum, 2007; Ovalle & Nahirney, 2013). In rats, the pancreas can be divided into a duodenal lobe, splenic lobe and gastric lobe (Figure 2.4), where the duodenal duct (main distal duct), splenic duct (main pancreatic duct) and gastric duct drain, respectively (Baetens *et al.*, 1979; Dolensek *et al.*, 2015).



Adapted from Dolensek *et al.* (2015)

**Figure 2.4 Diagram showing duodenal, splenic and gastric lobes of the rat pancreas**

The exocrine pancreas consists of parenchymal cells namely acinar and ductal cells (Figure 2.5). The apical portion of pancreatic acinar cells contain zymogen granules, which contain digestive enzymes (Kierszenbaum, 2007; Haschek *et al.*, 2009d).

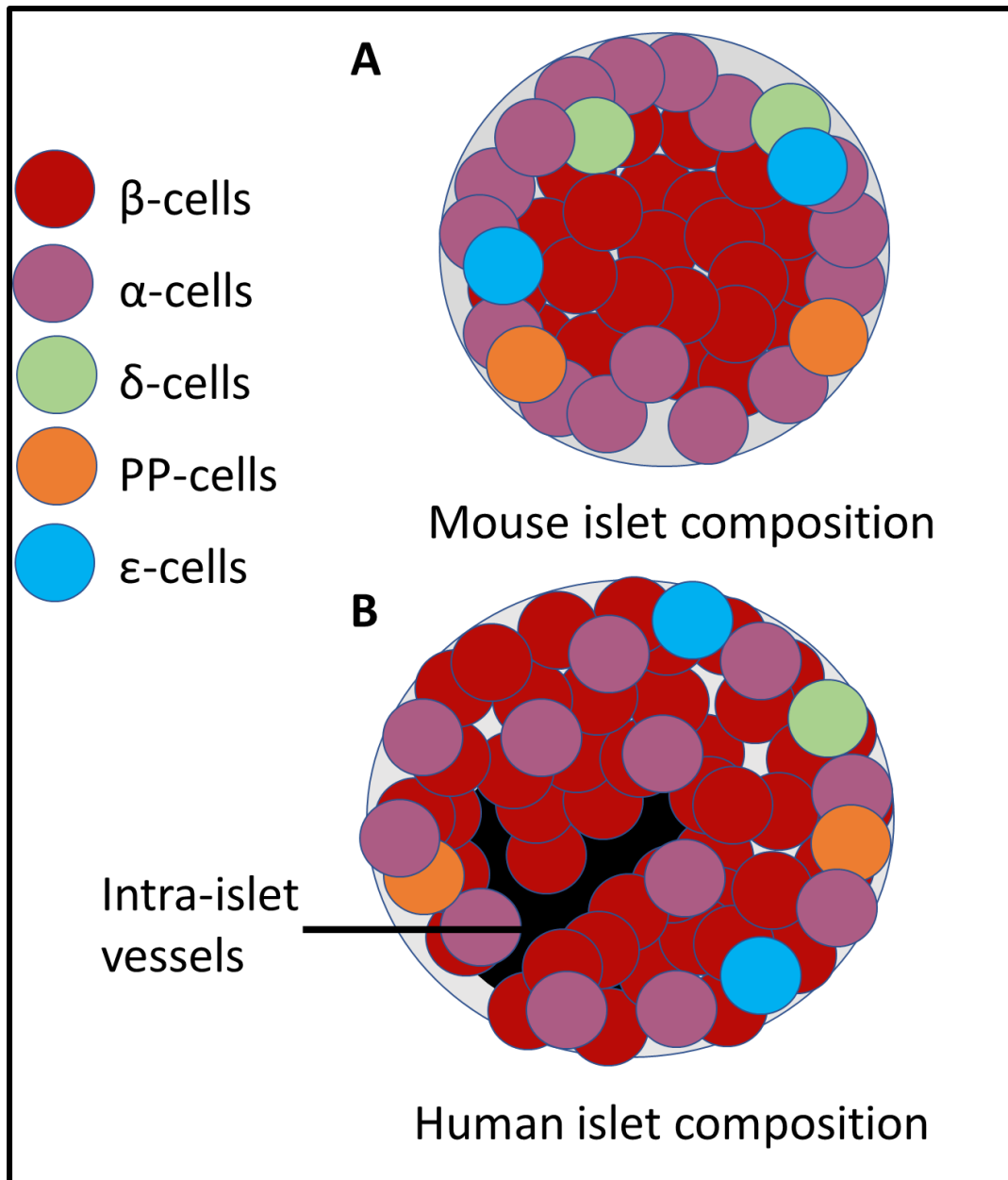


Micrograph by Dan lle Truter

**Figure 2.5 Rat pancreas showing acinar cells, pancreatic islet with capillaries and pancreatic duct (D) stained with H&E. Magnification = 200x; scale bar = 200  $\mu$ m**

The remaining 2% of the pancreas is an endocrine gland composed of the pancreatic islets (islets of Langerhans), which produced several hormones responsible for glucose metabolism (Motta *et al.* 1997; Kierszenbaum 2007; Ovalle & Nahirney 2013).

The pancreatic islets consist of four types of endocrine cells: alpha ( $\alpha$ ) -cells that produce glucagon, beta ( $\beta$ ) -cells that produce insulin, delta ( $\delta$ ) -cells which secrete gastrin and somatostatin and F-cells which synthesize pancreatic polypeptide (PP). In rodents, the  $\beta$ -cells are found in the core of the islet, whereas the  $\alpha$ -, delta and F cells are arranged around the mantle as shown in Figure 2.6A (Kierszenbaum, 2007; Migrenne, 2011). The pancreatic islets of rats in the ventral region are considered glucagon- and PP-poor in relation to the dorsal region (Baetens *et al.*, 1979).



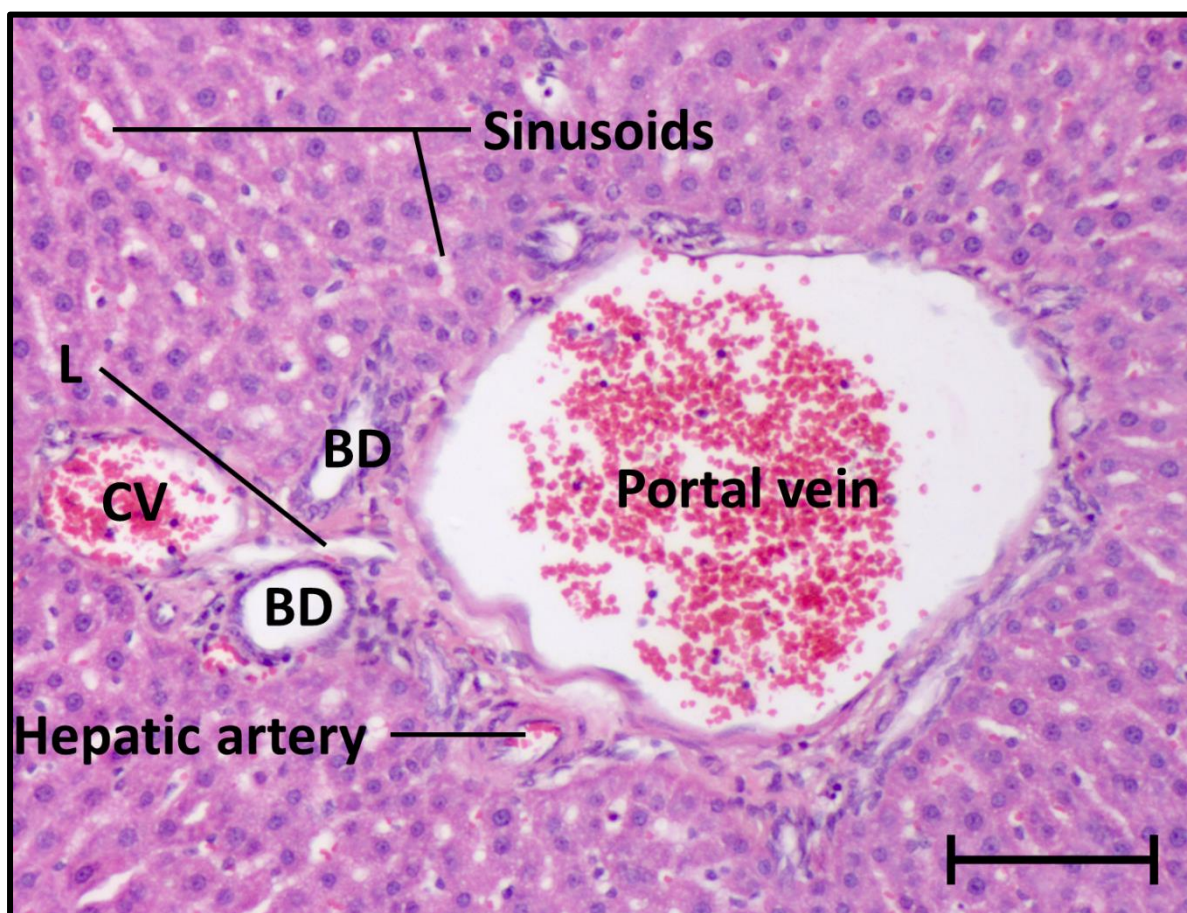
Adapted from Migrenne (2011)

**Figure 2.6 Arrangement of endocrine cells in islets of Langerhans of A) mice and B) humans.**

The distribution of the endocrine cells in human islets is shown in Figure 2.6B. The  $\beta$ -cells are mainly present in the core of the islet, with  $\alpha$ -cells arranged diffusely around the islet. The  $\delta$ - and PP-cells are arranged around the mantle of the pancreatic islet (Kierszenbaum, 2007; Migrenne, 2011).

## 2.5 HISTOLOGY OF THE LIVER

The liver is an accessory organ of the alimentary tract and is responsible for metabolism of glucose, proteins and fat, alteration of exogenous substances and formation of bile. The adult liver is comprised of 80% parenchyma, which consists of hepatocytes arranged as a maze of cellular plates. Stroma composes the other 20% of the organ (Ovalle and Nahirney, 2013).

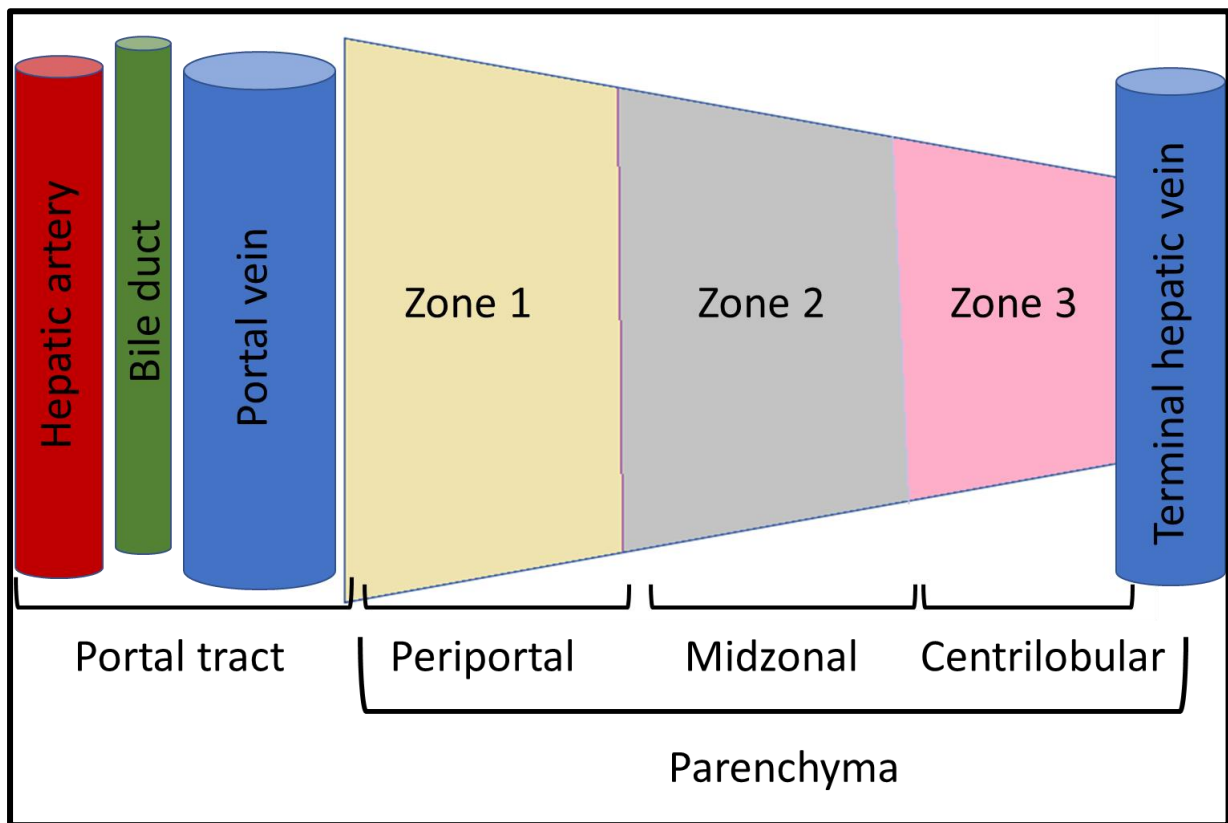


Micrograph by Dan lle Truter

**Figure 2.7 Histology of the liver parenchyma with the portal triad stained with H&E. CV= central vein, BD= biliary duct, L= lymphatic vessel. Magnification = 200x; scale bar = 200  $\mu$ m**

The liver has multiple accompanying structures that forms portal triads: each consists of a portal vein, hepatic artery and bile duct (Figure 2.7). Connective tissue divides the liver into classic hepatic lobules, which are classified as the structural units of the liver (Ovalle and Nahirney, 2013).





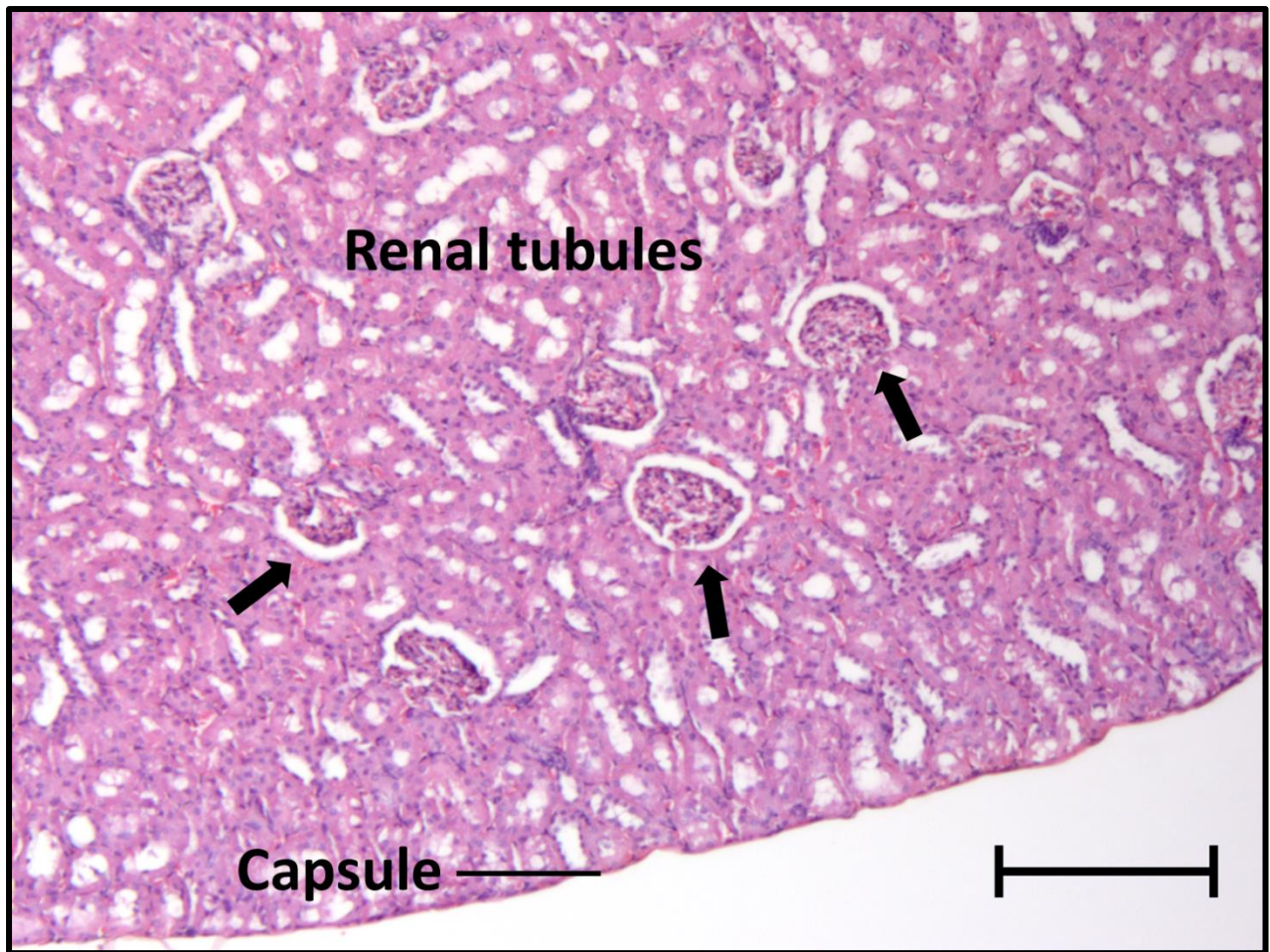
Adapted from Haschek *et al.* (2009e)

**Figure 2.8** Diagram of a part of the liver lobule illustrating the different zones

The parenchyma of the liver is divided into the periportal, midzonal and centrilobular areas as shown in Figure 2.8.

## 2.6 HISTOLOGY OF THE KIDNEYS

Kidneys are compound tubular glands, which are covered by a capsule of dense connective tissue. The outer capsule of the kidney consists of collagen fibres with fibroblasts. The renal parenchyma contains tightly packed renal tubules as shown in Figure 2.9.

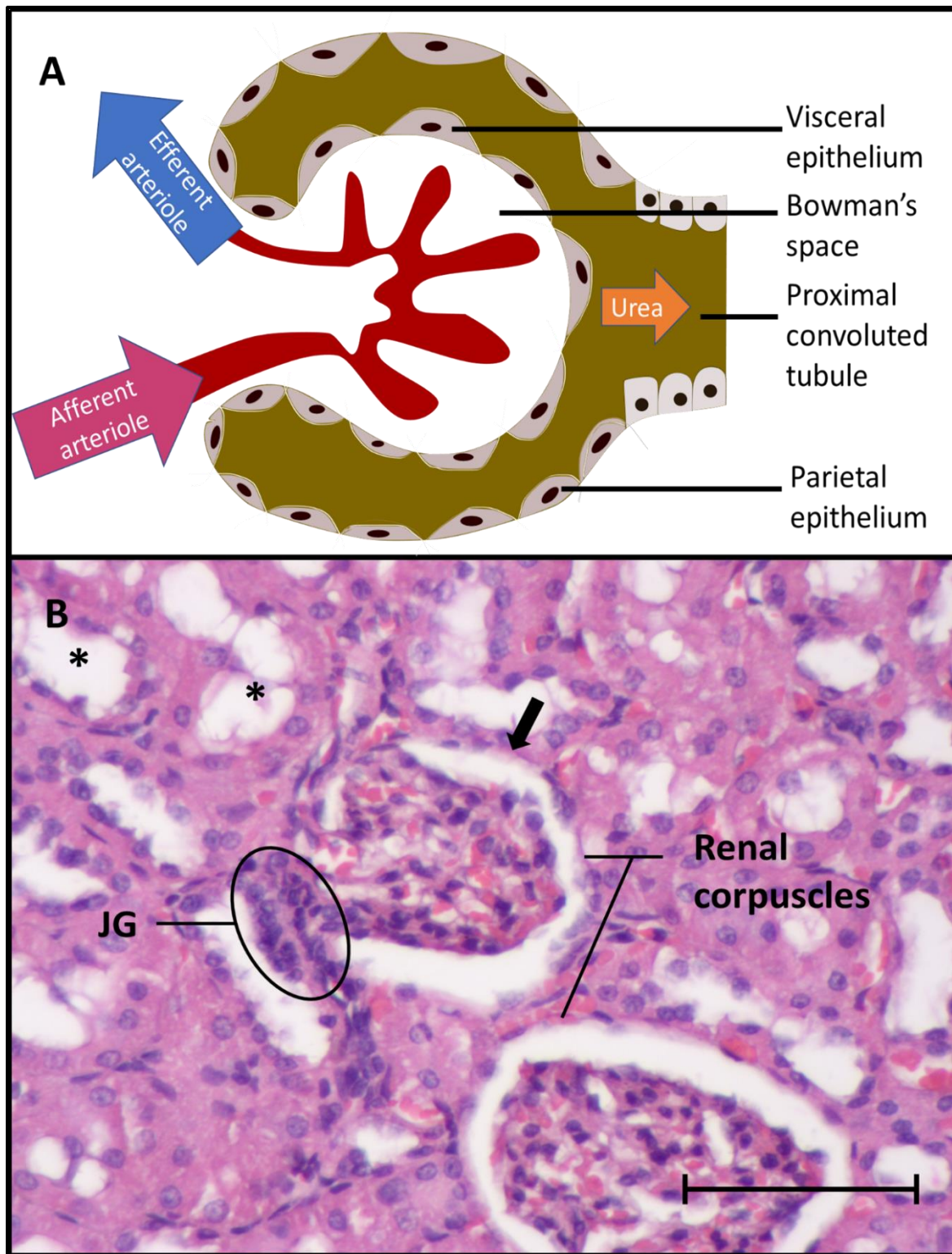


Micrograph by Dan lle Truter

**Figure 2.9 Histology of the kidney stained with H&E. Arrows indicate renal corpuscles in cortex. Magnification = 100x; scale bar = 500  $\mu$ m**

The functional unit of the kidney is called a nephron and consists of a renal corpuscle, proximal tubule, loop of Henle and distal tubule. The renal corpuscle contains a cluster of glomerular capillaries in the Bowman's capsule (Kierszenbaum, 2007).

Figure 2.10 displays a (A) schematic representation as well as a (B) histological representation of the components of the renal corpuscle.



(A) Adapted from Ovalle and Nahirney (2013); (B) micrograph by Dan lle Truter

**Figure 2.10** A) Schematic diagram of the renal corpuscle, B) Histology of the renal corpuscle stained with H&E. JG= juxtaglomerular complex, arrow indicates the Bowman's capsule; 400x magnification; scale bar = 100 μm

The glomerulus consists of a capillary network, podocytes (epithelial cells) and mesangium. Blood enters the glomerulus via the afferent arteriole and it is filtered to form and plasma filtrate (ultrafiltrate) which is composed of water, solute and other small molecules (Haschek *et al.*, 2009c; Sands and Veerlander, 2010). The Bowman's capsule consists of a visceral layer (podocytes) and parietal layer of simple squamous epithelium, of which the latter is continuous with the PCT (Haschek *et al.*, 2009c; Ovalle and Nahirney, 2013).

The PCT reabsorbs 50-60% of the ultrafiltrate from the glomerulus, which includes water, glucose, sodium and amino acids. The pars recta, thin descending, thin ascending and thick ascending limbs form the loop of Henle. The loop of Henle generates osmotic pressure via the counter-current multiplier system and the distal convoluted tubule (DCT) uses aldosterone to reabsorb sodium ions to ultimately dispose of acid in the body (Haschek *et al.*, 2009c; Sands and Veerlander, 2010; Ovalle and Nahirney, 2013).

## **2.7 DIFFERENT FIXATION AND STAINING METHODS**

### **2.7.1 Common fixatives**

Proper fixation to stabilize cell morphology and tissue architecture is integral in histomorphometric studies. Fixatives can be classified as either denaturing or cross-linking. Denaturing fixatives include alcohol-based fixatives and acts by creating hydrogen bonds, whereas cross-linking fixatives create covalent chemical bonds between proteins in the respective tissue (Howat and Wilson, 2014). Glutaraldehyde, neutral buffered formalin (NBF) and paraformaldehyde are classified as cross-linking fixatives. Alcohol-based fixatives has shown to create shrinkage of tissue and lysis or swelling of RBCs (Howat and Wilson, 2014).

Formaldehyde has been the golden standard for fixation since the 1900s. Paraformaldehyde (PFA) is a polymerized form of formaldehyde, which is methanol-free formaldehyde and is commonly used to fixate proteins, peptides and enzymes (Hassel and Hand, 1974). In the present study, 4% PFA was used as fixative for all tissues.

### **2.7.2 Haematoxylin and Eosin (H&E)**

Haematoxylin and Eosin (H&E) is commonly used for its ability to stain most tissue structures. In the present study, Mayer's Haematoxylin was used, which stains nuclei dark blue/black. Eosin stains the cytoplasm of various tissues pink. Erythrocytes, eosinophilic granules, other tissue elements stains varying shades of pink (Bancroft and Layton, 2013b). This stain was used for the evaluation of histopathology in the pancreas, liver and kidney. The staining protocol is outlined in addendum 1.

### **2.7.3 Periodic acid and Schiff (PAS)**

Periodic acid Schiff is used to highlight carbohydrate-rich molecules such as glycogen, glycoproteins, and proteoglycans typically found in connective tissue, glycocalyx and basal laminae. An important mechanism of PAS is the oxidizing action of periodic acid to bind with free •OH groups or amino/alkylamine groups to form dialdehydes. Schiff stains glycogen and glycoproteins magenta and nuclei blue (Bancroft and Layton, 2013a; Giri, 2015). This stain was used to distinguish between the PCTs and DCTs. Periodic acid Schiff stains the brush border of the PCTs and the discernible nuclei of the DCTs. The protocol for PAS is outlined in addendum 3. In this study, the stain was used to clearly distinguish between the proximal and distal convoluted tubules of the kidney.

### **2.7.4 Immunohistochemistry**

Immunohistochemistry (IHC) is a technique used to visualise an antigen using a labelled antibody of that specific antigen. This antigen can be a fluorescent dye, an enzyme, radioactive element or colloidal gold. The procedure for IHC includes fixation, antigen retrieval, blocking of endogenous enzymes and antibody labelling (Chen *et al.*, 2010). In the present study, double-staining was used to label  $\alpha$ - and  $\beta$ -cells with anti-glucagon and anti-insulin, respectively. The protocol is outlined in addendum 2 and will be discussed in the following chapter.

## CHAPTER 3 MATERIALS AND METHODS

The study consisted of four male Wistar rat groups as indicated in Figure 3.1: 1) a control group (C/ART-), 2) a group which received antiretroviral treatment C/ART+), 3) rats that received melatonin treatment (C/M+) and lastly, 4) a group that received melatonin and has been subjected to ART (ART+/M+) (Figure 3.1).

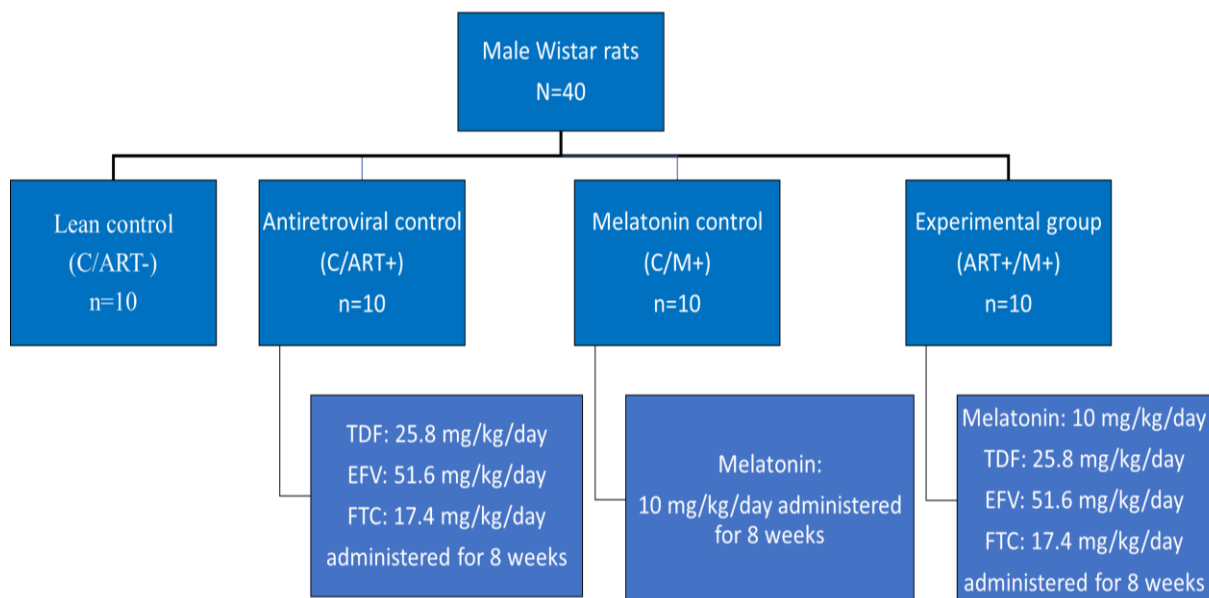


**Figure 3.1 Design of the experiment consists of four groups; C/ART-, C/ART+, C/M+ and ART+/M+. Each group consisted of 10 male Wistar rats. All treatments were administered for 8 weeks.**

The animal selection and care were conducted by the Division of Medical Physiology, Department of Biomedical Sciences, Faculty of Medicine and Health Sciences, Stellenbosch University. Male Wistar rats were housed (maximum of four animals per cage) in a controlled environment (temperature: 22°C; humidity: 40%; circadian rhythm: 12 hours of artificial light per day). All animals were on a normal rat chow diet for 16 weeks. The rats were 8 weeks old (180–200g) when the cART and melatonin treatment was initiated.

The ART was administered in adult male Wistar rats for eight weeks by means of oral gavage. The C/ART- and C/M+ groups were also gavage with 1 ml of water (without ART) to ensure

that no variation occurred due to the procedure. A generic version of Atripla® (Odimune™) was used in the fixed dose combination (FDC) of 300 mg TDF, 600 mg EFV and 200 mg FTC. The Odimune™ tablets were crushed and administered according to the rats' weekly weights. Each rat received TDF, EFV and FTC of 25.8 mg/kg/day, 51.6 mg/kg/day and 17.4 mg/kg/day, respectively.

The melatonin was administered for eight weeks in the drinking water of the rats. All rats received 10 mg/kg/day, depending on the rats' weight. The average weight of the rats in the cage were calculated weekly and multiplied by 0.01 mg/g/day. The melatonin was made up two days in advance and administered at the same time every day. The amount of water the rats drank were calculated after each day. The following equation was used to determine the grams of melatonin needed:

*Melatonin needed (mg) for 500 ml*

$$= \frac{[(\text{average weight of rats in cage} \div \text{amount of rats in cage}) \times 0.01]}{\text{average amount of water drank per rat per day} \div 500 \text{ ml}}$$

### **Equation 1 Calculation of melatonin needed for two days of stock**

The melatonin was firstly dissolved in 0.2% ethanol (500 µl) before 500 ml distilled water was added.

### **3.1 TISSUE SAMPLE COLLECTION**

Tissue samples (N=40; n=10 per group) of the pancreas, liver, kidney and blood samples were obtained after the rats were anesthetized, before 10:00 in the morning, using an intraperitoneal injection of 160 mg/kg sodium pentobarbitone into the lower right abdomen and euthanized via exsanguination. All rats were weighed with a scale before euthanasia.

Pancreata were isolated by detaching the connective tissue from the stomach to the small intestine. Thereafter, the connective tissue was loosened at the caudal end of the large intestine as well as the spleen, thus minimalizing the amount of fat retrieved. The duodenal lobe of the pancreas was used for analysis. The right median lobe of the liver and the right kidney were harvested. All three organs were immediately put in 4% paraformaldehyde (PFA) after

retrieval. Blood (approximately 1 ml) was collected after the removal of the heart and placed in a Becton Dickinson (BD) vacutainer serum tube.

Ethical approval to use tissue for this study was obtained from the Research Ethics Committee: Animal Care and Use of Stellenbosch University (SU-ACUM15-00003-Tissue).

## **3.2 TISSUE PROCESSING**

Tissue samples of the pancreas, liver and kidney were processed in the Histology Laboratory located in the Division of Anatomy and Histology, Department of Biomedical Sciences, Faculty of Medicine and Health Sciences, Stellenbosch University as described in the following subsections.

### **3.2.1 Fixation**

Fixation consists of several chemical events to preserve the tissues by preventing autolysis and bacterial attack (Bancroft & Stevens 1990). The tissues obtained for this study was immediately fixed in 4% PFA for 24-48 hours after retrieval, after which processing was initiated in the Histology laboratory.

### **3.2.2 Tissue processing**

The pancreas, liver and kidney were trimmed to an appropriate size. The excess fat was removed from the pancreas before inserting it into an embedding cassette (approximately 3 cm x 1 cm). The kidney was cut in cross-section at the pelvis as indicated by Figure 3.2 with a red line. Approximately 3-4 mm of the superior and inferior parts of the kidney was cut as indicated by the blue lines in Figure 3.2. The kidney (approximately 1 cm x 1 cm) was embedded with the pelvis to the bottom of the cassette and the superior and inferior parts towards the top of the cassette.



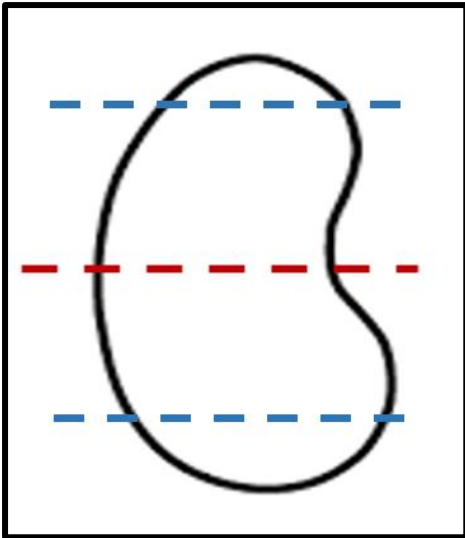


**Figure 3.2** Diagram showing how the kidney was cut before processing. The red line indicates where the kidney was cut at the pelvis. Blue lines indicate how the superior and inferior parts of the kidney was cut.

Tissue samples were then processed using a Leica XL automated tissue stainer (Manufacturer & Model: Leica St 5010; Serial Number 1732/07.2007). The steps of processing include dehydration, clearing and infiltration, where the tissue is put in 70%, 90%, 99%, 99%, 99% and 99% alcohol for 15 minutes, 15 minutes, 15 minutes, 15 minutes, 30 minutes and 45 minutes, respectively. Clearing was done by placing the tissues in xylene for 20 minutes, 20 minutes and 45 minutes. Wax infiltration was done for 30 minutes, 30 minutes and 45 minutes (Rolls, 2017).

### 3.2.3 Embedding

Paraffin wax, moulds and wax-infiltrated tissues was pre-heated to 60°C within the Leica embedder (Leica EG1160, Cat. No. 038630528). The embedding cassette was filled halfway with paraffin wax, after which the tissue was placed into the wax. The cassette was closed and set by adding the lid and filling the cassette completely with the paraffin wax. Thereafter, the cassette was immediately placed onto an iced surface to set the wax (Bancroft & Stevens 1990).

### 3.2.4 Sectioning

Wax tissue blocks were removed from the mould, after which it was trimmed by a Leica microtome (Leica RM2125RT, SMM Instruments, Cat. No. 045737987) to provide a smooth surface for cutting. The embedded pancreas tissue was cut into 3  $\mu\text{m}$  sections and the liver and kidney were cut into 5  $\mu\text{m}$  sections. Two serial sections were made for the pancreata and kidneys, and one section for the liver.

### 3.2.5 Heating

The specific sections were placed into the water bath (Electrothermal, Cat. No. MH 8501), where they were picked up onto a microscope slide at a 45° angle (Bancroft & Stevens 1990). One of the three slides of the pancreas were positively charged to enable IHC labelling. The tissue was then inserted into a heating oven to enable the slide with the respective tissue to dry.

### 3.2.6 Staining

The pancreas, liver and kidney sections were stained with H&E (addendum 1) to enable histopathology analysis. Haematoxylin and eosin stains the nuclei blue, the cytoplasm pink and the red blood cells, eosinophilic granules, other tissue elements varying shades of pink (Bancroft and Stevens, 1990).

Additionally, the pancreata were labelled using monoclonal anti-insulin and polyclonal anti-glucagon. The anti-insulin and anti-glucagon identifies the  $\alpha$ - and  $\beta$ -cells in the pancreatic islets, respectively. An envision G/2 System/AP, Rabbit/Mouse kit was used for the staining as described in addendum 2.

In summary, 3% hydrogen peroxide was used to block tissue against endogenous peroxidase activity. The tissue was then rinsed with both 0.05 M tris buffered saline (TBS) (pH = 7.2) and 0.1 M phosphate buffered saline (PBS) (pH = 7.2) to maintain a normal pH. Normal goat serum (NGS) of a 1:20 dilution was then used for 20 minutes to block non-specific binding of subsequent agents. The anti-glucagon antibody (100 $\mu\text{l}$ ) at a 1:100 dilution was then placed on the slides in a moisture chamber for 30 minutes. Biotinylated anti-rabbit immunoglobulin G

(IgG) antibody at a 1:200 dilution was placed on the slides for 30 minutes, followed by Vectastain® (ABC kit, North America) for 60 minutes to detect an unlabelled primary antibody. Then, a chromogen solution (K3468, Dako, North America) with liquid 3'3'-diaminobenzidine (DAB) was placed on the slides for 5 minutes to enhance the staining of the tissue. Normal horse serum (NHS) of a 1:20 dilution was added to the slides for 20 minutes in the moisture chamber to block non-specific binding of subsequent agents. Thereafter, the anti-insulin (100µl) of a 1:10 000 dilution was placed on the sections and incubated overnight at 4°C. The next day, the slides were warmed to room temperature and the Envision™ kit was placed on the slides to enable staining of more than one marker. Mayer's haematoxylin was then used to counterstain the tissue for 2 minutes. After the slides dried, a coverslip was added with distyrene/plasticizer/xylene (DPX) mounting medium.

In addition to H&E, the kidneys were also stained with PAS (addendum 3). The slides were oxidised with periodic acid for 5 minutes and rinsed with distilled water. Schiff's reagent was then placed in the slides for 15 minutes, which was rinsed with lukewarm water. The slides were counterstained with Mayer's haematoxylin for 1 minute and washed in tap water. The stained section was covered with a cover slide proportional to its size by using DPX mounting medium. In this study, the stain was used to clearly distinguish between the proximal and distal convoluted tubules of the kidney (Bancroft and Layton, 2013a; Giri, 2015).

### 3.3 ANALYSES OF PANCREATA, LIVERS AND KIDNEYS

The pancreata, kidneys and livers stained with H&E were screened for any histopathology present by the researcher, two histopathologists and a histologist. In addition, two interobservers also confirmed the findings.

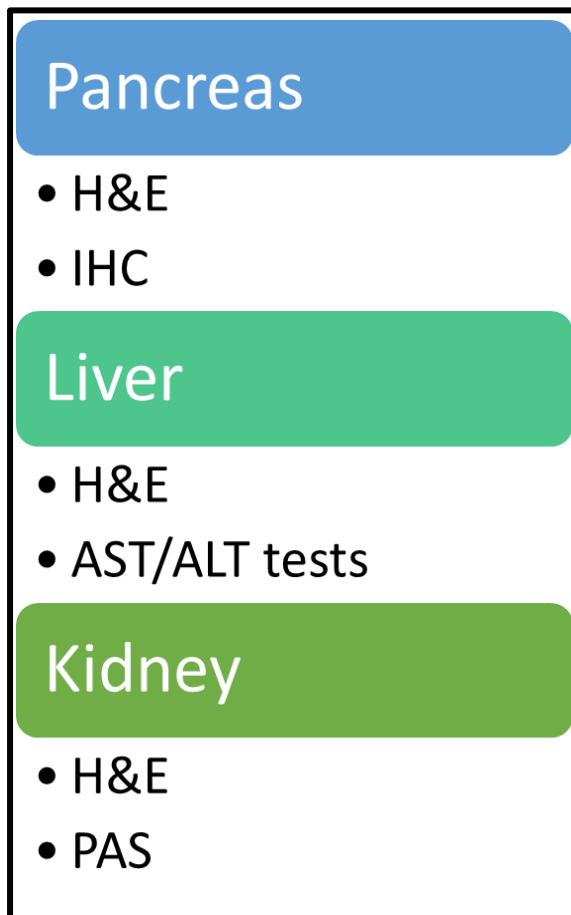


**Figure 3.3 Summary of stains and tests for the pancreas, liver and kidney**

Furthermore, the pancreata, kidneys and livers were analysed by IHC, PAS and liver function tests, respectively, which will be discussed in the following subsections. Figure 3.3 shows a summary of the methods for each of the three tissues.

### 3.3.1 Pancreas

The pancreata (N=40) were stained with H&E for histopathology analysis. Inflammatory cells, necrosis, loss of cell architecture, swelling of pancreatic ducts and fibrosis were considered. The observations were classified as absent (0), mild (1) or moderate (2).

The slides labelled with anti-insulin and anti-glucagon were used to quantify the insulin and glucagon secreting cells in the pancreatic islets (Figure 3.4A) (Michels *et al.*, 1986; Elayat *et al.*, 1995). To quantify the hormone secreting cells, the whole section of the pancreas was scanned with a Nikon Eclipse ProScan microscope at a 100x magnification (10 x objective lens). The images were taken with a 15% overlap and was stitched together to form a composite image of the tissue. The section area and islets were analysed using the Leica QWin Pro (version 3.5.0) software. Firstly, the tissue area on each individual photo was measured and added together to provide the complete tissue area for each specific animal. Normalisation of the data was ensured with a log transformation because the amount of pancreatic tissue retrieved differed per animal. The complete section area was converted from  $\mu\text{m}^2$  to  $\text{mm}^2$  and the number of islets per  $\text{mm}^2$  was then calculated. The area was converted to  $\text{mm}^2$  to enable the comparison of natural numbers rather than a very small number of  $10^{-6}$ .

After the section area was determined, the islets per area were analysed with the PancreasIsletMeasurements (v1.1) 13/02/2013.Q5R routine. Each islet was selected, and the area of the islet was measured as shown in Figure 3.4B, where the green shows the area of the pancreatic islet.

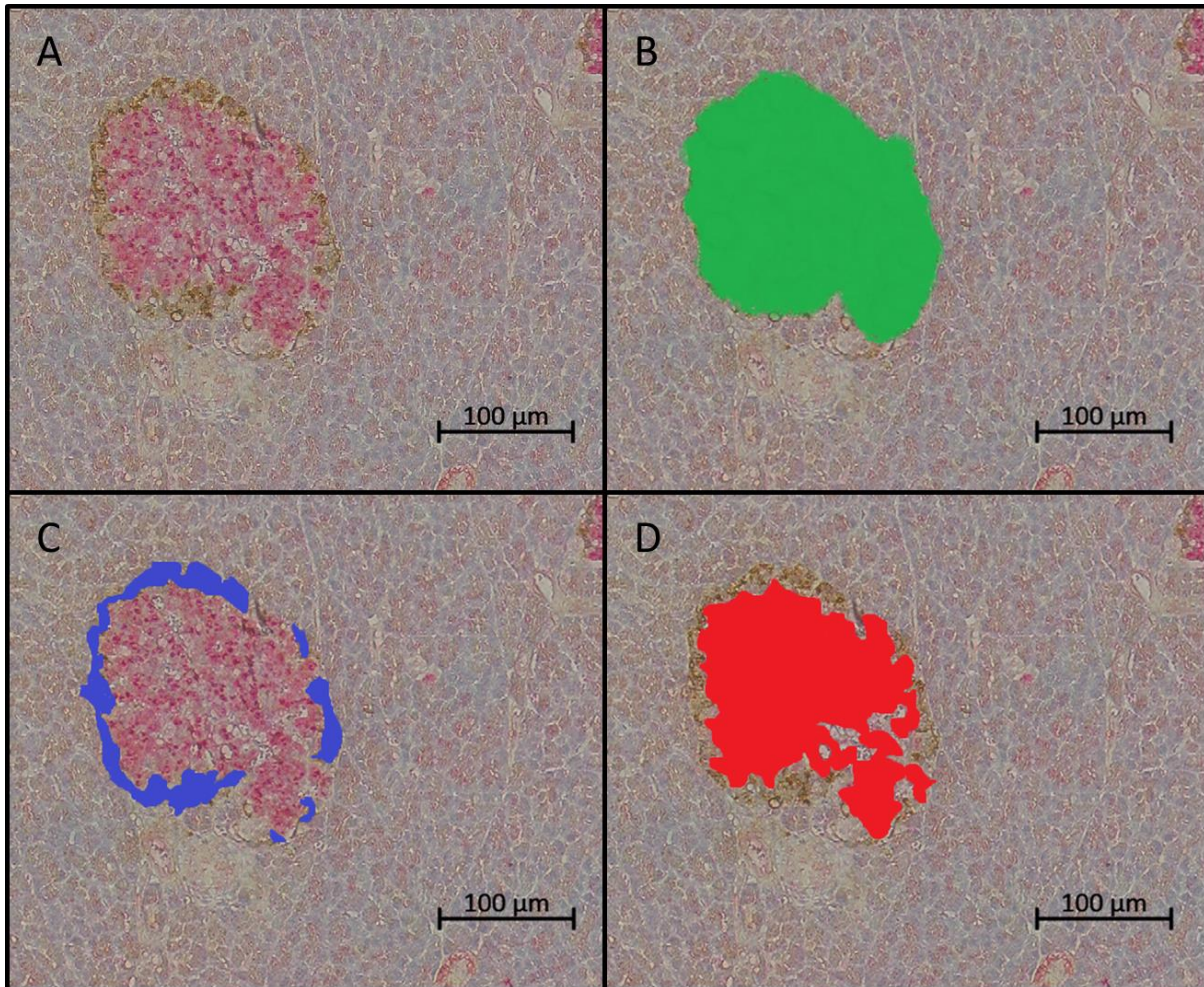


**Figure 3.4 Examples of measurements of the pancreas in a control rat, including the total islet area,  $\alpha$ -cell area and the  $\beta$ -cell area.** A) Pancreatic islet labelled with anti-insulin and anti-glucagon; B) Total islet area = green; C)  $\alpha$ -cell area = blue; D)  $\beta$ -cell area = red. Magnification = 100x; scale bar = 100  $\mu$ m

The area labelled with brown, which represents the  $\alpha$ -cells, was measured (Figure 3.4C). The area selected with blue highlighted the  $\alpha$ -cell area. The area labelled red, which represents the  $\beta$ -cells, was then measured (Figure 3.4D). Pancreatic islets which were not completely in view in the specific photo, were excluded.

The measurements were then used to determine each hormone's fraction per islet area by using equation 2 below:

$$\text{Hormone percentage} = \frac{\text{Hormone area}}{\text{Islet area}} \times 100$$

### **Equation 2 Hormone percentage calculation**

In total, 514, 733, 762 and 643 islets were analysed for the C/ART-, C/ART+, C/M+ and ART+/M+, respectively.

### **3.3.2 Liver analyses**

The liver was stained with H&E for histopathology analysis. Inflammatory cells, necrosis, loss of cell architecture and granular appearance were considered. The observations were classified as absent (0), mild (1) or moderate (2).

Blood from the thoracic aorta for liver function tests was collected into a yellow BD vacutainer tube. The tube was then placed in a centrifuge at 1 300 rpm for 20 minutes and the serum was collected and frozen at -80°C before sending it to the National Health Laboratory Services (NHLS) for analysis.

Liver function tests, including AST and ALT, haemoglobin and lipemia (Glick *et al.*, 1986; Thapa and Walia, 2007) was done by the NHLS of Tygerberg. The method of analysis is outlined in addendum 4. The AST value was divided by the ALT value to determine the ratio for each specific animal.

### 3.3.3 Kidney analyses

The kidneys were stained with H&E for histopathology analysis. Inflammatory cells, necrosis, loss of cell architecture, vacuolation and swelling of tubules were considered. The observations were classified as absent (0), mild (1) or moderate (2).

The kidneys stained with PAS were used for morphometric analyses (Kotyk *et al.*, 2016). Each kidney section was scanned with the Nikon automated tissue scanning software at a 200x magnification (20x objective lens). The images were taken with a 10% overlap and was stitched together to form a composite image of the tissue as seen in Figure 3.5.

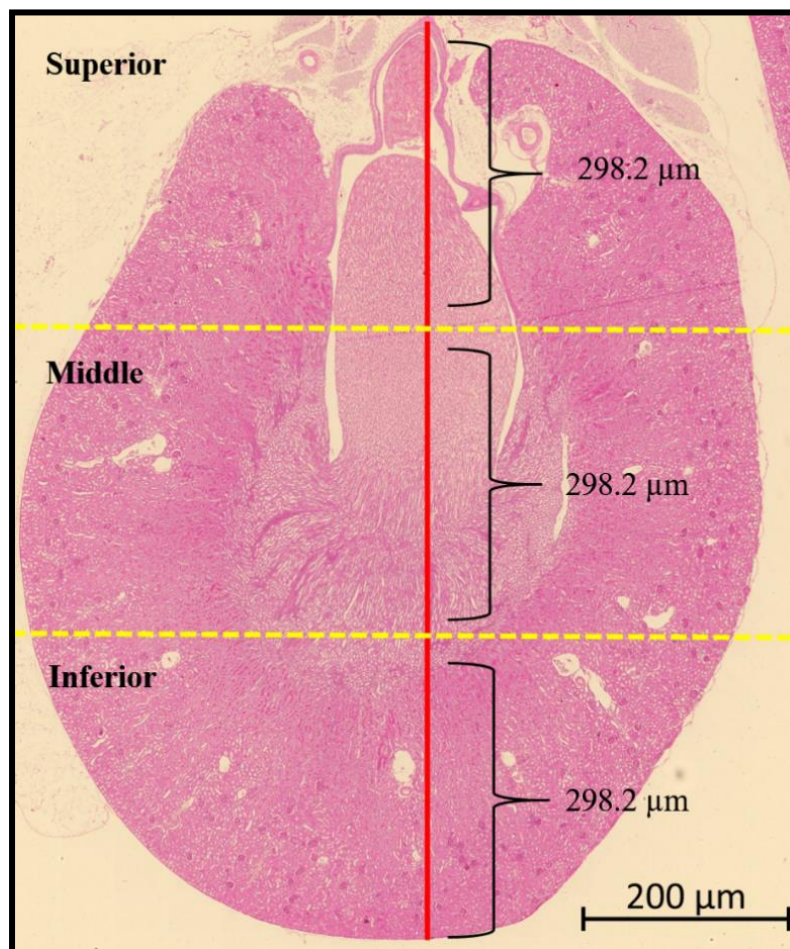


**Figure 3.5 Composite image of the kidney showing the superior, middle and inferior part.**

The red line indicates the complete length of the kidney tissue on the specific slide (894.68 μm). The yellow lines indicate the various parts the kidney tissue was divided into. Magnification = 200x; scale bar = 200 μm



Thirty renal corpuscles were analysed per animal (10 per part). To randomise the renal corpuscles that are analysed, the area of the kidneys was divided into a superior, middle and inferior part. Every fifth renal corpuscle was analysed to amount for ten renal corpuscles analysed per part. For each renal corpuscle, the following was measured:

1. Renal corpuscle area
2. Renal corpuscle circumference
3. Renal corpuscle diameter
4. Renal corpuscle radius
5. Glomerular area
6. Glomerular circumference
7. Glomerular diameter
8. Glomerular radius
9. Renal space

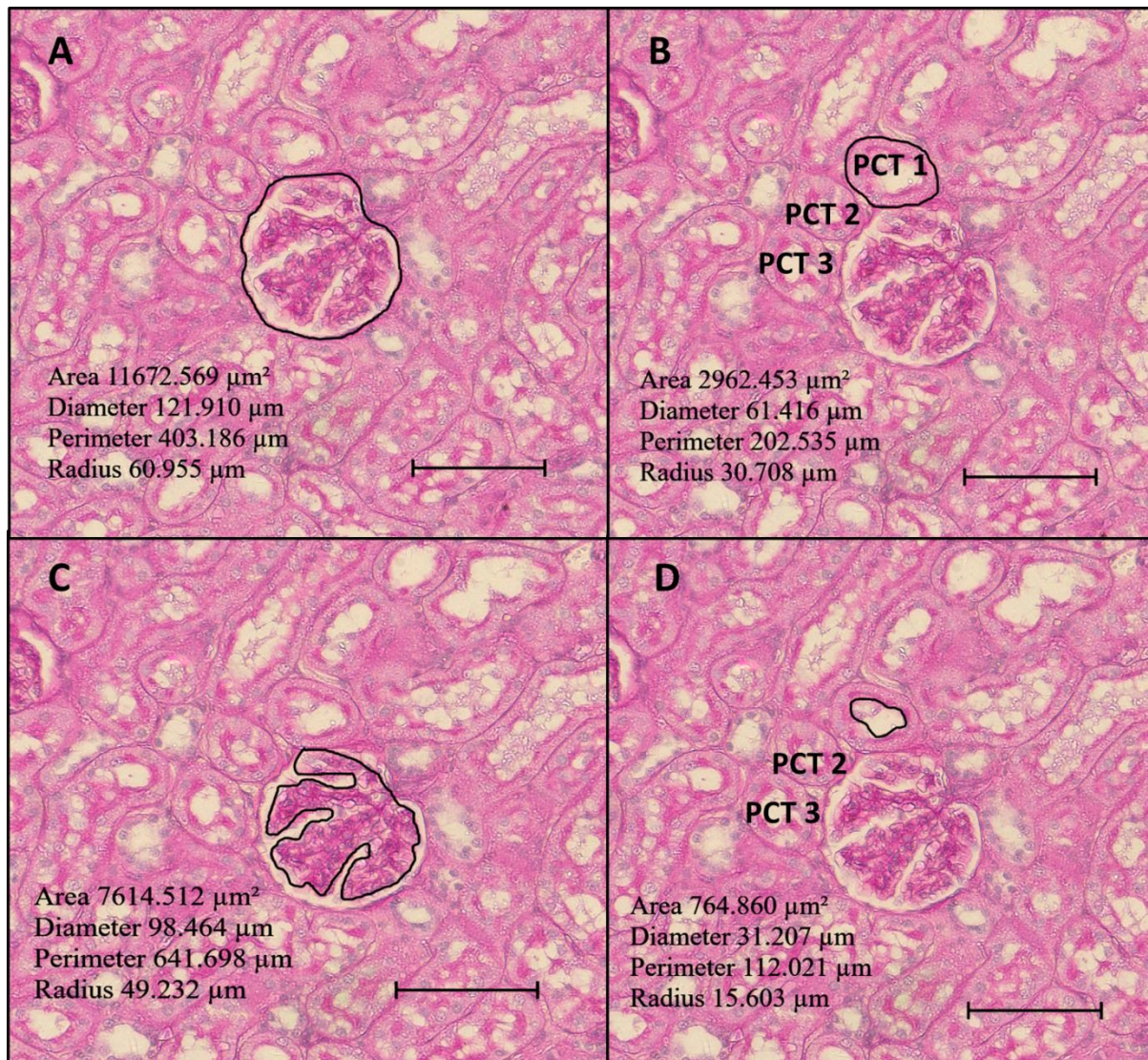


**Figure 3.6** Examples of measurements of the kidney of a control rat, including the renal corpuscle, glomerulus, PCTs and lumen of the PCTs. A) Renal corpuscle area, diameter, perimeter and radius B) Proximal convoluted tubule area with lumen (LPCT), diameter, perimeter and radius C) Glomerular area, diameter, perimeter and radius D) Lumen of PCT area, diameter, perimeter and radius. Magnification = 200x; scale bar = 50  $\mu\text{m}$

Figure 3.6A shows measurement of renal corpuscle and 16C measurement of glomerulus.

In addition to the measurements of the renal corpuscles, three PCT's adjacent to the specific renal corpuscles measured, was also analysed (Figure 3.6 B&D). The following was measured per PCT:

1. PCT area

2. PCT circumference
3. PCT diameter
4. PCT radius
5. Luminal area

The thickness of the PCT (PCT area) were calculated as the PCT area with the lumen (LPCT) minus the luminal area.

### 3.3.4 Statistical analyses

All data was statistically analysed by a biostatistician using Microsoft Excel and Statistica software (version 13). All p-values smaller than 0.05 were considered significant and p-values smaller than 0.01 were considered highly significant. The following tests were used to analyse the data:

**Mean:** The mean or average of a sample is the sum of all the values divided by the amount of observations (McKillup, 2012).

**Standard error of the mean (SEM):** The standard error of the mean is the standard deviation (SD) of the dispersal of the sample mean. The SEM increases as the sample size increases, which improves the accuracy of the statistic (McKillup, 2012).

**Analysis of variance (ANOVA):** A single-factor ANOVA is used to compare the means of a sample between three or more treatments. A single-factor ANOVA only determines that one or more treatment differs from the rest. A multiple-comparison ANOVA identifies which treatment differs from the other(s) (McKillup, 2012).

**Levene's Test:** A Levene test determines the absolute variation between each duplicate and its treatment mean and does a one-way ANOVA on that variation.

## CHAPTER 4 RESULTS

### 4.1 BODY MASS

The body mass of the rats was measured before euthanasia was administered. The mean body mass of the rats were 297.2 g, where no significant difference ( $p=0.4$ ) was seen in body mass between the four treatment groups (Figure 4.1). The C/ART+ group had the lowest mean body mass of 288.6 g and the C/M+ group had the highest mean body mass of 303.3 g.

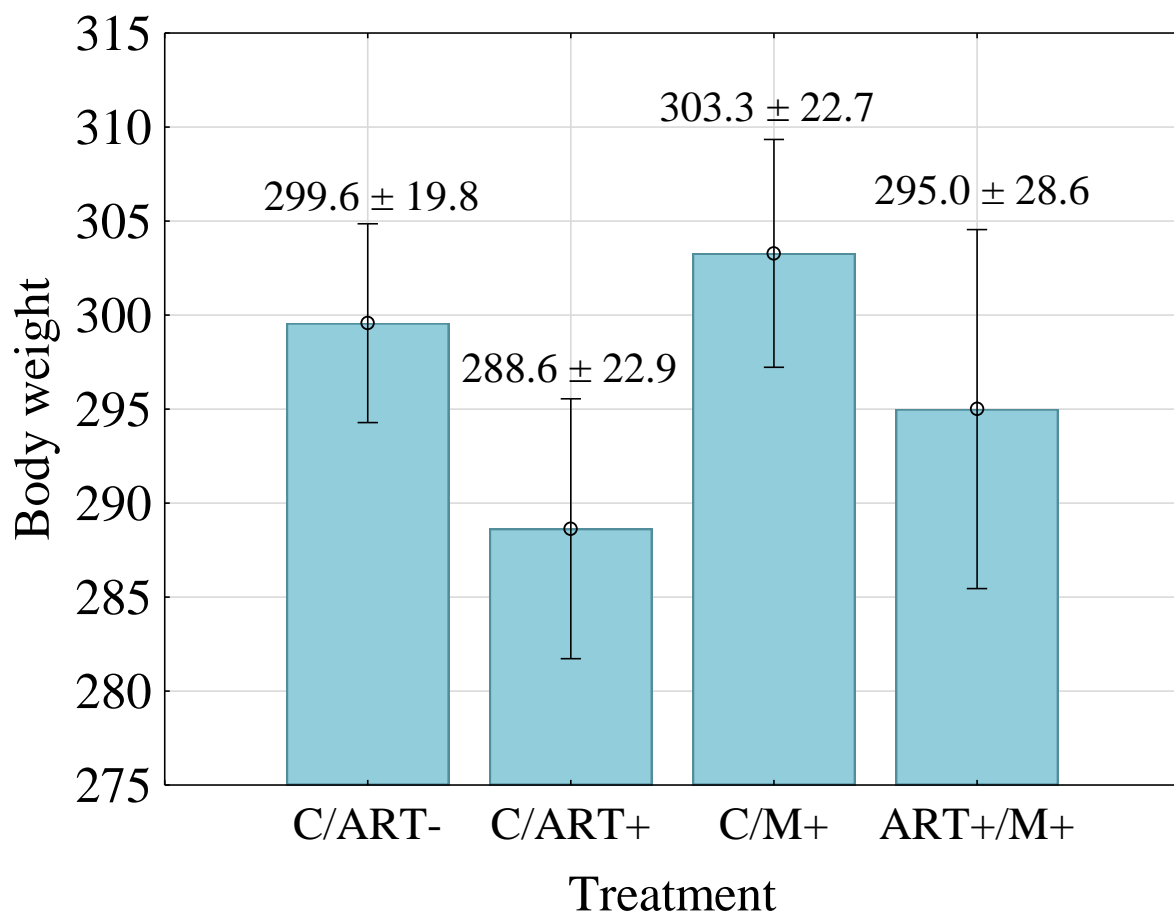


**Figure 4.1** Body mass of the rats did not differ significantly between the four treatment groups.

The C/M+ group showed an increased body weight in comparison to the C/ART+ group ( $p=0.1$ ).

## 4.2 PANCREAS

Sections of the pancreas were stained using H&E and labelled using monoclonal anti-insulin and polyclonal anti-glucagon antibodies.

### 4.2.1 Histopathology of the pancreas

Sections of the pancreas (n=40) stained with H&E were used for histopathologic evaluation and confirmed by the researcher, two histopathologists and a histologist. In addition, two interobservers also confirmed the findings. The observations were classified as absent (0), mild (1) or moderate (2). Histopathology observed were extremely mild and included proteinaceous material outside of the ducts. Furthermore, other incidental findings included mildly and moderately active lymph nodes as well as proteinaceous casts.

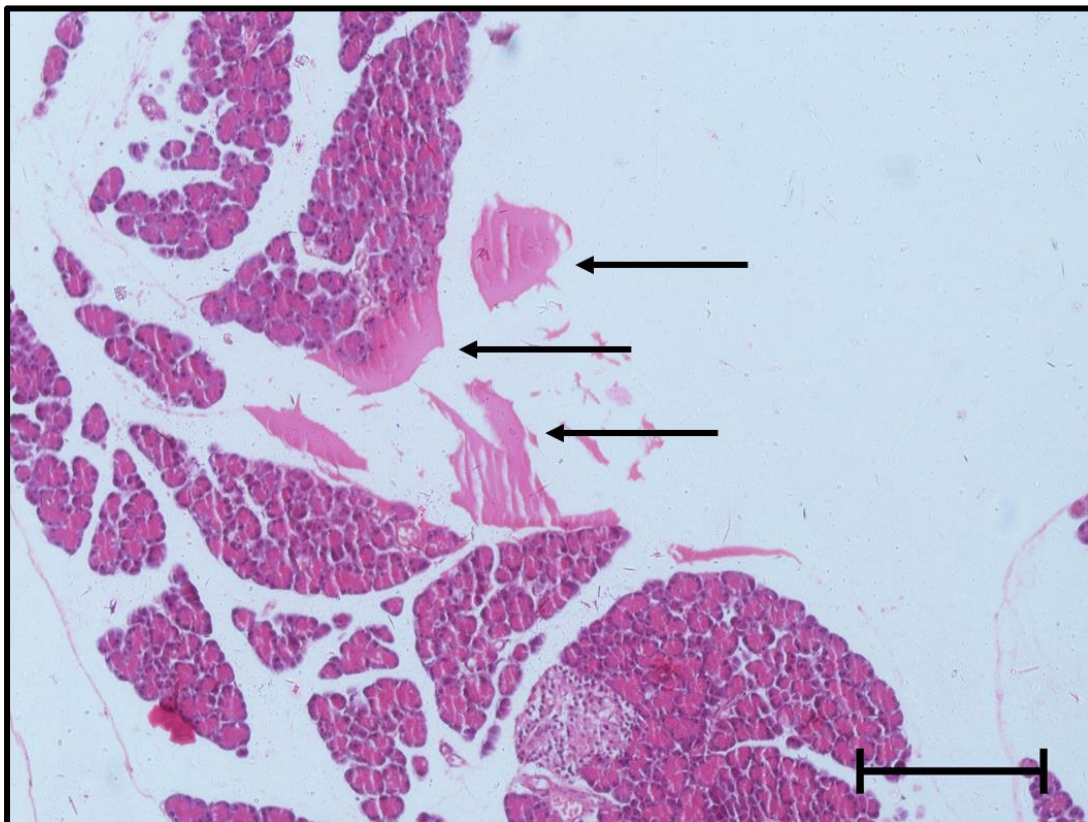


**Figure 4.2 Proteinaceous material outside of ducts as indicated by the arrows in a rat from the C/ART+ group. Magnification = 100x; scale bar = 200  $\mu$ m**

As seen in Figure 4.2, 2.5% (1/40) of the pancreata showed proteinaceous material outside of the pancreatic ducts, which was seen in the C/M+ group.

#### 4.2.2 Other findings

Proteinaceous material was seen in the ducts of 21% (8/39) of the pancreata, as seen in Figure 4.3.

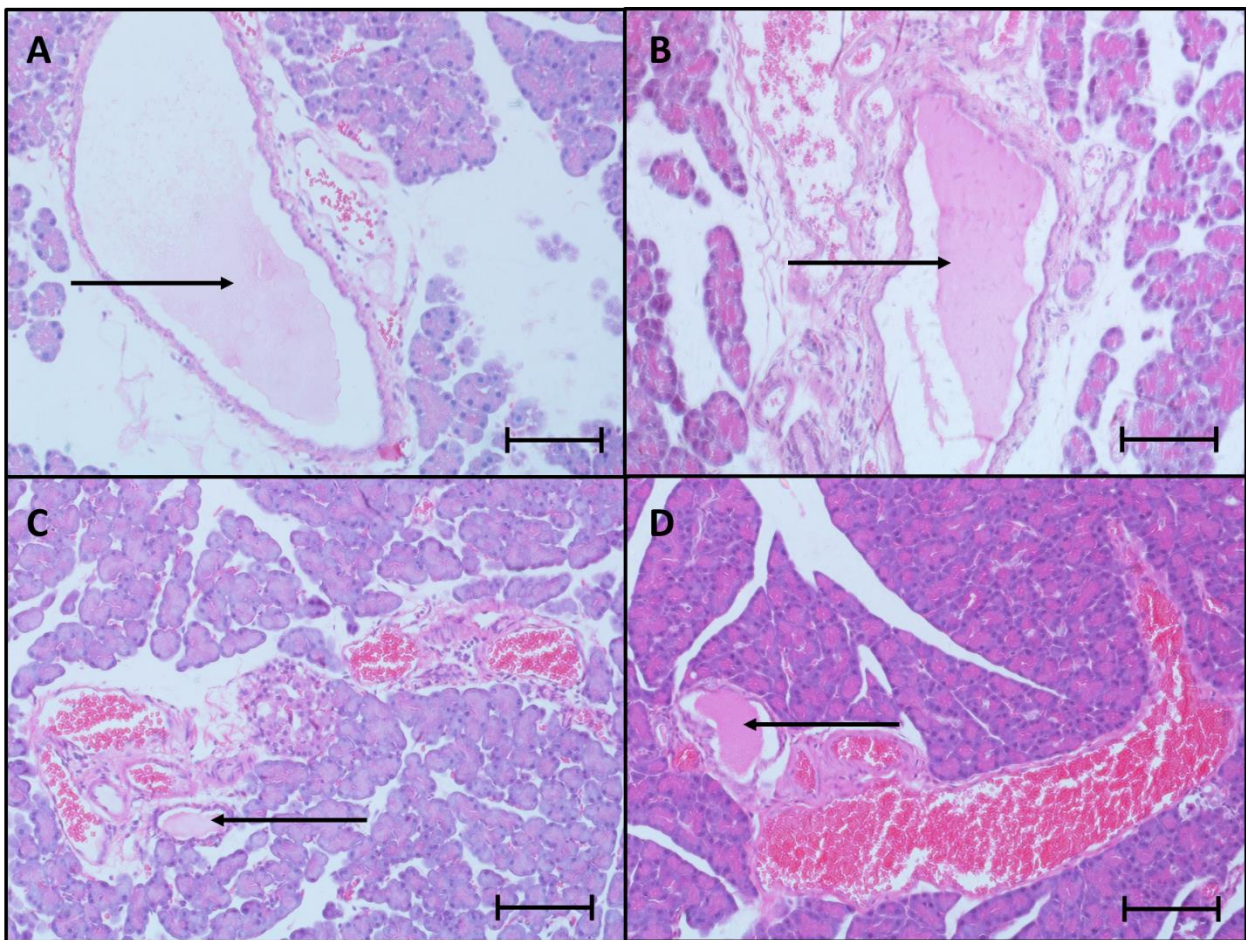


**Figure 4.3 Proteinaceous material in ducts of all four groups of the pancreas as indicated by the arrows. A) C/ART-; B) C/ART+; C) C/M+; D) ART+/M+. Magnification = 100x; scale bar =100  $\mu$ m**

The proteinaceous material is observed in all treatment groups as seen in Figure 4.3 A, B, C and D.

The accompanying lymph tissue outside of the pancreas parenchyma appeared active in 15% (6/39) of the pancreata; of which 10% (4/39) were mildly active and 5% (2/39) were moderately active. Figure 4.4 shows the included lymph tissue, including lymph nodes and gut-associated lymphoid tissue (GALT) in the ART+/M+ group, which appeared mildly active, especially in the paracortical area of the lymph tissue.

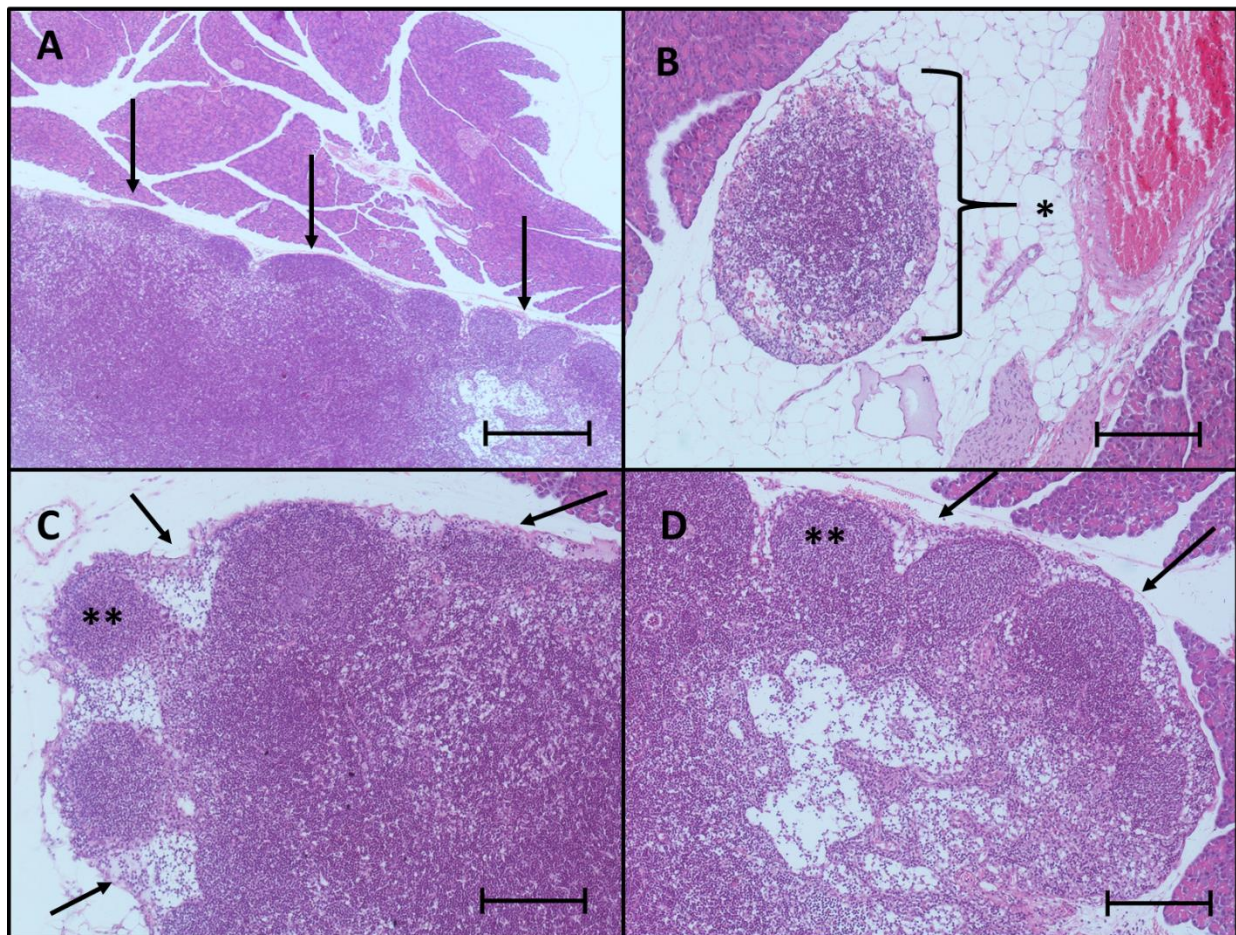


**Figure 4.4 Included lymph tissue of ART+/M+ group appears mildly active. Arrows indicate the lymphoid tissue.** A) The cortical area of the lymph tissue appears mildly active, but it does not penetrate the parenchyma. Magnification = 50x; scale bar = 500  $\mu$ m; B) Included GALT (\*) appears mildly active, but is well circumscribed. Magnification = 100x; scale bar = 200  $\mu$ m C) & D) The cortex of the included lymph tissue appears mildly active. \*\* indicate follicles in cortex. Magnification = 100x; scale bar = 200  $\mu$ m

The groups that had active lymph tissue included C/M+ (3/6), C/ART+ (2/6) and ART+/M+ (1/6).



### 4.2.3 Analysis of the pancreatic islets

The pancreatic islets were labelled with monoclonal anti-insulin and polyclonal anti-glucagon antibodies, respectively. A total of 1056 pancreatic islets with their accompanying  $\alpha$ -cells and  $\beta$ -cells were measured in the C/ART- group, 1512 in the C/ART+ group, 1570 in the C/M+ group and 1320 in the ART+/M+ group. The islet cells positive for glucagon ( $\alpha$ -cells) labelled brown and the cells positive for insulin ( $\beta$ -cells) labelled red (Figure 4.6). Islet numbers were normalised to the respective total section areas ( $\text{mm}^2$ ). Table 4.1 shows a summary of the measurements obtained in the pancreas.

**Table 4-1 Summary of the measurements on the pancreatic islets in the pancreas labelled with anti-insulin and anti-glucagon  $\pm$  SD of the four treatment groups.**

Treatment	Islets per $\text{mm}^2$	Islet area ( $\mu\text{m}^2$ )	$\alpha$ -cell area ( $\mu\text{m}^2$ )	$\beta$ -cell area ( $\mu\text{m}^2$ )
C/ART-	<b>1.53 <math>\pm</math> 0.72<sup>b</sup></b>	4755.68 $\pm$ 1595.80 <sup>a</sup>	443.58 $\pm$ 240.66 <sup>ab</sup>	1902.76 $\pm$ 1003.85 <sup>a</sup>
C/ART+	2.06 $\pm$ 0.52 <sup>ab</sup>	4113.95 $\pm$ 852.20 <sup>a</sup>	<b>352.71 <math>\pm</math> 105.55<sup>a</sup></b>	1468.57 $\pm$ 343.98 <sup>a</sup>
C/M+	<b>2.30 <math>\pm</math> 0.69<sup>a</sup></b>	5249.80 $\pm$ 1738.86 <sup>a</sup>	<b>582.72 <math>\pm</math> 311.35<sup>b</sup></b>	1838.75 $\pm$ 802.11 <sup>a</sup>
ART+/M+	<b>1.66 <math>\pm</math> 0.55<sup>b</sup></b>	4928.76 $\pm$ 1919.92 <sup>a</sup>	442.87 $\pm$ 171.85 <sup>ab</sup>	1880.72 $\pm$ 1021.24 <sup>a</sup>
Mean	1.89 $\pm$ 0.68	4762.05 $\pm$ 1574.64	455.47 $\pm$ 228.16	1772.70 $\pm$ 825.33

Statistical significance ( $p < 0.05$ ) is indicated by a bold font and different letters of the alphabet. If the same letter/s is/are present above each of the groups, there were no significant differences.

No significant difference ( $p=0.5$ ) was seen in the islet area between the four groups. The mean islet areas for the C/ART-, C/ART+, C/M+ and ART+/M+ groups were each 4755.68  $\mu\text{m}^2$ , 4113.95  $\mu\text{m}^2$ , 5249.80  $\mu\text{m}^2$  and 4928.76  $\mu\text{m}^2$ , respectively.

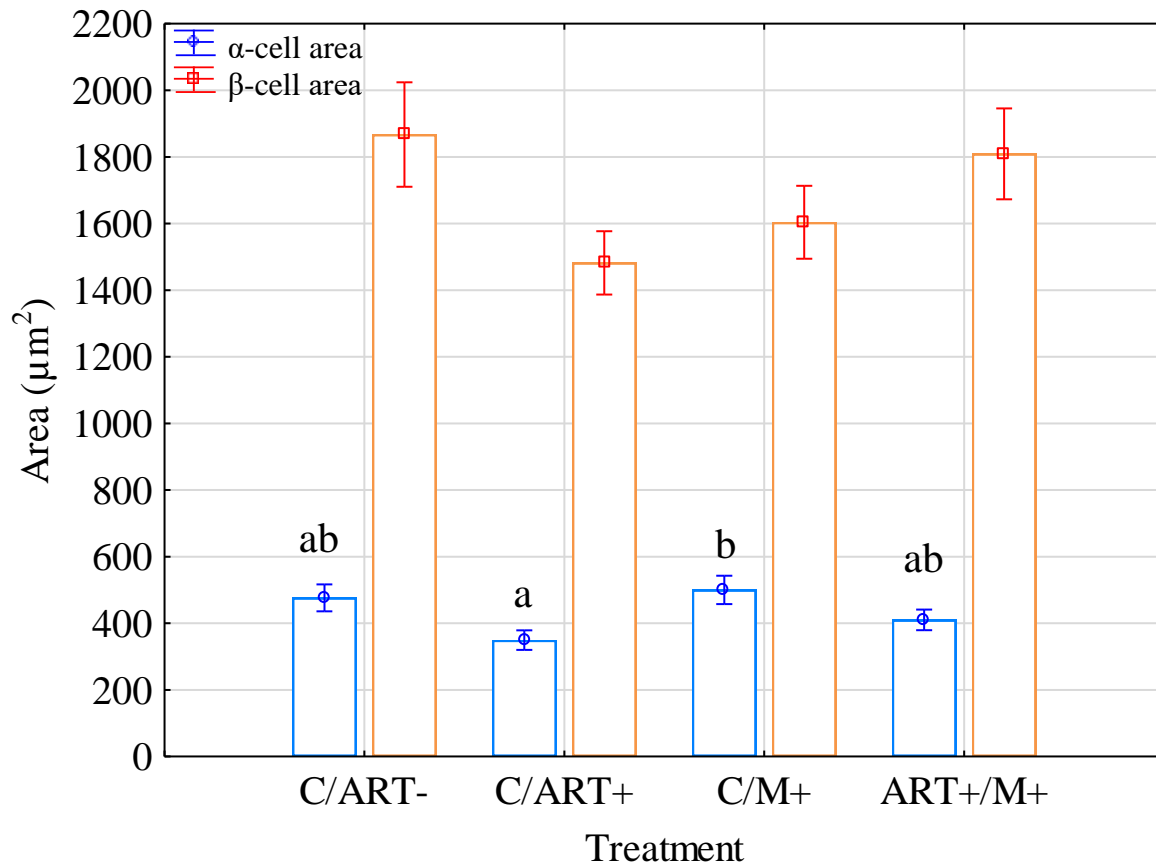


**Figure 4.5** The area of the  $\alpha$ - and  $\beta$ -cells did not differ between the four treatment groups. The  $\beta$ -cell area (blue line) was higher than the  $\alpha$ -cell area (red line) in all four treatment groups. Statistical significance ( $p < 0.05$ ) is indicated by a bold font and different letters of the alphabet. If the same letter/s is/are present above each of the groups, there were no significant differences.

As seen in Figure 4.5, in all treatment groups, the  $\alpha$ -cell area was smaller than the  $\beta$ -cell area with an area mean of  $455.47 \mu\text{m}^2$   $\alpha$ -cells and  $1772.70 \mu\text{m}^2$   $\beta$ -cells per islet. The  $\alpha$ -cell area of the C/ART+ group was the lowest with  $352.71 \mu\text{m}^2$  and the  $\alpha$ -cell area of the C/M+ group was the highest with  $582.72 \mu\text{m}^2$ . Post hoc tests showed the  $\alpha$ -cell area differed significantly ( $p=0.03$ ) between the C/ART+ and C/M+ groups.

The  $\beta$ -cell area of the C/ART- group was the highest with  $1902.76 \mu\text{m}^2$  and the  $\beta$ -cell area of the C/ART+ group was the lowest with  $1468.57 \mu\text{m}^2$ . Neither the  $\alpha$ -cell area ( $p=0.2$ ) nor  $\beta$ -cell area of  $\alpha$ -cells and  $\beta$ -cells ( $p=0.6$ ) showed significant difference between the four groups.

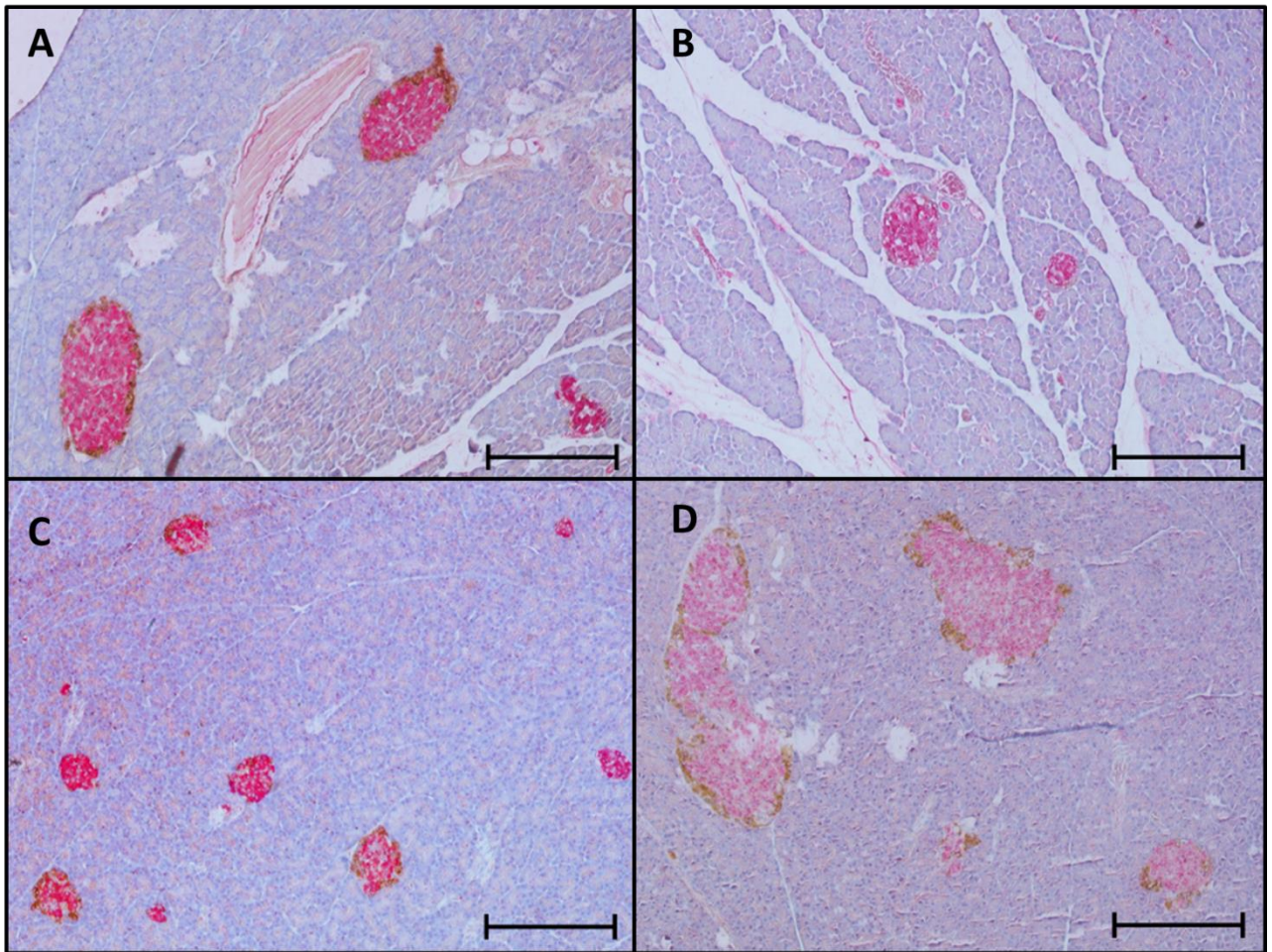
The mean percentage of  $\alpha$ -cells and  $\beta$ -cells of the four treatment groups was 6.57% and 34.45%, respectively (Table 4.2). No significant difference was observed in either  $\alpha$ -cell percentages ( $p=0.8$ ) and  $\beta$ -cell percentages ( $p=0.8$ ) between the four treatment groups.

**Table 4-2 Percentage of  $\alpha$ -cell area and  $\beta$ -cell area in the pancreatic islets  $\pm$  SD of the four treatment groups.**

Treatment	$\alpha$ -cell percentage	$\beta$ -cell percentage
C/ART-	6.65 $\pm$ 3.14 <sup>a</sup>	36.07 $\pm$ 8.63 <sup>a</sup>
C/ART+	5.86 $\pm$ 2.51 <sup>a</sup>	34.90 $\pm$ 7.19 <sup>a</sup>
C/M+	6.86 $\pm$ 1.97 <sup>a</sup>	33.61 $\pm$ 6.49 <sup>a</sup>
ART+/M+	6.89 $\pm$ 2.26 <sup>a</sup>	33.21 $\pm$ 7.30 <sup>a</sup>
Mean	6.57 $\pm$ 2.44	34.45 $\pm$ 7.24

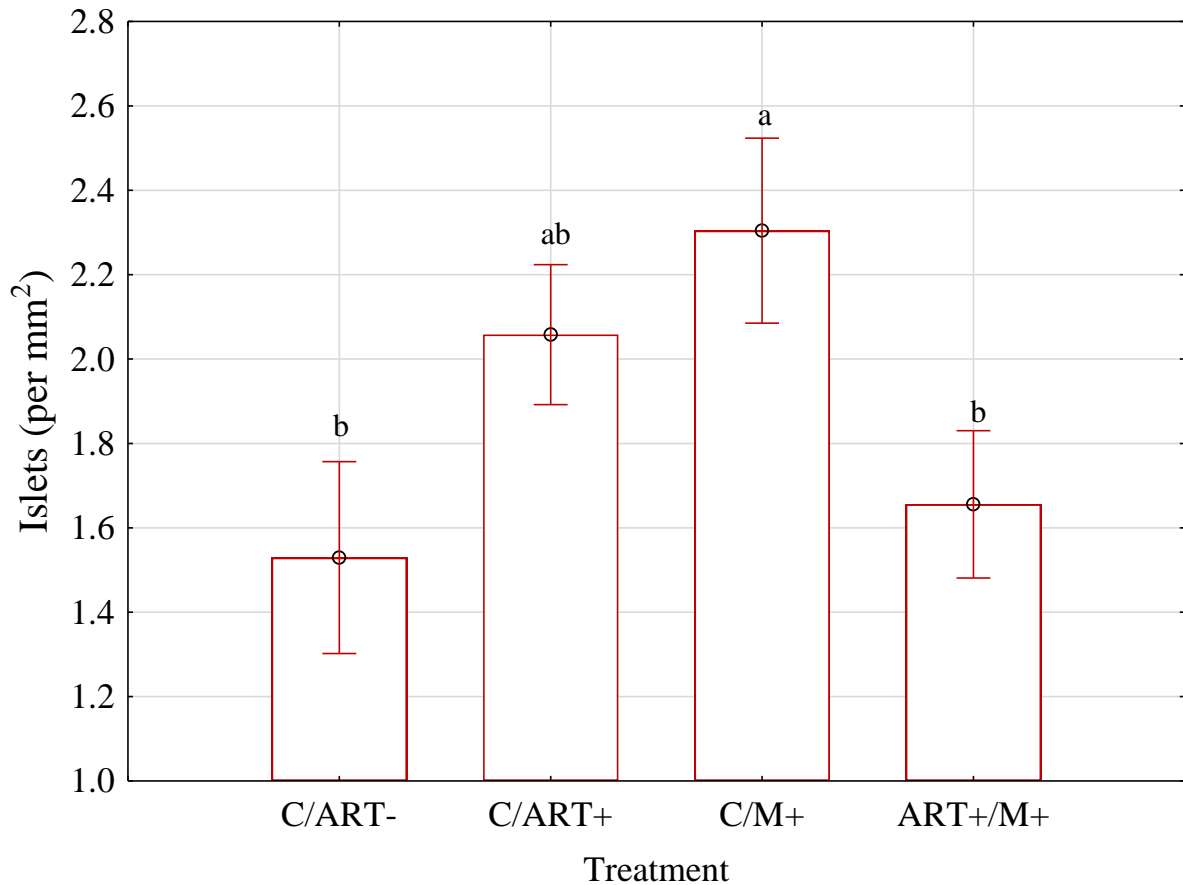
Statistical significance ( $p < 0.05$ ) is indicated by a bold font and different letters of the alphabet. If the same letter/s is/are present above each of the groups, there were no significant differences.

Figure 4.6 shows the  $\alpha$ -cell area (brown) in the mantle of the pancreatic islets and the  $\beta$ -cell area (red) in the core of the pancreatic islets of the four treatment groups.



**Figure 4.6** Examples of the islet area and  $\alpha$ - and  $\beta$ -cell area of the four treatment groups showed no significant differences. The C/M+ group had more islets per  $\text{mm}^2$  than the other groups. A) C/ART- group B) C/ART+ group C) C/M+ group D) ART+/M+ group. Magnification = 100x; scale bar = 100  $\mu\text{m}$ .

The mean number of islets observed between the four groups per  $\text{mm}^2$  was 1.89. The C/ART- group had 1.53 per  $\text{mm}^2$ , the C/ART+ group had 2.06 per  $\text{mm}^2$ , the C/M+ group 2.30 per  $\text{mm}^2$  and the ART+/M+ group 1.66 per  $\text{mm}^2$ . The number of islets per  $\text{mm}^2$  differed significantly ( $p=0.03$ ) between the four groups as shown in Figure 4.7.



**Figure 4.7** The number of pancreatic islets per mm<sup>2</sup> differed significantly between the treatment groups. Statistical significance ( $p < 0.05$ ) is indicated by different letters of the alphabet. If the same letter/s is/are present above each of the groups, there were no significant differences.

Post hoc analysis showed highly significant difference in the C/M+ group compared to the C/ART- ( $p=0.01$ ) and ART+/M+ ( $p=0.02$ ) groups.

### 4.3 LIVER

Sections of the liver were stained using H&E. Additionally, liver enzymes tests, specifically AST, ALT, lipaemia and haemoglobin were done on blood samples.

#### 4.3.1 Histopathology of the liver

Sections of the liver (n=40) stained with H&E were used for histopathologic evaluation and confirmed by the researcher, two histopathologists and a histologist. In addition, two interobservers also confirmed the findings. The observations were classified as absent (0), mild (1) or moderate (2). Histopathology observed was extremely mild and included granular appearance of hepatocytes, loss of hepatocyte architecture and lymphocyte infiltration. The histopathology observed was expressed as a percentage of the total amount of liver sections observed.

The specific histopathology that was seen in the liver included granular appearance, loss of hepatocyte architecture and lymphocyte infiltration. Mild granular appearance of hepatocytes was observed in 23% (9/40) of livers (Figure 4.8A). Loss of hepatocyte architecture (Figure 4.8B) and lymphoid infiltration (Figure 4.8C) were seen in 3% (1/40) of the livers, which was also classified as mild. Hydropic changes expressed as mild vacuolation (Figure 4.8D) were seen in 15% (6/40) of the livers.

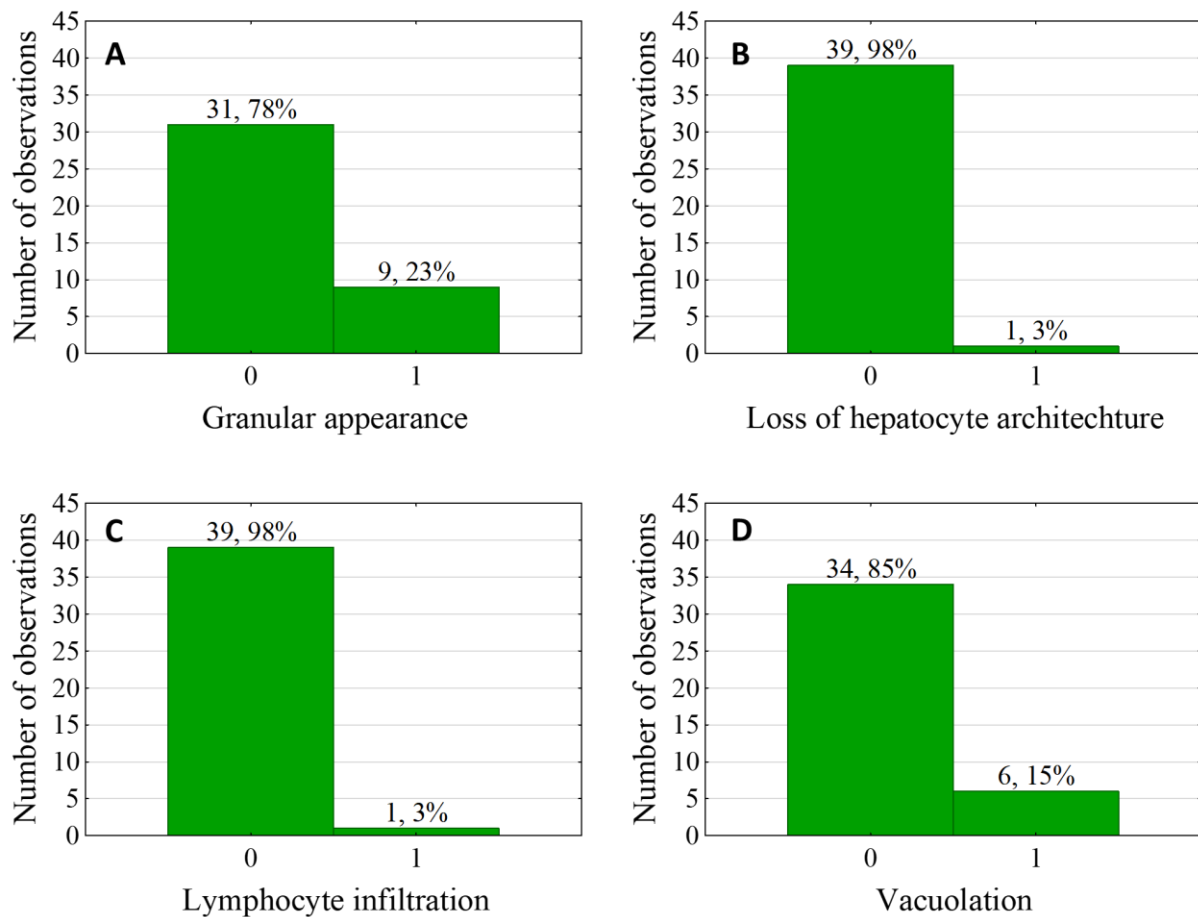


**Figure 4.8 Percentages of the histopathology seen in the liver in the total of four treatment groups.** No histopathology = 0; mild activity = 1. A) Granular appearance of hepatocytes; B) Loss of hepatocyte architecture; C) Lymphocyte infiltration; D) Vacuolation

Granular appearance of hepatocytes was seen in 40% of the C/ART- group, 20% in the C/ART+ group, 20% in the C/M+ group and 10% in the ART+/M+ group (Figure 4.9).

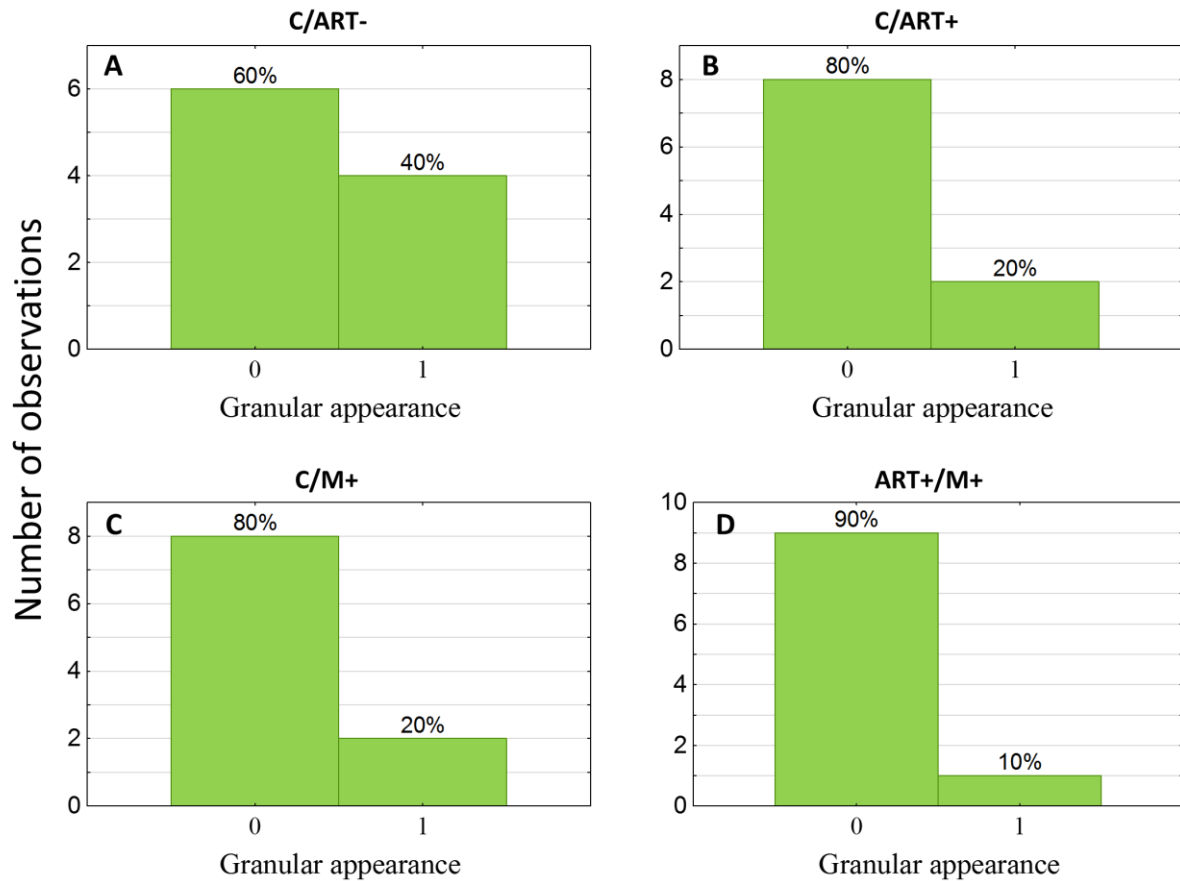


**Figure 4.9** The percentages of the granular appearance of hepatocytes did not differ significantly between the four treatment groups. A) C/ART- group; B) C/ART+ group; C) C/M+ group; D) ART+/M+ group

The granular appearance of hepatocytes did not differ significantly ( $p=0.4$ ) between the four treatment groups. Figure 4.10B shows an example of mild granular appearance observed in the affected livers in contrast with a normal appearance of the hepatocytes (Figure 4.10A).



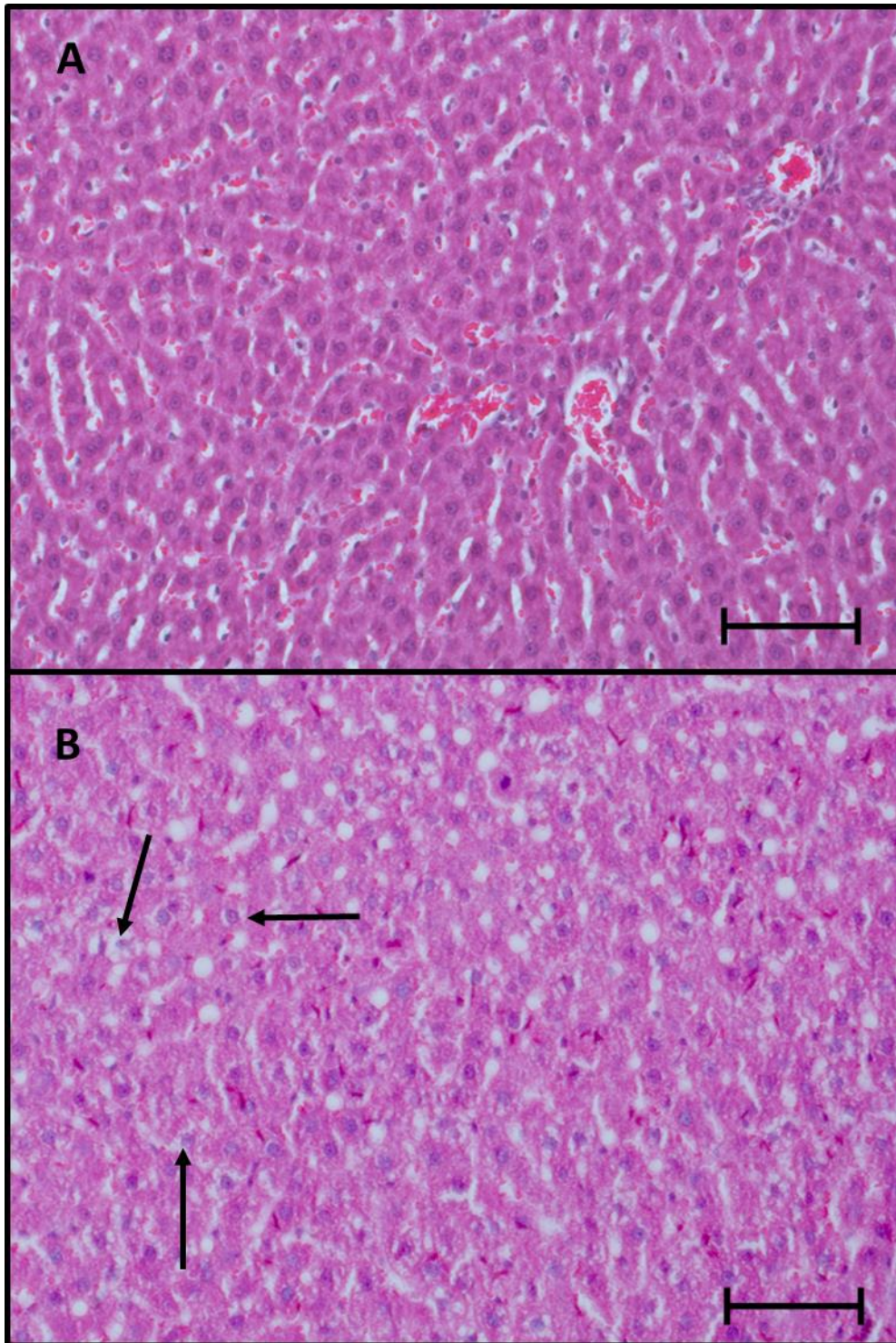


**Figure 4.10 Granular appearance and vacuolation of hepatocytes.** A) Normal appearance of hepatocytes B) Mild granular appearance of hepatocytes. Arrows indicate vacuoles. Magnification =200x, scale bar = 100  $\mu$ m

The prevalence of vacuolation did not differ significantly between the four treatment groups, but showed a trend ( $p=0.06$ ) between the four treatment groups (Figure 4.11). The C/ART-

group had 40% vacuolation, the C/ART+ group 10%, the C/M+ group 10% and the ART+/M+ group 0%. Mild vacuolation, as seen in these groups, is indicated in Figure 4.10B.

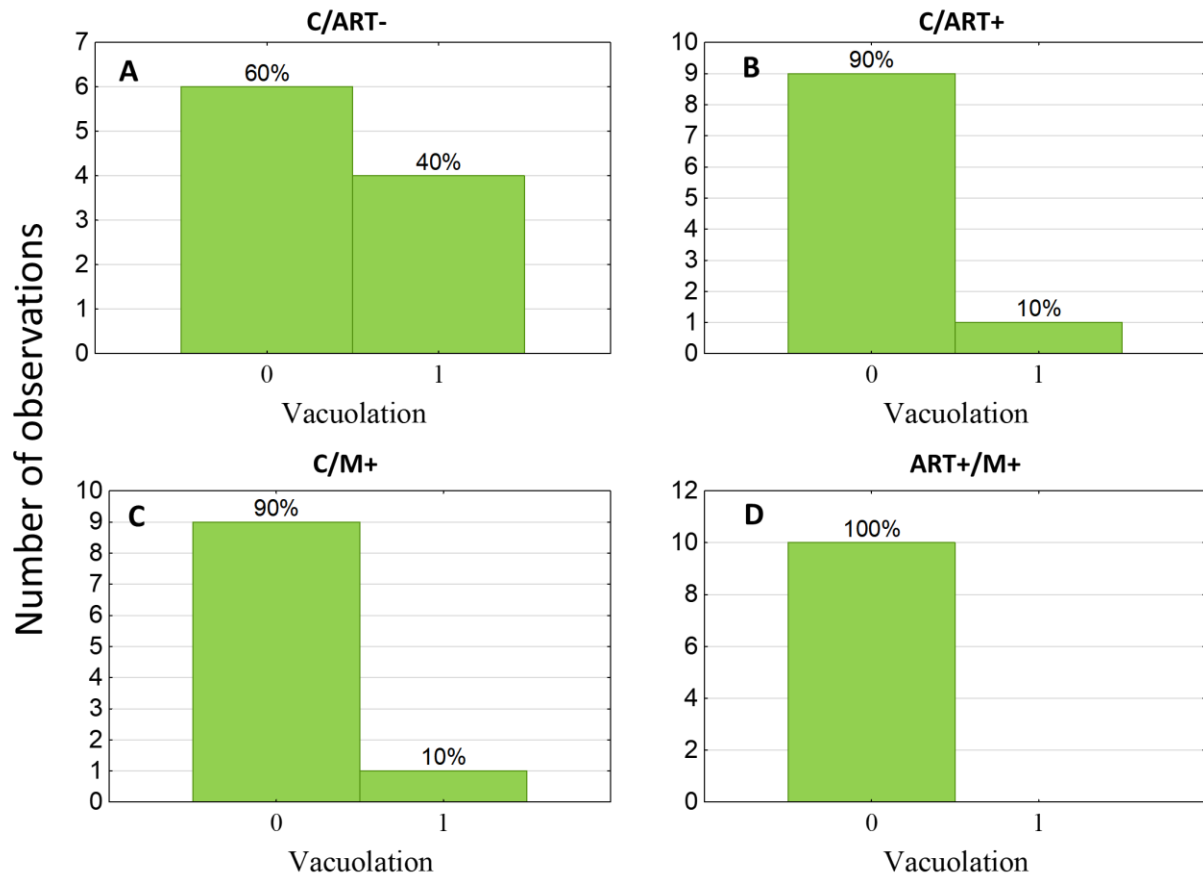


**Figure 4.11** The percentages of the mild vacuolation of hepatocytes did not differ significantly between the four treatment groups. A) C/ART- group; B) C/ART+ group; C) C/M+ group; D) ART+/M+ group

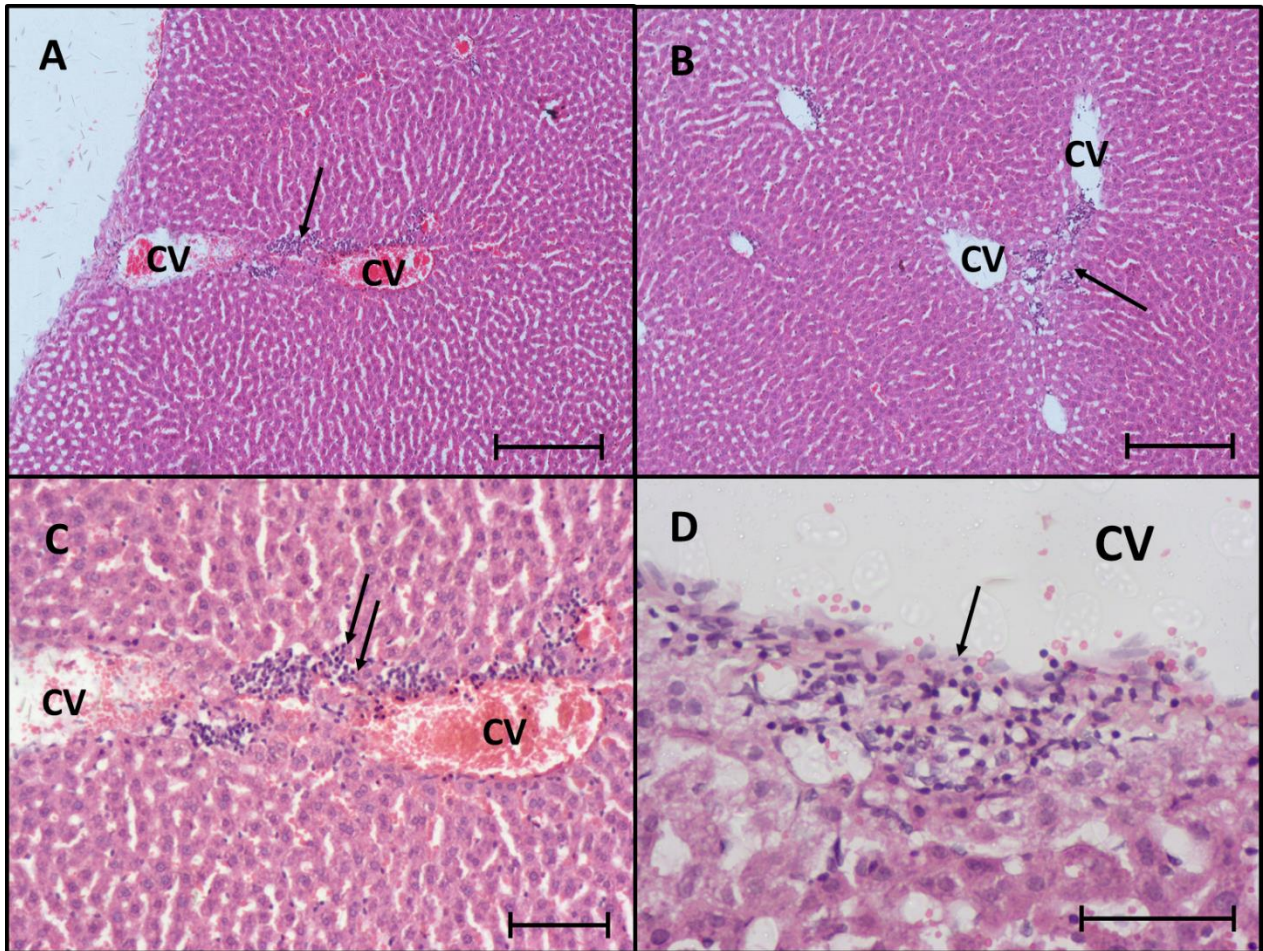


**Figure 4.12 Lymphocyte infiltration in various areas around the central veins of a C/M+ liver.** CV= central vein; arrows indicate lymphocytes. A) 100x magnification, scale bar = 200  $\mu\text{m}$ ; B) 100x magnification, scale bar = 200  $\mu\text{m}$ ; C) 200x magnification, scale bar = 100  $\mu\text{m}$ ; D) 400x magnification, scale bar = 100  $\mu\text{m}$ .

Lymphocyte infiltration around the central veins was seen in the C/M+ group (Figure 4.12). The infiltration was seen around the central veins.

### 4.3.2 Liver enzyme analysis

Blood samples (n=37) were used to do liver function tests, specifically ALT, AST, serum haemoglobin and serum lipaemia. Three of the blood samples for the ART+/M+ group could not be collected due to an inadequate amount of blood from three of the rats.

**Table 4-3 Summary of the values from liver function tests  $\pm$  SD of the four treatment groups.**

Treatment	ALT (U/L)	AST (U/L)	AST/ALT ratio	Haemoglobin (g/dl)	Lipaemia (mg/dl)
C/ART-	62.40 $\pm$ 6.44 <sup>a</sup>	181.50 $\pm$ 107.14 <sup>a</sup>	2.92 $\pm$ 0.60 <sup>a</sup>	<b>50.90 <math>\pm</math> 27.91<sup>b</sup></b>	<b>12.00 <math>\pm</math> 7.23<sup>a</sup></b>
C/ART+	54.40 $\pm$ 0.55 <sup>a</sup>	160.80 $\pm$ 75.50 <sup>a</sup>	3.02 $\pm$ 0.70 <sup>a</sup>	<b>98.00 <math>\pm</math> 65.29<sup>a</sup></b>	8.33 $\pm$ 2.24 <sup>ab</sup>
C/M+	59.40 $\pm$ 9.52 <sup>a</sup>	188.60 $\pm$ 85.60 <sup>a</sup>	3.32 $\pm$ 0.76 <sup>a</sup>	66.20 $\pm$ 30.26 <sup>ab</sup>	<b>6.90 <math>\pm</math> 2.42<sup>b</sup></b>
ART+/M+	68.14 $\pm$ 2.50 <sup>a</sup>	217.71 $\pm$ 61.65 <sup>a</sup>	3.30 $\pm$ 0.73 <sup>a</sup>	92.17 $\pm$ 39.93 <sup>ab</sup>	9.67 $\pm$ 1.97 <sup>ab</sup>
Mean	60.51 $\pm$ 9.84	184.68 $\pm$ 84.49	3.13 $\pm$ 0.69	74.46 $\pm$ 45.51	9.20 $\pm$ 4.61

Statistical significance ( $p < 0.05$ ) is indicated by a bold font and different letters of the alphabet. If the same letter/s is/are present above each of the groups, there were no significant differences.

No significant differences were seen in ALT ( $p=0.83$ ) nor AST (0.61) values between the four groups (Table 4.3). The mean of the ALT of the four groups was 60.51, whereas the mean of the AST was 184.68. The highest ALT value was 68.14 and the highest AST value was 217.71, both in the ART+/M+ group. The AST/ALT ratio was above 2:1 for all groups ( $p<0.01$ ), with the C/M+ group being the highest with 3.32:1. The lowest AST/ALT ratio was 2.92:1 and in the C/ART- group. No statistical difference ( $p=0.51$ ) was, however, observed between the four groups for the AST/ALT ratio.

Bilirubin, haemoglobin and lipaemia tests were conducted to determine interference on AST and ALT. All bilirubin values were 0 mg/dl. Figure 4.13 and Figure 4.14 shows the serum haemoglobin and serum lipaemia values, respectively.

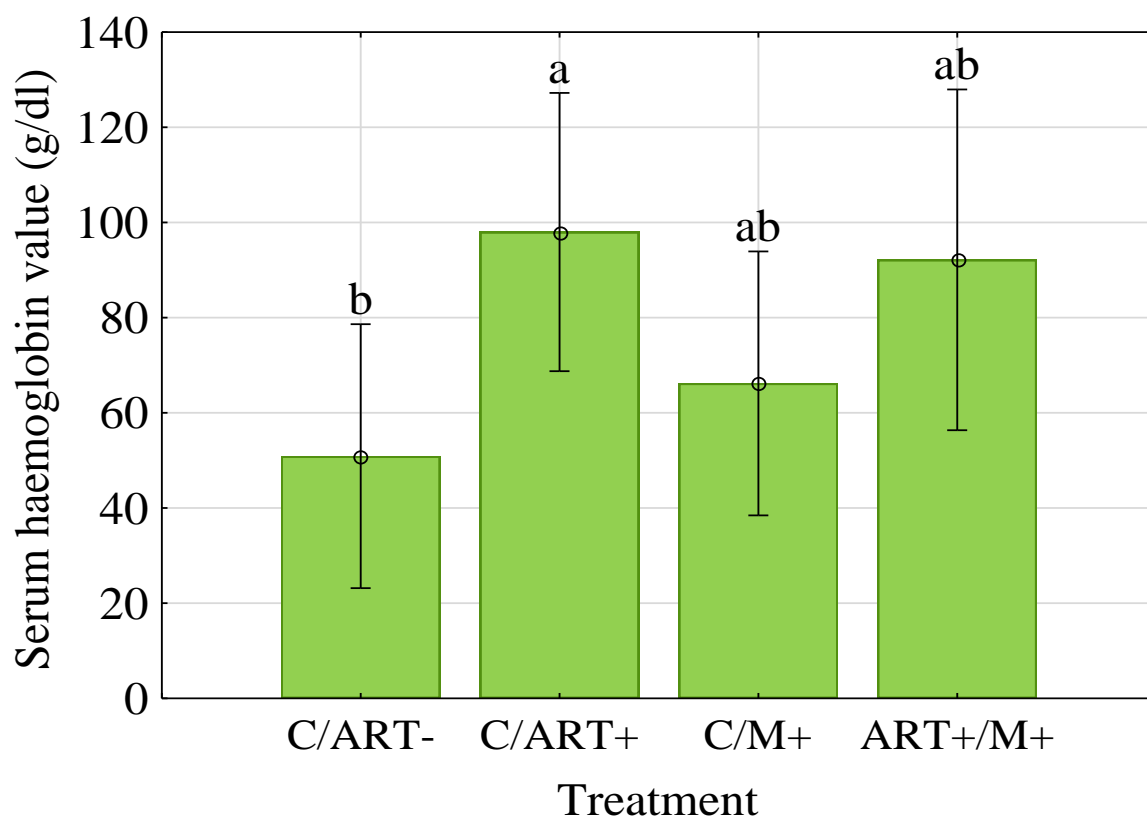


**Figure 4.13 Serum haemoglobin value differed significantly between the C/ART- group and C/ART+ group.** Statistical significance ( $p < 0.05$ ) is indicated by different letters of the alphabet. If the same letter/s is/are present above each of the groups, there were no significant differences.

The serum haemoglobin (Figure 4.13) and lipaemia (Figure 4.14) values could be determined for 35 animals; C/ART- ( $n=10$ ), C/ART+ ( $n=9$ ), C/M+ ( $n=10$ ) and ART+/M+ ( $n=6$ ). The combined treatment effect was not significant ( $p=0.09$ ), but showed a trend (Table 4.3) between the four treatment groups. However, post hoc analysis showed the C/ART- group had the lowest haemoglobin value at 50.90 and differed significantly ( $p=0.02$ ) with the C/ART+ group, which had a haemoglobin value of 98.00. A trend ( $p=0.07$ ) was also seen between the C/ART- and ART+/M+ groups with a haemoglobin value of 92.17 for the latter.

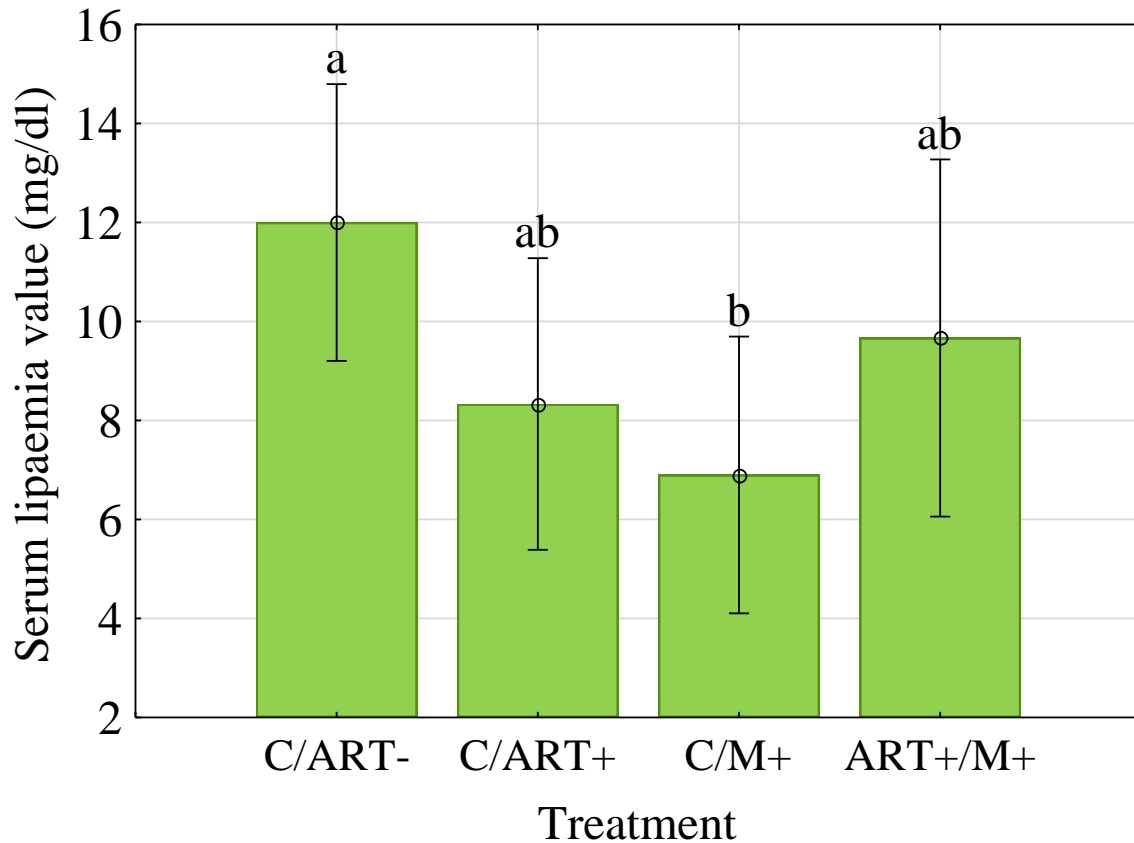


**Figure 4.14 Serum lipaemia value differed significantly between the C/ART- group and C/M+ group.** Statistical significance ( $p < 0.05$ ) is indicated by different letters of the alphabet. If the same letter/s is/are present above each of the groups, there were no significant differences.

The serum lipaemia value did not differ significantly between the four treatments, but showed a trend ( $p=0.08$ ) (Figure 4.14). Post hoc analysis showed that the C/ART- group, which had a lipid value of 12.00, differed highly significantly ( $p=0.01$ ) with the C/M+ group, which had a lipid value of 6.90. The C/ART- and C/ART+ groups also showed a trend ( $p=0.08$ ) with a lipid value of 12.00 and 8.33, respectively.

## 4.4 KIDNEY

The kidneys were stained using both H&E and PAS.

### 4.4.1 Histopathology of the kidney

Sections of the kidney (n=40) stained with H&E were used for histopathologic evaluation and confirmed by the researcher, two histopathologists and a histologist. In addition, two interobservers also confirmed the findings. The observations were classified as absent (0), mild (1) or moderate (2). Histopathology observed were mild and moderate hydropic changes, which included swelling of proximal and distal convoluted tubules and vacuolation of proximal convoluted tubules. The amount of histopathology observed were expressed as a percentage of the total amount of kidneys observed.

Mild swelling of the PCTs and DCTs were observed in 45% (18/40) of the kidneys (Figure 4.15A), which was accompanied by 55% (22/40) of PCTs and DCTs which presented with vacuolation (Figure 4.15B).

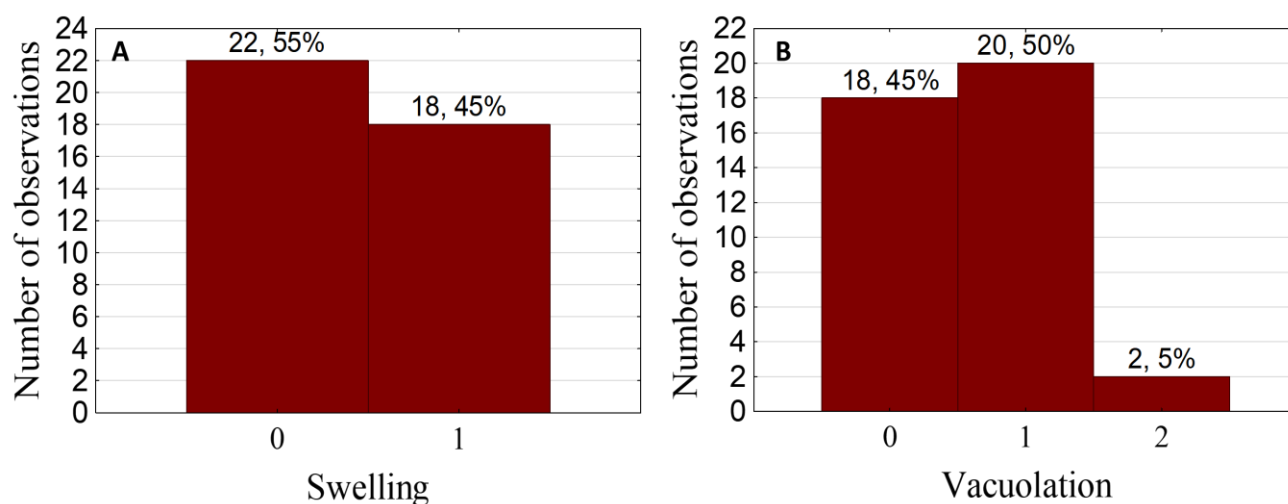


**Figure 4.15 Percentage of A) swelling and B) vacuolation seen in the kidneys in the total of four treatment groups.** No histopathology = 0; mild activity = 1; moderate activity = 2.

Swelling of the PCTs and DCTs showed no significant differences ( $p=0.2$ ) between the four groups, but as seen in Figure 4.16, the C/ART- and C/ART+ group varies from the C/M+ and

ART+/M+ groups. The prevalence of swelling in the C/ART- and C/ART+ group was 40% and 20%, respectively, whereas it was 60% in both the C/M+ and ART+/M+ groups.

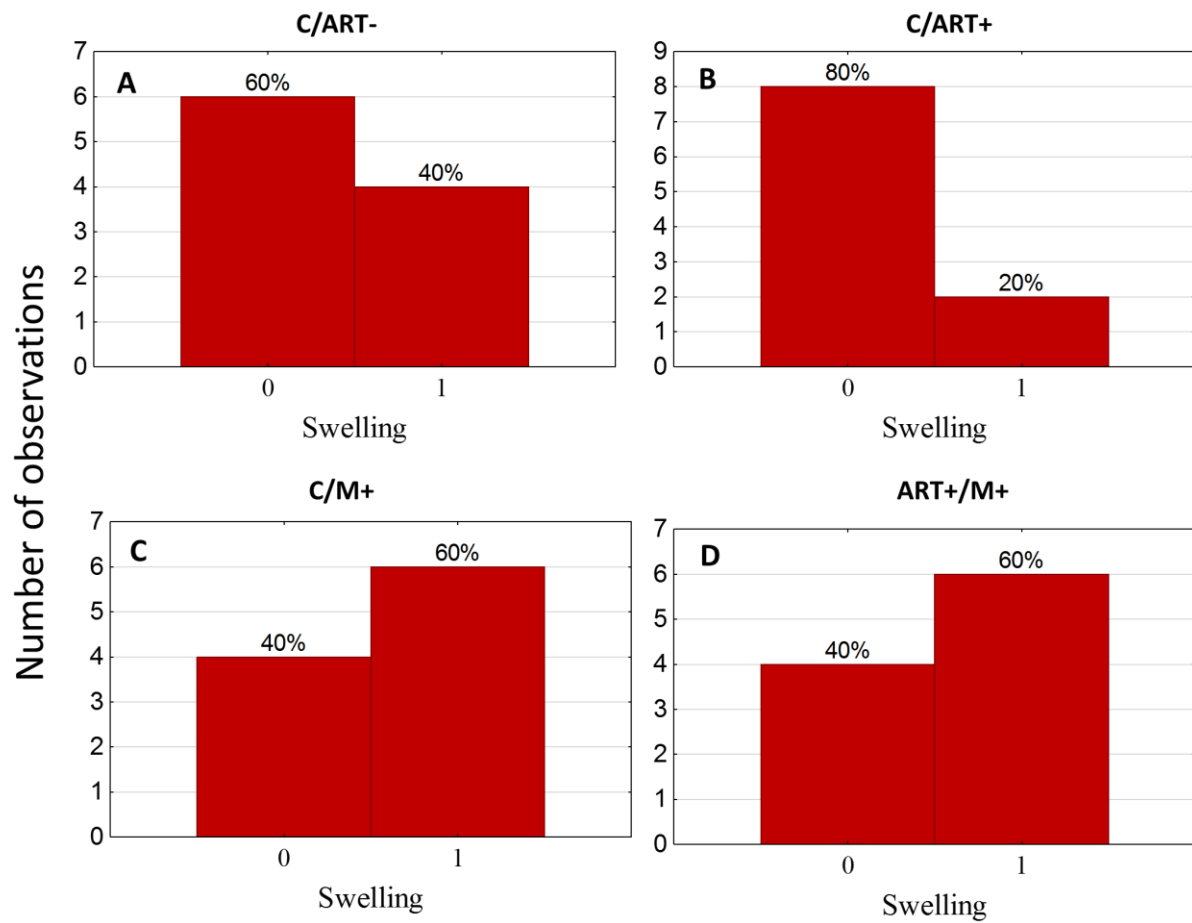


**Figure 4.16 Percentage of mild swelling seen in the kidneys did not differ significantly between the four treatment groups. A) C/ART-; B) C/ART+; C) C/M+; D) ART+/M+**

Of the 54% (21/40) affected kidneys which presented with vacuolation in the PCTs and DCTs, 50% (20/40) were classified as mild and 5% (2/40) as moderate.



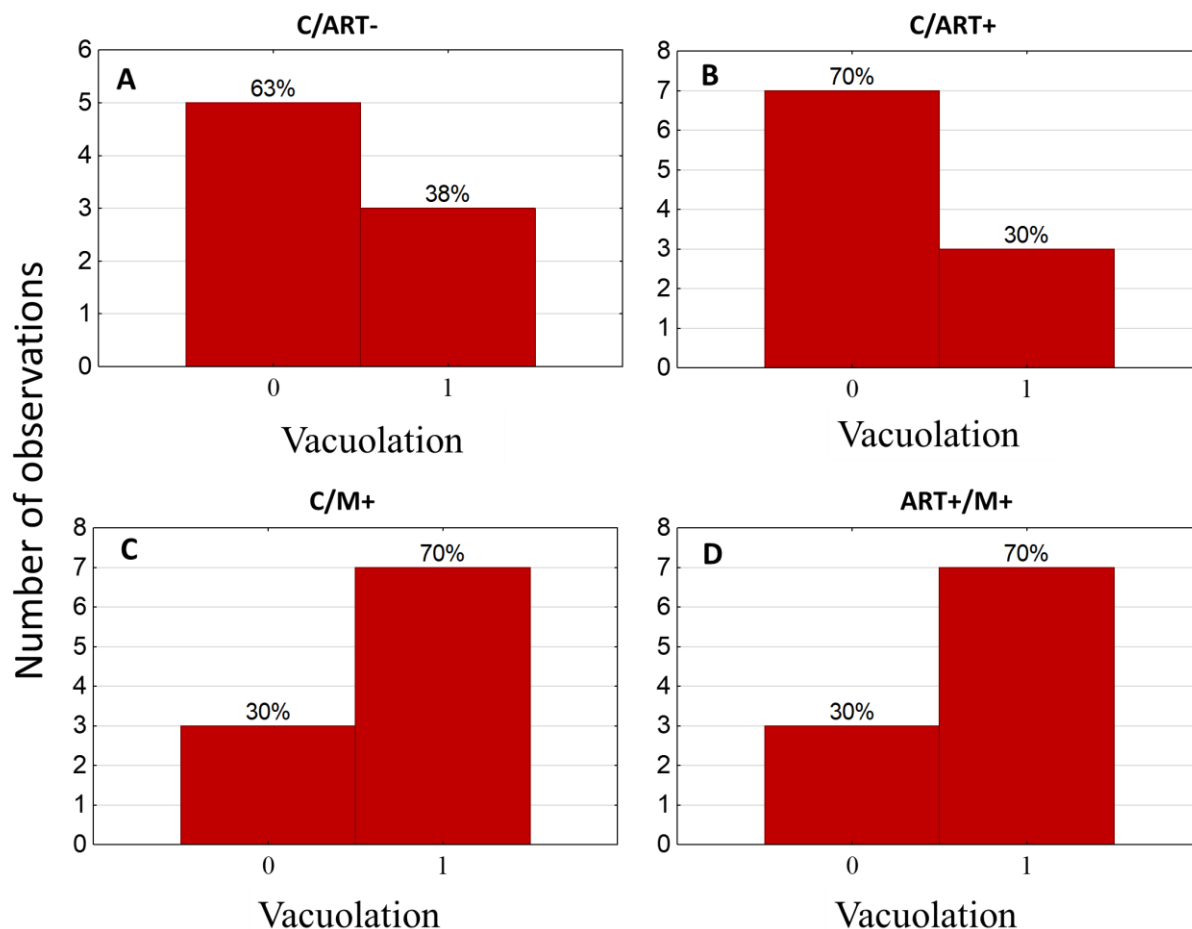


**Figure 4.17 Percentage of mild and moderate vacuolation seen in the kidneys did not differ significantly between the four treatment groups. A) C/ART-; B) C/ART+; C) C/M+; D) ART+/M+**

Vacuolation of the PCTs and DCTs showed no significant differences, but showed a trend ( $p=0.1$ ) between the four groups. Figure 4.17 shows the C/ART- and C/ART+ group varies from the C/M+ and ART+/M+ groups. The prevalence of vacuolation in the C/ART- and C/ART+ group was 38% and 30%, respectively, whereas it was 70% in both the C/M+ and ART+/M+ groups.

#### 4.4.2 Analysis of renal corpuscles with accompanying proximal convoluted tubules

The kidneys (n=40) stained with PAS were used for histomorphometric measurements of the renal corpuscle, glomerulus and proximal convoluted tubules. Figure 4.18 shows staining of the kidney with PAS to distinguish between the DCT and PCT.

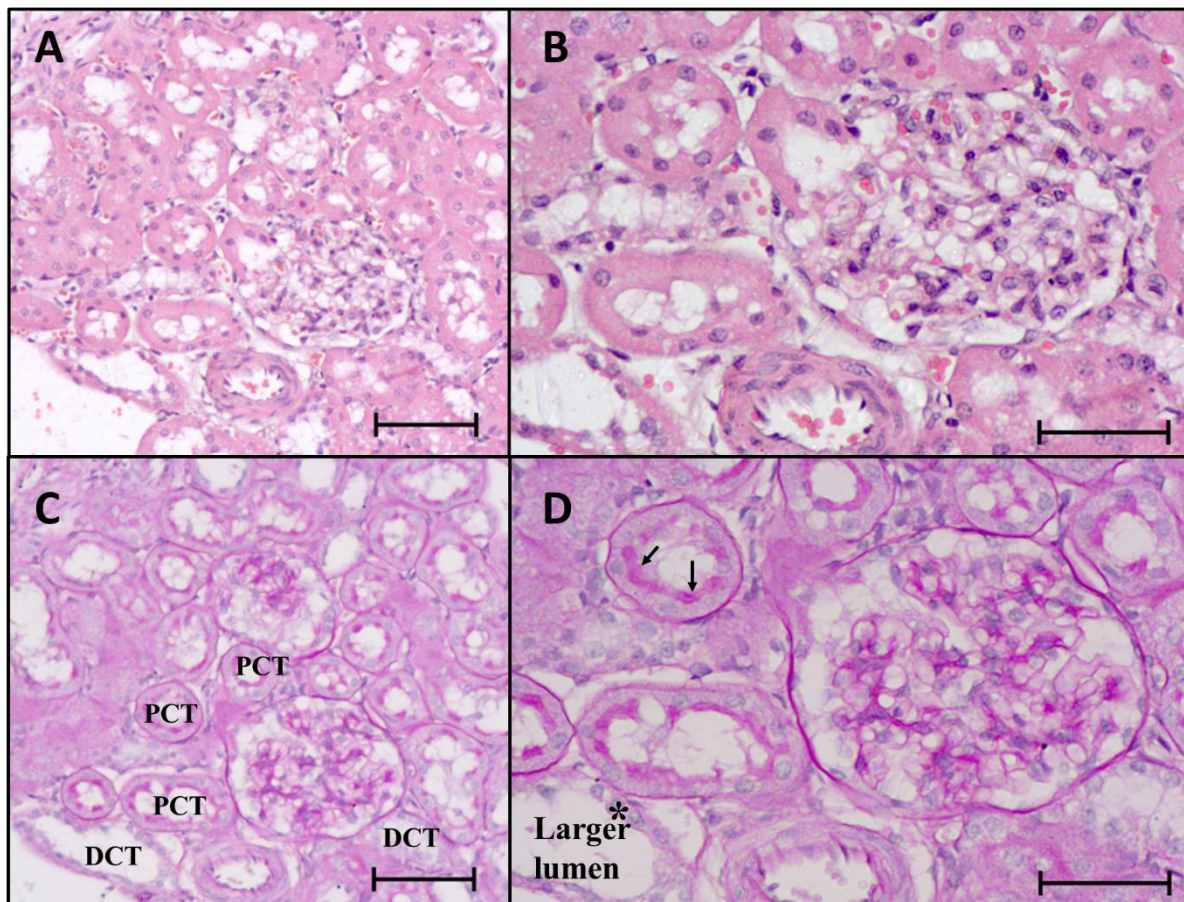


**Figure 4.18** Serial sections of slides stained with H&E and PAS. PAS distinguishes between the DCTs and PCTs. A&B shows no discernible nuclei or brush border as stained with H&E. C & D shows discernible nuclei (\*) of the DCT and the brush border (arrows) of the PCT as stained with PAS. The DCT also has a larger lumen than the PCT. A & C magnification = 100x; scale bar = 100  $\mu$ m. B & D magnification = 200x; scale bar = 100  $\mu$ m.

Each kidney was divided into three sections and the area, diameter, perimeter and renal space of 10 renal corpuscles per area with their glomeruli was measured. The area, diameter, perimeter and PCT thickness of three proximal convoluted tubules adjacent to the associated renal corpuscle was measured. A total of 300 renal corpuscles, glomeruli and renal spaces and 900 PCT's were measured per treatment group.

## 4.4.2.1 Renal corpuscle

A summary of the measurements of the renal corpuscle is outlined in Table 4.4.

**Table 4-4 Summary of the measurements of the renal corpuscle of the four treatment groups  $\pm$  SD.**

Treatment	Area ( $\mu\text{m}^2$ )	Diameter ( $\mu\text{m}$ )	Perimeter ( $\mu\text{m}$ )	Radius ( $\mu\text{m}$ )
C/ART-	<b>9381.97 <math>\pm</math> 3435.95<sup>a</sup></b>	<b>107.44 <math>\pm</math> 20.11<sup>a</sup></b>	<b>355.76 <math>\pm</math> 64.76<sup>a</sup></b>	<b>53.72 <math>\pm</math> 10.05<sup>a</sup></b>
C/ART+	<b>7672.45 <math>\pm</math> 2989.24<sup>b</sup></b>	<b>97.08 <math>\pm</math> 18.59<sup>b</sup></b>	<b>323.23 <math>\pm</math> 60.17<sup>b</sup></b>	<b>48.54 <math>\pm</math> 9.30<sup>b</sup></b>
C/M+	<b>8239.66 <math>\pm</math> 2879.72<sup>b</sup></b>	<b>100.12 <math>\pm</math> 19.89<sup>b</sup></b>	<b>333.74 <math>\pm</math> 64.27<sup>b</sup></b>	<b>50.06 <math>\pm</math> 9.94<sup>b</sup></b>
ART+/M+	8390.83 $\pm$ 3528.32 <sup>ab</sup>	101.68 $\pm$ 20.40 <sup>ab</sup>	336.70 $\pm$ 66.84 <sup>ab</sup>	<b>50.57 <math>\pm</math> 10.45<sup>b</sup></b>
Mean	8421.23 $\pm$ 3274.84	101.58 $\pm$ 20.09	337.36 $\pm$ 66.84	50.72 $\pm$ 10.11

Statistical significance ( $p < 0.05$ ) is indicated by a bold font and different letters of the alphabet. If the same letter/s is/are present above each of the groups, there were no significant differences.

The area of the renal corpuscle differed significantly ( $p=0.02$ ) between all treatment groups (Figure 4.19A). Specifically, the C/ART- differed highly significantly from the C/ART+ ( $p<0.01$ ) and significantly from the C/M+ ( $p=0.03$ ) group. A trend ( $p=0.06$ ) was seen between the C/ART- and ART+/M+ groups. The renal corpuscle area of the C/ART- group was the highest at  $9381.97 \mu\text{m}^2$  and the C/ART+ group the lowest at  $7672.45 \mu\text{m}^2$ .

The diameter of the renal corpuscle differed highly significantly ( $p=0.01$ ) between all treatment groups (Figure 4.19B). Post hoc analysis showed that the C/ART- group's renal corpuscle diameter was the highest at  $107.44 \mu\text{m}$  and differed highly significantly from the C/ART+ ( $p<0.01$ ) group, which had the lowest renal corpuscle diameter of  $97.08 \mu\text{m}$ . The C/ART- group differed significantly from the C/M+ ( $p=0.02$ ) group, whereas a trend ( $p=0.07$ ) was seen between the C/ART- and ART+/M+ groups.

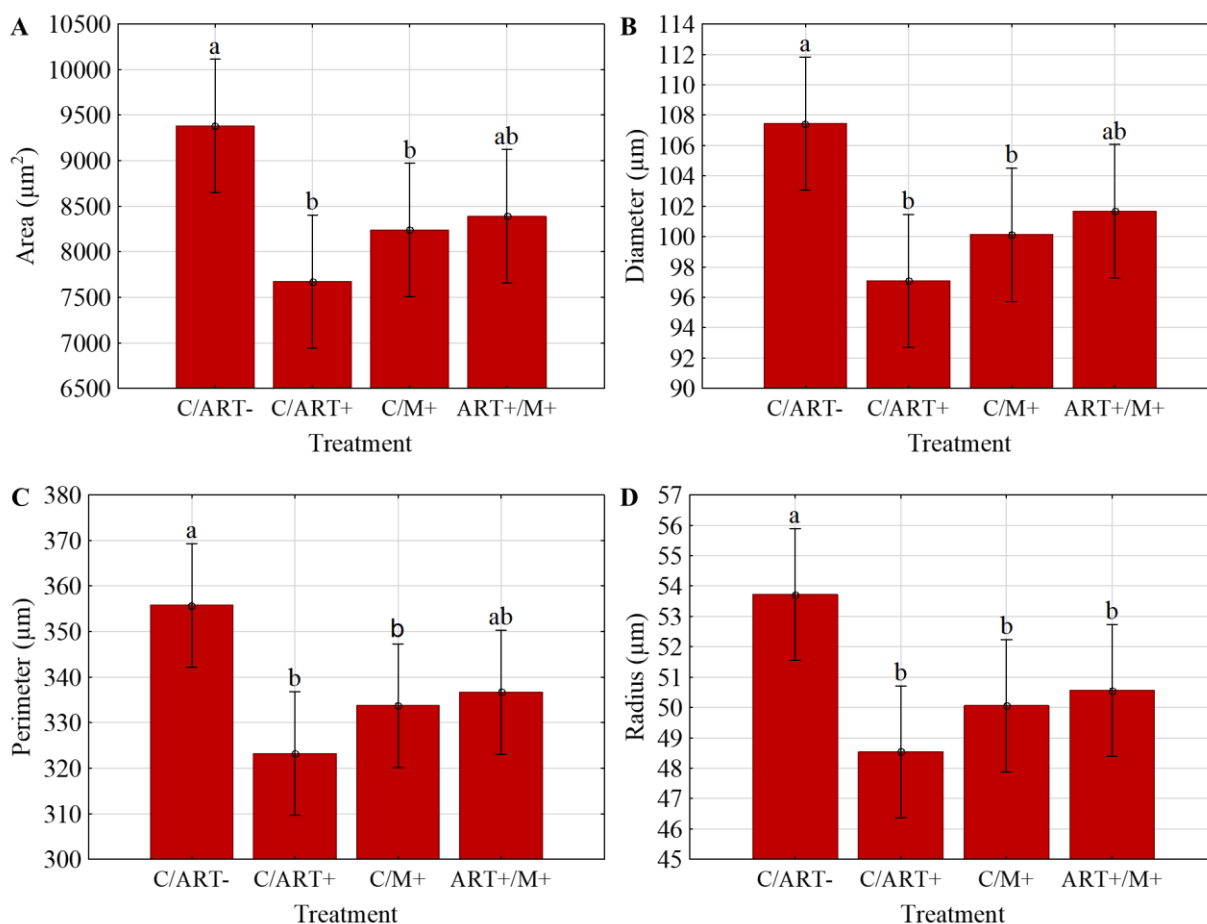


**Figure 4.19** The area, diameter, perimeter and radius of the renal corpuscle differed significantly between the four treatment groups. Statistical significance ( $p < 0.05$ ) is indicated by different letters of the alphabet. If the same letter/s is/are present above each of the groups, there were no significant differences.

The perimeter of the renal corpuscle differed highly significantly ( $p=0.01$ ) between the four treatment groups (Figure 4.19C). Post hoc tests showed that the C/ART- group had the highest renal corpuscle perimeter of  $355.76 \mu\text{m}$  and differed highly significantly ( $p<0.01$ ) from the C/ART+ group with a renal corpuscle perimeter of  $323.23 \mu\text{m}$  and from the C/M+ group ( $0.03$ ), which had a renal corpuscle perimeter of  $333.74 \mu\text{m}$ .

The radius of the renal corpuscle differed highly significantly ( $p=0.01$ ) between the four treatment groups (Figure 4.19D). The C/ART- group, which had the highest renal corpuscle radius, differed significantly from the C/ART+ ( $p<0.01$ ), C/M+ ( $p=0.02$ ) and ART+/M+ ( $p=0.04$ ) groups.

## 4.4.2.2 Glomerulus

A summary of the measurements of the glomerulus is outlined in Table 4.5.

**Table 4-5 Summary of the measurements of the glomeruli of the four treatment groups  $\pm$  SD**

Treatment	Area ( $\mu\text{m}^2$ )	Diameter ( $\mu\text{m}$ )	Perimeter ( $\mu\text{m}$ )	Radius ( $\mu\text{m}$ )
C/ART-	<b>5512.37 <math>\pm</math> 2519.59<sup>a</sup></b>	<b>81.41 <math>\pm</math> 19.83<sup>a</sup></b>	363.38 $\pm$ 120.47 <sup>a</sup>	<b>40.70 <math>\pm</math> 9.91<sup>a</sup></b>
C/ART+	<b>4670.64 <math>\pm</math> 2079.68<sup>b</sup></b>	<b>75.25 <math>\pm</math> 16.91<sup>b</sup></b>	346.48 $\pm$ 103.19 <sup>a</sup>	<b>37.62 <math>\pm</math> 8.46<sup>b</sup></b>
C/M+	<b>5519.37 <math>\pm</math> 2370.49<sup>a</sup></b>	<b>81.75 <math>\pm</math> 18.59<sup>a</sup></b>	354.19 $\pm$ 105.50 <sup>a</sup>	<b>40.88 <math>\pm</math> 9.29<sup>a</sup></b>
ART+/M+	<b>5501.12 <math>\pm</math> 2505.78<sup>a</sup></b>	<b>81.20 <math>\pm</math> 19.63<sup>a</sup></b>	357.73 $\pm$ 113.90 <sup>a</sup>	<b>41.28 <math>\pm</math> 13.44<sup>a</sup></b>
Mean	5300.86 $\pm$ 2400.28	79.90 $\pm$ 18.94	355.44 $\pm$ 111.01	40.12 $\pm$ 10.54

Statistical significance ( $p < 0.05$ ) is indicated by a bold font and different letters of the alphabet. If the same letter/s is/are present above each of the groups, there were no significant differences.

The area of the glomerulus showed a trend, but did not differ significantly ( $p=0.06$ ) between the four treatment groups (Figure 4.20A). Post doc tests, however, showed that the C/ART+ group differed significantly with the C/ART- group ( $p=0.03$ ), C/M+ ( $p=0.03$ ) and ART+/M+ ( $p=0.03$ ) groups. The C/ART+ group had the lowest glomerular area of  $4670.64 \mu\text{m}^2$ , whereas the C/M+ group had the highest of  $5519.37 \mu\text{m}^2$ .

The diameter of the glomerulus showed a trend, but did not differ significantly ( $p=0.09$ ) between the four treatment groups (Figure 4.20B). Post doc tests, however, showed that the C/ART+ group differed significantly with the C/ART- group ( $p=0.04$ ), C/M+ ( $p=0.03$ ) and ART+/M+ ( $p=0.05$ ) groups. The C/ART+ group had the lowest glomerular diameter of  $75.25 \mu\text{m}$ , whereas the C/M+ group had the highest of  $81.75 \mu\text{m}$ .

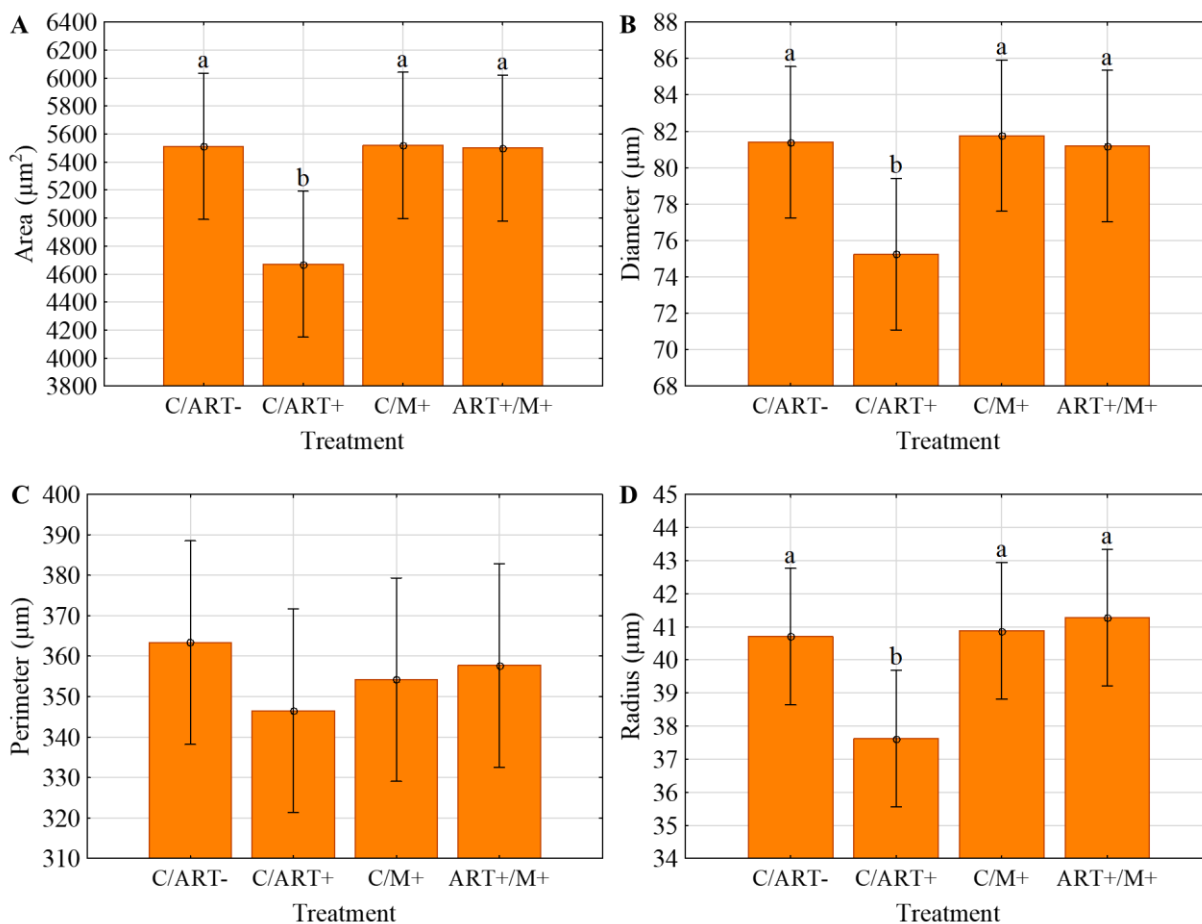


**Figure 4.20** The area, diameter, perimeter and radius of the glomerulus differed significantly between the four treatment groups. Statistical significance ( $p < 0.05$ ) is indicated by different letters of the alphabet. If the same letter/s is/are present above each of the groups, there were no significant differences.

The perimeter of the glomerulus did not differ significantly ( $p=0.8$ ) between the four treatment groups (Figure 4.20C). The C/ART- group had the largest perimeter and the C/ART+ group the smallest of 363.38 µm and 346.48 µm, respectively. The perimeter mean of the glomeruli between the four groups was 355.44 µm.

The glomerular radius showed a trend ( $p=0.06$ ), but was not statistically different for the four treatment groups (Figure 4.20D). However, statistical difference was seen between the C/ART+ group and the C/ART- ( $p=0.04$ ), C/M+ ( $p=0.03$ ) and ART+/M+ ( $p=0.02$ ) groups. The C/ART+ group had the smallest radius of 37.62 µm and the ART+/M+ group the largest of 41.28 µm.

#### 4.4.2.3 Proximal convoluted tubules

The area, diameter, perimeter, radius and thickness of three PCT's adjacent to the measured renal corpuscle was measured in all animals. Only PCT's which were cut cross-sectionally were selected to enable an accurate depiction of the tubule thickness and luminal properties. The PCT area with the lumen (LPCT) minus the luminal area was used to calculate the PCT area (Table 4.6).

**Table 4-6 Summary of the measurements of the LPCT and the PCT of the four treatment groups  $\pm$  SD**

Treatment	LPCT Area ( $\mu\text{m}^2$ )	Diameter ( $\mu\text{m}$ )	Perimeter ( $\mu\text{m}$ )	Radius ( $\mu\text{m}$ )
<b>Proximal convoluted tubules</b>				
C/ART-	<b>2199.64 <math>\pm</math> 705.79<sup>a</sup></b>	<b>52.28 <math>\pm</math> 8.25<sup>a</sup></b>	<b>173.75 <math>\pm</math> 29.09<sup>a</sup></b>	<b>26.14 <math>\pm</math> 4.12<sup>a</sup></b>
C/ART+	<b>1790.34 <math>\pm</math> 528.78<sup>b</sup></b>	<b>47.28 <math>\pm</math> 6.62<sup>b</sup></b>	<b>157.86 <math>\pm</math> 23.39<sup>b</sup></b>	<b>23.64 <math>\pm</math> 3.31<sup>b</sup></b>
C/M+	1944.93 $\pm$ 578.00 <sup>ab</sup>	49.29 $\pm$ 6.82 <sup>ab</sup>	162.90 $\pm$ 23.79 <sup>ab</sup>	24.65 $\pm$ 3.41 <sup>ab</sup>
ART+/M+	1998.76 $\pm$ 823.41 <sup>ab</sup>	49.61 $\pm$ 8.74 <sup>ab</sup>	165.28 $\pm$ 29.82 <sup>ab</sup>	25.32 $\pm$ 8.58 <sup>ab</sup>
Mean	1983.52 $\pm$ 684.55	49.62 $\pm$ 7.86	164.95 $\pm$ 27.29	24.94 $\pm$ 5.40
<b>Proximal convoluted tubule area minus lumen</b>				
	Area ( $\mu\text{m}^2$ )			
C/ART-	<b>1769.15 <math>\pm</math> 578.80<sup>a</sup></b>			
C/ART+	<b>1485.03 <math>\pm</math> 450.80<sup>b</sup></b>			
C/M+	<b>1548.56 <math>\pm</math> 518.99<sup>b</sup></b>			
ART+/M+	1614.71 $\pm$ 638.80 <sup>ab</sup>			
Mean	1604.44 $\pm$ 561.12			

Statistical significance ( $p < 0.05$ ) is indicated by a bold font and different letters of the alphabet. If the same letter/s is/are present above each of the groups, there were no significant differences.

The LPCT area (Figure 4.21A) differed significantly ( $p=0.04$ ) between the four groups. Post hoc analysis showed that the C/ART- group and C/ART+ groups' LPCT area differed highly significantly ( $p=0.01$ ). The C/ART- group had a PCT area of 2199.64  $\mu\text{m}^2$  and the C/ART+ group a PCT area of 1790.34  $\mu\text{m}^2$ .

The diameter of the total PCT and its lumen differed significantly ( $p=0.04$ ) between the four groups (Figure 4.21B). Specifically, the C/ART- and C/ART+ groups had highly significant differences ( $p<0.01$ ) between them with diameters of  $52.28 \mu\text{m}$  and  $47.28 \mu\text{m}$ , respectively.

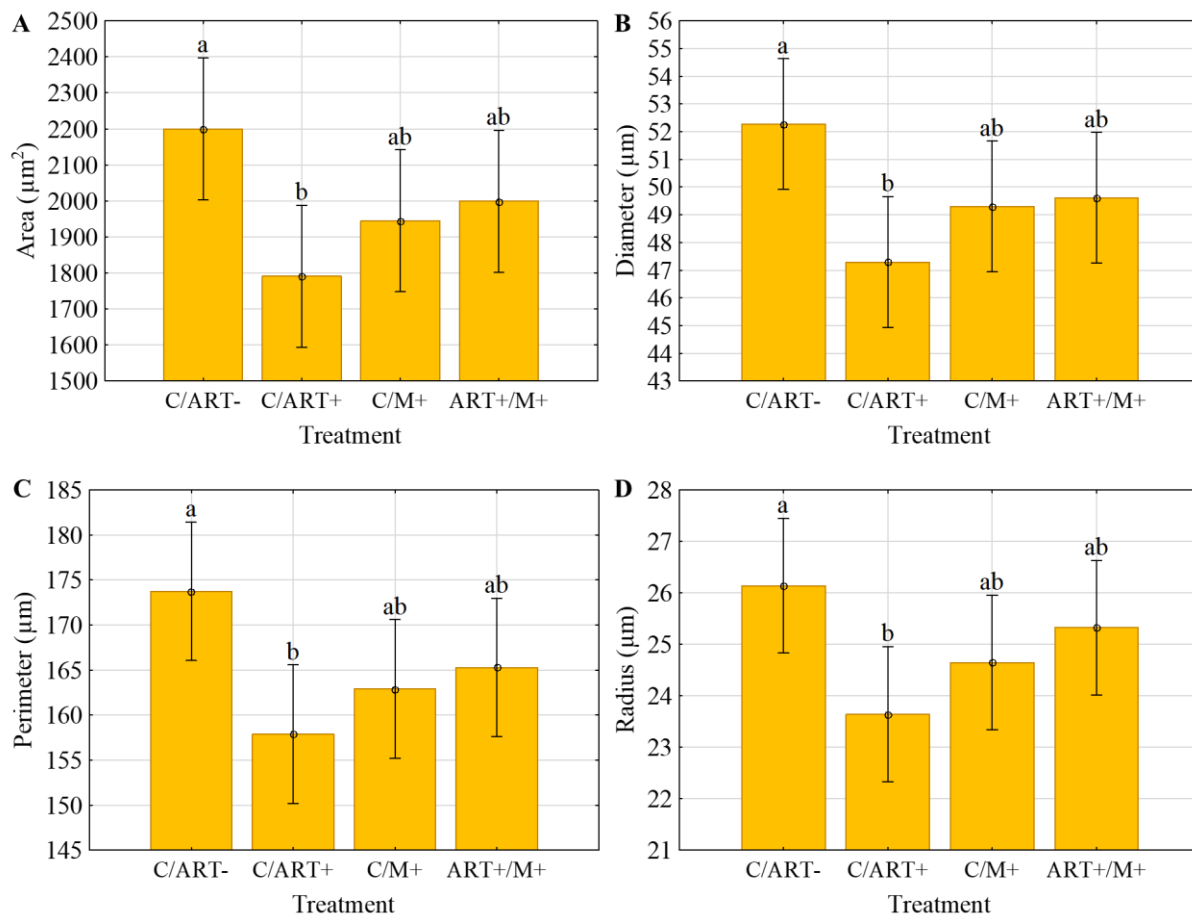


**Figure 4.21 The area, diameter, perimeter and radius of the renal corpuscle differed significantly between the four treatment groups.** Statistical significance ( $p < 0.05$ ) is indicated by different letters of the alphabet. If the same letter/s is/are present above each of the groups, there were no significant differences.

The PCT's of the C/ART- group had the largest perimeter at  $173.75 \mu\text{m}$ , whereas the C/ART+ group had the lowest at  $157.86 \mu\text{m}$  (Figure 4.21C). The perimeter of the PCT's of the four treatment groups differed significantly ( $p=0.04$ ). Post hoc analysis showed the C/ART- and C/ART+ groups had highly significant differences ( $p=0.01$ ) in the perimeter of their PCT's.



The radius of the PCT's showed a trend ( $p=0.06$ ) between the four treatment groups (Figure 4.21D). Highly significant difference ( $p=0.01$ ) was observed in the radius between the C/ART- and C/ART+ groups with  $26.14\ \mu\text{m}$  and  $23.64\ \mu\text{m}$  respectively.

The area of the PCT was measured by subtracting the LPCT area with the luminal area. The four treatment groups showed statistical difference ( $p=0.04$ ) between them with the C/ART- group being the largest at  $1769.15\ \mu\text{m}^2$  and the C/ART+ group the smallest at  $1485.03\ \mu\text{m}^2$  (Figure 4.22).

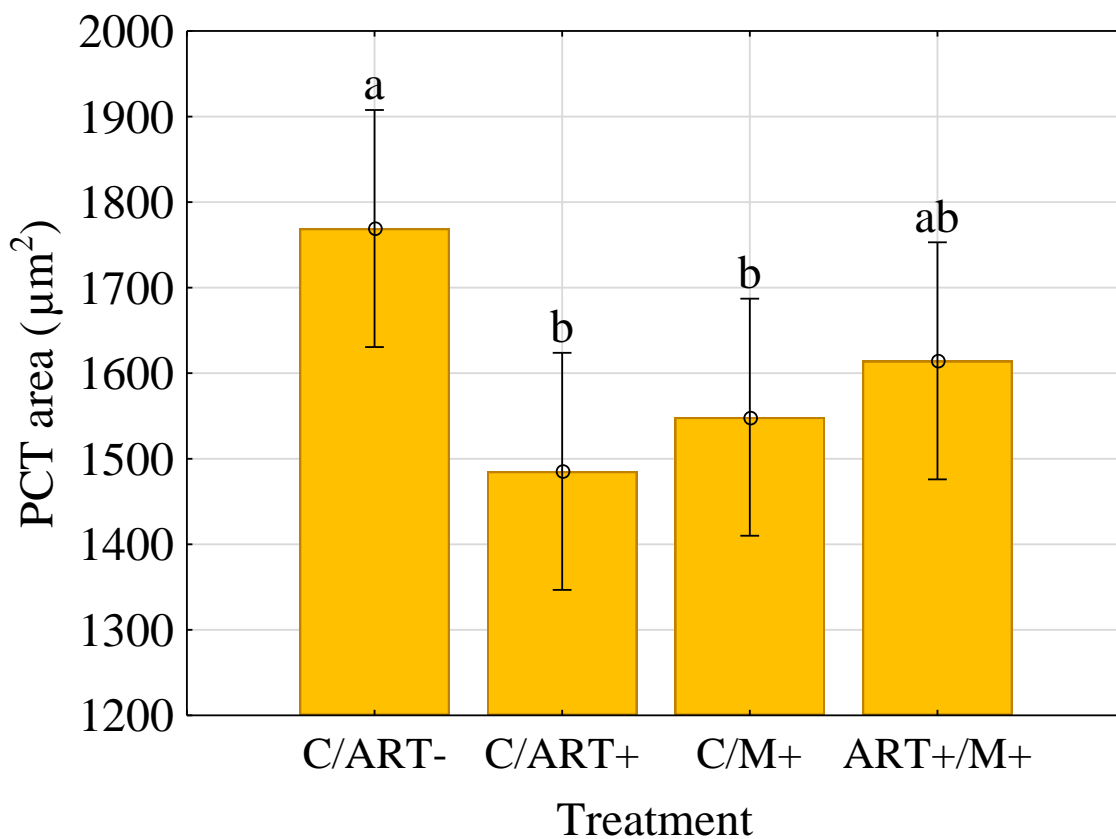


**Figure 4.22 Proximal tubule area differed significantly between the four treatment groups.** Statistical significance ( $p < 0.05$ ) is indicated by different letters of the alphabet. If the same letter/s is/are present above each of the groups, there were no significant differences.

Highly significant difference ( $p < 0.01$ ) was seen between the C/ART- and C/ART+ groups. The C/ART- and C/M+ groups also had significant difference ( $p=0.03$ ) in the PCT area.

#### 4.4.2.4 Renal space

The renal space (Table 4.7) was calculated by subtracting the glomerular area from the corpuscle area.

**Table 4-7 Summary of the measurements of the renal space of the four treatment groups  $\pm$  SD**

Treatment	Area ( $\mu\text{m}^2$ )
<b>Renal space</b>	
C/ART-	<b>3869.60 <math>\pm</math> 1463.54<sup>a</sup></b>
C/ART+	<b>3001.81 <math>\pm</math> 1408.68<sup>b</sup></b>
C/M+	<b>2720.29 <math>\pm</math> 1175.45<sup>b</sup></b>
ART+/M+	<b>2889.71 <math>\pm</math> 1525.16<sup>b</sup></b>
Mean	3120.35 $\pm$ 1463.54

Statistical significance ( $p < 0.05$ ) is indicated by a bold font and different letters of the alphabet. If the same letter/s is/are present above each of the groups, there were no significant differences.

Highly significant ( $p < 0.01$ ) difference was seen in the renal space between the four treatment groups (Figure 4.23).

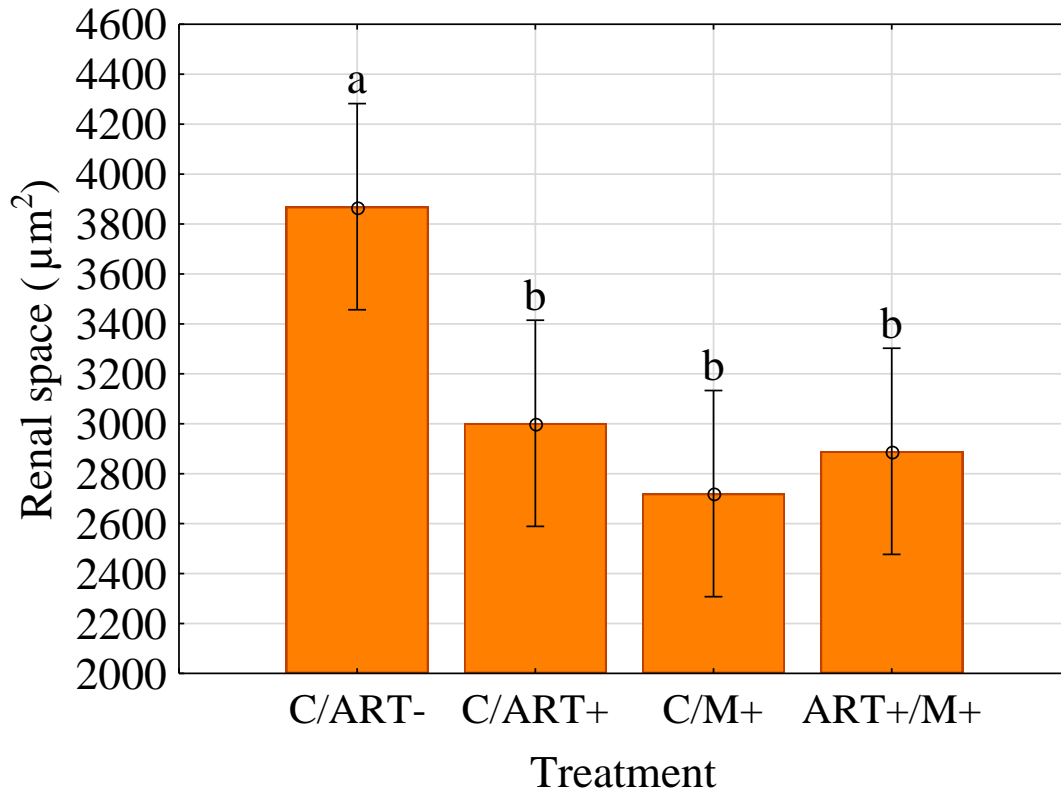


**Figure 4.23 The renal space differed significantly between the four treatment groups.**

Statistical significance ( $p < 0.05$ ) is indicated by different letters of the alphabet. If the same letter/s is/are present above each of the groups, there were no significant differences.

The renal space of the C/ART- group differed highly significantly with the C/ART+ ( $p < 0.01$ ), C/M+ ( $p < 0.01$ ) and ART+/M+ ( $p < 0.01$ ) groups (Figure 4.23). The C/ART- group had the largest renal space of  $3120.35 \mu\text{m}^2$ . The C/M+ group had the lowest renal space of  $2720.29 \mu\text{m}^2$ , followed by the ART+/M+ group of  $2889.71 \mu\text{m}^2$ .

## CHAPTER 5 DISCUSSION

The body mass of rats differs greatly between rats of different strains and stock, but they usually weigh between 500 g and 600 g (Hofstetter *et al.*, 2006). In the present study, the body mass of each rat (8 weeks old) was between 180 g and 200 g when treatment was initiated. After 8 weeks of treatment, the mean body mass of all the rats were 297.2 g, with no significant differences between the four treatment groups. Shikuma *et al.* (2004) found that HIV positive patients on HAART with very low cluster of differentiation (CD) 4 immune cell counts, and thus higher immune compromise, had a larger increase in body weight than patients who have been previously exposed to HAART and thus have a higher CD4 count. It was concluded that an increase in body mass is higher in patients with a higher virological count and immunological compromise. Furthermore, a significant increase in weight was only observed after 16 weeks of HAART (Shikuma *et al.*, 2004). In the present study, the treatment was administered for eight weeks and no known immune compromise was present due to the HIV negative rat model, thus weight gain was not significant with administration of TDF/EFV/FTC.

The melatonin group had the highest body mass in the present study, although melatonin has shown to decrease body mass in obese rats or rats on a high fat diet (HFD) (Wolden-Hanson *et al.*, 2000; Puchalski *et al.*, 2003; Hussein *et al.*, 2007). This decrease is accompanied by a decrease in plasma insulin levels, triglycerides and glucose (Wolden-Hanson *et al.*, 2000; Ríos-Lugo *et al.*, 2010). In the absence of a HFD in the present study, no significant increase in body mass or  $\beta$ -cell area were observed in the present study.

The pancreatic islets were successfully labelled with monoclonal anti-insulin and polyclonal anti-glucagon, respectively. The cells in the islets positive for glucagon ( $\alpha$ -cells) labelled brown and the cells positive for insulin ( $\beta$ -cells) red. As seen in Migrenne (2011) and Kierszenbaum (2013), the cells positive for insulin and the cells positive for glucagon, in the present study, were observed in the core and mantle, respectively. In addition, the  $\beta$ -cell area was significantly larger than the  $\alpha$ -cell area in all of the treatment groups, as described by King *et al.* (2007) and Kierszenbaum (2013) as the standard relationship of  $\beta$ -cell and  $\alpha$ -cell area ratio.

Rat pancreatic islets are composed of 60-85%  $\beta$ -cells and 15-25%  $\alpha$ -cells as originally described by Erlandsen *et al.* (1976) and Wieczorek *et al.* (1998). In the present study, the  $\beta$ -

cells comprised 33-36% of the pancreatic islets, with no significant differences between the four treatment groups. Similarly, the  $\alpha$ -cells in the present study comprised 6-7% of the total pancreatic islet area, with no significant differences between the four treatment groups. The duodenal region of the rat pancreas has been described to be glucagon-poor, as opposed to the splenic region (Baetens *et al.*, 1979; Dolensek *et al.*, 2015). In the present study, the pancreatic islets of the duodenal lobe of the pancreas were analysed, which may explain the smaller percentages of glucagon and insulin expression in the islets. Furthermore, King *et al.* (2007) showed that  $\beta$ -cells are not dependant on non- $\beta$ -cells for optimal functioning as seen in islet transplantation of mice.

It has been well-described that pancreatic islets of various mammals, including rats and humans, express melatonin trans-membrane receptors MT1 and MT2 (Peschke *et al.*, 2007; Ramracheya *et al.*, 2008; Bähr *et al.*, 2012; Peschke *et al.*, 2013). According to Bähr *et al.* (2011), melatonin stimulates glucagon secretion *in vivo* and *in vitro* in Wistar rats by inhibiting insulin secretion and stimulating glucagon synthesis (Farhadi *et al.*, 2015). In the present study, the  $\alpha$ -cell area was significantly higher in the melatonin group compared to the group subjected to cART, which indicates that melatonin stimulated glucagon expression in the pancreatic islets.

No significant difference in insulin expression was seen between the four treatment groups. The latter contradicts studies done by la Fleur *et al.* (2001), Peschke *et al.*, (2006) and Peschke *et al.* (2007), which indicates that melatonin inhibits insulin secretion. However, in the present study, the number of pancreatic islets per mm<sup>2</sup> were significantly more in the melatonin group than in both the control and the experimental groups. The groups affected suggest that melatonin treatment stimulates a higher number of pancreatic islets, whereas cART has no significant effect on the number of pancreatic islets. It is possible that melatonin stimulates pancreatic islet production and thus the ability to secrete glucagon and insulin, but not necessarily the hormones themselves.

Blümer *et al.* (2008) and van Vonderen *et al.* (2010) concluded that NRTIs affect glucose metabolism and induce insulin resistance humans, which in turn will increase insulin levels in the body. In the present study, no significant differences were seen in groups subjected to cART in neither glucagon nor insulin expression. This may be due to the treatment only being administered for eight weeks, which is equivalent to approximately 5-6 years for humans

(Adami Andreollo *et al.*, 2012). The specific combination of TDF/EFV/FTC may not induce insulin resistance and alteration in glucose metabolism in patients as early (within three months) or aggressively as zidovudine and lamivudine (Blümer *et al.*, 2008; Paik and Kotler, 2011).

No histopathology was observed in the pancreas of any of the four treatment groups, which is contradicting to studies conducted by Muñoz-Casares *et al.* (2006), Barbosa *et al.* (2013) and Oliveira *et al.* (2014). Barbosa *et al.* (2013) describes pancreatitis, steatosis and apoptosis in the pancreas of HIV positive patients on cART. In the present study, no lymphocyte infiltration, oedema, necrosis, haemorrhage, apoptosis or necrosis were observed in the exocrine part of the pancreata, which showed that the TDF/EFV/FTC combination did not induce pancreatitis or cellular injury after 8 weeks of treatment in rats.

Various authors have commented on the protective effects of melatonin on the exocrine and endocrine pancreas (Baydas *et al.*, 2002; Picinato *et al.*, 2002b; Muñoz-Casares *et al.*, 2006; Radogna *et al.*, 2010). These studies describe the action of melatonin during oxidative stress, necrosis, acute pancreatitis and inflammatory conditions. In the present study, the ameliorating effects of melatonin could not be observed as cART did not induce any histologically observable changes on tissue level.

Most of the changes in histopathology were reversible (Haschek *et al.*, 2009a; Cha *et al.*, 2016) or may have been incidental findings due to fixation, however, it was included for complete disclosure of the findings. Formaldehyde derivatives such as 4% PFA has proven to be effective in preserving tissue for histological examination (Hassel and Hand, 1974). As all samples were collected simultaneously in the present study, a fixative which is appropriate for multiple organs and purposes (H&E, special staining and IHC) had to be used for all organs.

All tissue samples were immediately immersed in 4% PFA after the specific rat was euthanised. Although extreme care was taken to ensure that proper fixation took place, some control animals showed histopathology, which might indicate that autolysis took place. Multiple researchers were collecting tissue from each rat in order to reduce the number of animals sacrificed for research purposes as stated by the three R's of animal ethics (Prescott and Lidster, 2017). This caused suboptimal waiting periods for tissue collection. However, all

samples were treated consistently, and thus statistically significant changes observed are most likely treatment dependant or incidental.

In the present study, proteinaceous material was seen in the pancreatic ducts, which was noted to be normal pancreatic enzymes produced by the zymogen granules of the acinar cells (Kierszenbaum, 2007). Some pancreata had included lymph tissue, which appeared mildly and moderately active, respectively. These observations were in the cART, melatonin and experimental groups, with no statistical significance between the groups. As lymph nodes are sensitive to both endogenous and exogenous factors, the cause of the activity is hard to determine (Ibraheem *et al.*, 2013). In addition, no inflammatory cells or necrosis was observed, neither did the lymph tissue penetrate the parenchyma and thus it is likely that the lymph tissue activity observed in the present study is incidental and due to exogenous factors (Ibraheem *et al.*, 2013).

In the livers observed in the present study, very mild hepatocyte changes were seen, although none of the observations were significant. Mild granular appearance and vacuolation of the hepatocytes were seen in all treatment groups, but were most prevalent in the control group, which indicates that autolysis may have been initiated. As vacuolation of hepatocytes causes a granular appearance of the tissue (Haschek *et al.*, 2009a), the granular appearance observed in the present study may be due to artefactual vacuolation. Additionally, one rat in the melatonin group showed mild lymphocyte infiltration around the portal areas, which may be incidental as it was only observed in one animal.

The findings in the present study does not correspond with hepatic steatosis, cellular injury, nodular hyperplasia, fibrosis and hepatitis as described by Sulkowski (2004), Chang and Schiano (2007), Núñez (2010), Neuman *et al.* (2013) and Gallien *et al.* (2015) in HIV positive patients receiving cART. It is possible that the immune compromise of HIV enhances possible side effects or histopathology as it allows for opportunistic infections to manifest (Kim and Rutstein, 2010). Similar to the pancreas, melatonin had no effect on the histology of the liver as there was no histologically significant changes induced by cART.

Furthermore, liver enzyme tests were done to determine the hepatocellular integrity of the liver. Elevated AST and ALT serum levels indicate membrane permeability, cellular degeneration or cellular necrosis, which is indicative of hepatotoxicity (Haschek, *et al.*, 2009b). No significant

differences were seen in serum AST or ALT levels between the four treatment groups. The normal AST value in male Sprague Dawley rats range between 74-143 U/L and the normal ALT value range between 18-45 U/L (Giknis and Clifford, 2008). In the present study, the AST and ALT values ranged between 161-218 U/L and 54-68 U/L, respectively. The values in the present study are higher than reported as the standard, but similar to a study conducted by Alarifi *et al.* (2012), who measured AST and ALT values of 143-224 U/L and 34-61 U/L, respectively, in control albino Wistar rats.

Mild significant elevations (1-3 times the normal) in AST and ALT may indicate, non-alcoholic steatohepatitis (NASH), drug toxicity or myositis in humans (Thapa and Walia, 2007). However, these conditions are highly unlikely to be the cause of elevated liver enzyme levels in the present study, due to the insignificant differences in AST and ALT between the treatment groups. According to Haschek *et al.* (2009), female B6C3F1 mice which received oral gavage had a significantly higher ALT value than mice that were not gavaged. In the present study, the rats received oral gavage, which may have caused an increase in liver enzyme values. The normal AST and ALT values indicate that no significant hypoxia, fatty change, necrosis or liver injury were induced by cART treatment or melatonin supplementation.

Similarly, no significant difference was seen in the AST/ALT ratio between the four treatment groups. However, the ratio of AST/ALT was higher than 1 in all treatment groups, which indicates chronic liver disease (CLD) observed as cirrhosis and fibrosis on tissue level (Parise *et al.*, 2006; Thapa and Walia, 2007; Nsiah *et al.*, 2011). Furthermore, a decrease in ALT specifically may indicate pyridoxine deficiency (Thapa and Walia, 2007). In the present study, the high ratio of approximately 3 is most likely due to the above average values of both AST and ALT. Liver injury is also highly unlikely in the present study, as no fibrosis or cirrhosis was observed with the histopathology analysis. Bilirubin, haemoglobin and lipaemia tests were conducted to determine interferences in the sample values of AST and ALT (Glick *et al.*, 1986; Thapa and Walia, 2007).

In the present study, the mean haemoglobin value of the control group was 50.9 g/dl, which is much higher than the reported range of 13.7-17.6 g/dl for laboratory rats under anaesthesia (Car *et al.*, 2006; Giknis and Clifford, 2008). Increased haemoglobin in the blood may be indicative of haemolysis of the red blood cells (RBCs). This rupturing of RBCs elevates AST, ALT and bilirubin values of liver enzyme tests (Car *et al.*, 2006). Bilirubin values should be



between 0.10 mg/dl and 0.21 mg/ dl in rats under anaesthesia (Car *et al.*, 2006; Giknis and Clifford, 2008). In the present study, all samples with significant haemolysis was discarded, although the abnormally high haemoglobin values in all four treatment groups, may still have affected the AST and ALT values reported. This is, however, unlikely due to the bilirubin values, which was < 0.21 mg/dl in all the blood samples in the present study.

Patients with HIV have significantly lower haemoglobin values as the disease progresses, which could lead to anaemia (Obirikorang and Yeboah, 2009). In the present study, the group which was subjected to cART had a significantly higher haemoglobin value than the control group. This indicates that cART may not only restore haemoglobin levels in anaemic HIV positive patients (Johannessen *et al.*, 2011; Kibaru *et al.*, 2015), but also increases haemoglobin in the absence of HIV in a rat model. Although no significant difference was observed in the haemoglobin values of the melatonin group compared to the control group in the present study, previous research has indicated that melatonin increases haemoglobin levels in animals and humans (Hlutkin and Zinchuk, 2008; Ahmed and Salem, 2011). As melatonin may be transported through the blood by binding to haemoglobin, a decrease in haemoglobin may thus affect the antioxidant and hormone action of melatonin (Gilad and Zisapel, 1995).

Melatonin has shown to inhibit lipid peroxidation in the liver, by binding the free radicals that cause this lipid degradation (Sigala *et al.*, 2006). Lipaemia can be expressed as the accumulation of triglycerides and lipoprotein particles such as chylomicrons and very low density lipoprotein (VLDL), LDL and HDL in the blood (Rudel *et al.*, 1990; Nikolac, 2014). Several ARTs such as EFV and nevirapine have shown to increase various lipid parameters such as lipoprotein size and abundance in HIV positive patients. Although EFV has shown to increase hypercholesterolemia in HIV positive patients, (Fisher *et al.*, 2006; Olivero-David *et al.*, 2011) the present study showed no significant differences in the lipaemia index of the cART group.

In the present study, the melatonin group had a significant decrease in serum lipids compared to the control, which correlates with studies conducted by Sener *et al.* (2002a) and Sener *et al.* (2002b). The fore-mentioned studies in rats highlighted that melatonin scavenges free radicals generated by renal ischemia and nephrotoxicity before these radicals can degrade lipids from cell membranes (Mylonas and Kouretas, 1999; Sener *et al.*, 2002a; Sener *et al.*, 2002b).

Adjene, *et al.* (2011) found that chronic EFV administration in rats decreased kidney weight, which may have been caused by non-pathological cellular distortion or disruption or intracellular swelling. Furthermore, Adjene, *et al.* (2011) postulates that these changes are due to the cytotoxic effect of EFV. In the present study, the area, diameter, perimeter and radius of the renal corpuscles were significantly lower in both the cART and melatonin groups compared to the control group. Although EFV has shown to induce apoptosis (Eweka, 2009; Adjene *et al.*, 2011) and melatonin has been reported to modulate the immune system by inducing apoptosis (Hara *et al.*, 2013), no changes in histopathology were observed in the present study.

In the present study, the area, diameter and radius of the glomeruli was significantly lower in the cART group compared to the other three groups. Tenofovir DF may cause a decrease in eGFR due to its effects on tubular function in the absence and presence of altered glomerular structure (Post *et al.*, 2010; Squillace *et al.*, 2017). The decrease of glomerular size, in the cART group can be due to damaged podocytes as seen in herbicide poisoning in mice (Gu *et al.*, 2016). It is thus postulated that the eGFR may have been decreased in rats treated with TDF/EFV/FTC due to the compromise of glomerular structure together with possible altered tubular function in the present study.

The renal space was significantly lower in the cART, melatonin and experimental groups compared to the control. A smaller renal space can either be due to a decrease in the renal corpuscle area or an increase in the glomerular area. In the present study, both the renal corpuscle and glomerular parameters were smaller than the cART groups. It is possible that the cellular disruption of the renal corpuscles in this study were more significant than the cellular disruption of the glomeruli, which lead to the decrease in the renal space. This finding differs from Adjene *et al.* (2011) who found that a dilated renal space is associated with EFV-associated glomerulonephritis in rats. The results in the present study varies from Bellés *et al.* (2007), who reported a normal appearance of glomeruli in rats exposed to uranium-induced nephrotoxicity and melatonin. However, the study conducted by Bellés *et al.* (2007) did not conduct morphometric measurements, but evaluated the glomeruli using a semi-quantitative method. It is thus possible that changes in glomerular size as observed in the present study, using morphometric measurements, may have been overlooked by Bellés *et al.* (2007).

In the present study, the LPCT area (PCT area plus lumen), diameter, perimeter and radius of the PCTs was significantly lower in the cART group compared to the control. Degeneration of

tubular cells is a characteristic of nephrotoxicity induced by cART (Jao and Wyatt, 2010; Achhra *et al.*, 2016). Thus, the smaller PCT parameters is indicative of the early stages of nephrotoxicity in the cART group, whereas no possible degradation of the PCT parameters were seen in the groups exposed to melatonin. Lipid peroxidation and protein oxidation, which leads to nephrotoxicity, may be restored by the cytoprotective role of melatonin in the kidneys (Hara *et al.*, 2001; Sener *et al.*, 2002b).

The area of the PCT minus lumen (PCT) was significantly lower in the cART and melatonin groups in the present study compared to the control. This is suggestive of a larger lumen, which may have been caused by luminal ectasia (dilation of a tubular structure) as seen in Labarga *et al.* (2009) and Jao and Wyatt (2010) with the administration of TDF in rats. As TDF is secreted into the PCTs, it may cause cellular injury which can lead to nephrotoxicity (Jao and Wyatt, 2010). It is also possible that the larger luminal area was seen due to a loss in the brush border of the PCTs, which would severely affect the reabsorption of essential molecules in the body (Haschek *et al.*, 2009c; Jao and Wyatt, 2010). Although TDF has been shown to affect the tubular function in the kidneys or rats, Post *et al.* (2010) postulates that TDF does not cause tubular injury per se. This correlates with the findings in the present study, where no observable histopathology was seen, but a significant difference in various parameters of the nephron was measured. As discussed above, melatonin may induce apoptosis and necrosis in unfavourable conditions (Muñoz-Casares *et al.*, 2006; Diger Hardeland *et al.*, 2010). However, no necrosis or apoptosis were observed with evaluation of histopathology and it is unclear whether melatonin had a protective role in restoring morphometric parameters as seen in cART administration due to cART, which did not induce such changes.

Hydropic changes expressed swelling and vacuolation were observed in the kidneys of all treatment groups, with no significant differences in the present study. However, the prevalence of vacuolation of the PCTs in the melatonin and experimental groups in comparison with the control and cART groups showed a trend. The two groups that were exposed to melatonin both had 70% of vacuolation, compared to 38% in the control and 30% in the cART group. Hara *et al.* (2013) found that the mechanism by which melatonin modulates the immune system in humans can induce apoptosis of colostrum mononuclear cells. As hydropic changes are one of the first changes observed after cellular injury on tissue level, vacuolation observed in the present study may be indicative of the early stages of apoptosis. These changes are, however, still reversible (Haschek, *et al.*, 2009a). In addition, no fibrosis, degenerative changes of tubular

epithelial cells or glomerulonephritis were observed in the cART group as described by Van Rompay *et al.* (2004) and Adjene *et al.* (2011) in rhesus monkeys and rats, respectively.

As mentioned with the pancreas and liver, the treatment duration of TDF/EFV/FTC may not cause histologically observable histopathological changes in eight weeks in Wistar rats. Melatonin may be more effective in HIV positive patients receiving cART, as the compounding effects may induce histologically observable changes. However, the focus of this study was to observe changes in an HIV negative model to distinguish between the symptoms of HIV and the side effects of the specific combination of TDF/EFV/FTC on tissue level.

## CHAPTER 6 CONCLUSION

### 6.1 CONCLUDING REMARKS

This project aimed to address the lack of research regarding the histomorphometric changes of cART in the pancreas, liver and kidney. It also aimed to evaluate melatonin as a possible therapeutic option to eradicate these side effects.

In the present study, significant morphometric changes caused by cART were seen in all components of the nephron. Administration of TDF/EFV/FTC for 8 weeks in a rat model decreased the parameters of the renal corpuscle, glomerulus, renal space and PCTs, possibly due to the cytotoxic effects and decrease in tubular function induced by cART. Melatonin decreased renal corpuscle parameters, the renal space and the PCT area. It is possible that melatonin induced apoptosis and necrosis in these structures to prevent further tissue damage induced by possible inflammation. It is also possible that excess melatonin levels in the body may cause negative changes in the kidney's histomorphology due to difficulty in excretion or reabsorption of this molecule.

Haemoglobin and lipaemia values were affected by cART and melatonin, respectively. Administration of cART restores the anaemic haemoglobin values in HIV positive patients and thus the results show that the mechanism in which cART elevates serum haemoglobin is still active in the absence of anaemia or immunodeficiency. Melatonin decreased serum lipids in the present study, due to its inhibitory effect on peroxidation of cellular lipids by free radicals.

This study concluded that melatonin at the dose of 0.01 mg/g/day and 25.8 mg/kg/day TDF, 51.6 mg/kg/day EFV and 17.4 mg/kg/day FTC will exert a histologically observable effect on the kidneys in a Wistar rat model in the absence of HIV. Care must be taken in prescribing melatonin or TDF/FTC/EFV in HIV positive patients with renal damage or the susceptibility thereof.

## 6.2 LIMITATIONS OF THE STUDY AND PROSPECTIVE RESEARCH

The experiment was designed to reduce the number of rats sacrificed as much as possible and thus multiple researchers utilised the tissue from each rat. This caused suboptimal harvesting time in some cases and autolysis may have occurred in some samples. This also caused that three blood samples had to be excluded from analyses of liver enzymes due to insufficient blood collection.

Prospective research may include the measurement of free radicals in the same rat model to determine whether the changes in morphometry that melatonin induced in the kidney was restorative. Urea of the rats can also be monitored and tested daily to determine kidney function in the same rat model. The expression of melatonin receptors in  $\beta$ -cells (M1 and M2) can also be observed in different doses and conditions. Lastly, blood parameters such as growth hormone can also be evaluated to observe the physiological effects of melatonin on the normal hormone homeostasis in the body.

## REFERENCES

- Achhra AC, Nugent , Mocroft A, Ryom L, W. C. (2016) ‘Chronic Kidney Disease and Antiretroviral Therapy in HIV-Positive Individuals: Recent Developments.’, *Current HIV/AIDS reports*, Apr 30, pp. 149–157. doi: 10.1007/s11904-016-0315-y.
- Acuña-Castroviejo, D., Escames, G., Venegas, C., Díaz-Casado, M. E., Lima-Cabello, E., López, L. C., Rosales-Corral, S., Tan, D. X. and Reiter, R. J. (2014) ‘Extrapineal melatonin: Sources, regulation, and potential functions’, *Cellular and Molecular Life Sciences*, 71(16), pp. 2997–3025. doi: 10.1007/s00018-014-1579-2.
- Adami Andreollo, N., Freitas Dos Santos, E., Rachel Araújo, M., Roberto Lopes, L. and Adami Andreollo, N. (2012) ‘Rat’s age versus human’s age: what is the relationship?’, *Arquivos Brasileiros De Cirurgia Digestiva*, 25(1), pp. 49–51. doi: 10.1590/S0102-67202012000100011.
- Adjene, J. O., Ajakaye, I. O. and Nosakhare, P. O. (2011) ‘Morphological effects of chronic efavirenz administration on the kidney of adult Wistar rats’, *Genomic Medicine, Biomarkers, and Health Sciences*. Elsevier Taiwan LLC, 3(2), pp. 76–80. doi: 10.1016/j.gmbhs.2011.08.002.
- Ahmed, H. H. and Salem, H. A. (2011) ‘Effect of Melatonin on Some Hematological Parameters and Immune Status of Broiler Chicks’, 3(2), pp. 243–254. doi: 10.5539/jas.v3n2p243.
- Alarifi, S., Al-Doaiss, A., Alkahtani, S., Al-Farraj, S. A., Saad Al-Eissa, M., Al-Dahmash, B., Al-Yahya, H. and Mubarak, M. (2012) ‘Blood chemical changes and renal histological alterations induced by gentamicin in rats’, *Saudi Journal of Biological Sciences*, 19, pp. 103–110. doi: 10.1016/j.sjbs.2011.11.002.
- Allegra, M., Reiter, R. J., Tan, D.-X., Gentile, C., Tesoriere, L. and Livrea, M. A. (2003) ‘The chemistry of melatonin’s interaction with reactive species’, *Journal of Pineal Research*. Munksgaard International Publishers, 34(1), pp. 1–10. doi: 10.1034/j.1600-079X.2003.02112.x.
- Amorosa, V., Synnestvedt, M., Gross, R., Friedman, H., MacGregor, R. R., Gudonis, D., Frank, I. and Tebas, P. (2005) ‘A tale of 2 epidemics: the intersection between obesity and HIV infection in Philadelphia.’, *Journal of acquired immune deficiency syndromes (1999)*, 39(5),

pp. 557–561.

- Apostolova, N., Gomez-Sucerquia, L. J., Moran, A., Alvarez, A., Blas-Garcia, A. and Esplugues, J. V. (2010) 'Enhanced oxidative stress and increased mitochondrial mass during Efavirenz-induced apoptosis in human hepatic cells', *British Journal of Pharmacology*, 160(8), pp. 2069–2084. doi: 10.1111/j.1476-5381.2010.00866.x.
- Baetens, D., Malaisse-Lagae, F., Perrelet, A. and Orci, L. (1979) 'Endocrine Pancreas: Three-Dimensional Reconstruction Shows Two Types of Islets of Langerhans', *Science*, 206(4424), pp. 1323–1325.
- Bähr, I., Mühlbauer, E., Albrecht, E. and Peschke, E. (2012) 'Evidence of the receptor-mediated influence of melatonin on pancreatic glucagon secretion via the Gαq protein-coupled and PI3K signaling pathways', *Journal of Pineal Research*. Blackwell Publishing Ltd, 53(4), pp. 390–398. doi: 10.1111/j.1600-079X.2012.01009.x.
- Bahr, I., Mühlbauer, E., Schucht, H. and Peschke, E. (2011) 'Melatonin stimulates glucagon secretion in vitro and in vivo', *Journal of Pineal Research*, 50(3), pp. 336–344. doi: 10.1111/j.1600-079X.2010.00848.x.
- Bancroft, J. D. and Layton, C. (2013a) 'Carbohydrates', in Suvarna, S. Kim; Layton, Christopher; Bancroft, J. D. (ed.) *Bancroft's Theory and Practice of Histological Techniques*. Elsevier, pp. 215–238.
- Bancroft, J. D. and Layton, C. (2013b) 'The hematoxylin and eosin', in Suvarna, S. Kim; Layton, Christopher; Bancroft, J. D. (ed.) *Bancroft's Theory and Practice of Histological Techniques*. Elsevier, pp. 173–186.
- Bancroft, J. and Stevens, A. (eds) (1990) *Theory and Practice of Histological Techniques*. 3rd edn. Edinburg, London: Churchill Livingstone.
- Barbosa, A. G., Chehter, E. Z., Bacci, M. R., Mader, A. a and Fonseca, F. La (2013) 'AIDS and the pancreas in the HAART era: a cross sectional study.', *International archives of medicine*, 6(1), p. 28. doi: 10.1186/1755-7682-6-28.
- Baydas, G., Canatan, H. and Turkoglu, A. (2002) 'Comparative analysis of the protective effects of melatonin and vitamin E on streptozocin-induced diabetes mellitus', *Journal of Pineal Research*, pp. 225–230.
- Baykara, B., Tekmen, I., Pekcetin, C., Ulukus, C., Tuncel, P., Sagol, O., Ormen, M. and Ozogul, C.



- (2009) 'The protective effects of carnosine and melatonin in ischemia-reperfusion injury in the rat liver', *Acta Histochemica*, 111(1), pp. 42–51. doi: 10.1016/j.acthis.2008.03.002.
- Bekyarova, G. and Tzaneva, M. (2015) 'Melatonin Ameliorates Burn-Induced Liver Injury by Modulation of Nrf2 and Nf- $\kappa$ B Signaling Pathways', *Immunology*, 3(September), pp. 1–8. doi: 10.15226/soji/3/3/00128.
- Bellés, M., Linares, V., Luisa Albina, M., Sirvent, J., Sanchez, D. J. and Domingo, J. L. (2007) 'Melatonin reduces uranium-induced nephrotoxicity in rats', *Journal of Pineal Research*, 43(1), pp. 87–95. doi: 10.1111/j.1600-079X.2007.00447.x.
- Bergamini, C. M., Gambetti, S., Dondi, A. and Cervellati, C. (2004) 'Oxygen, reactive oxygen species and tissue damage.', *Current pharmaceutical design*, 10(14), pp. 1611–1626. doi: 10.2174/1381612043384664.
- Blümer, R. M., van Vonderen, M. G., Sutinen, J., Hassink, E., Ackermans, M., van Agtmael, M. A., Yki-Jarvinen, H., Danner, S. A., Reiss, P. and Sauerwein, H. P. (2008) 'Zidovudine/lamivudine contributes to insulin resistance within 3 months of starting combination antiretroviral therapy', *Aids*, 22(2), pp. 227–236. doi: 10.1097/QAD.0b013e3282f33557.
- Bobek, V., Kolostova, K., Pinterova, D., Kacprzak, G., Adamiak, J., Kolodziej, J., Boubelik, M., Kubecova, M. and Hoffman, R. M. (2010) 'A clinically relevant, syngeneic model of spontaneous, highly metastatic B16 mouse melanoma', *Anticancer Research*, 30(12), pp. 4799–4804. doi: 10.1002/jmv.
- Bonacini, M. (2004) 'Liver Injury during Highly Active Antiretroviral Therapy: The Effect of Hepatitis C Coinfection', *Clinical Infectious Diseases*, 38(SUPPL. 2), pp. S104–S108.
- Brown, T., Tassiopoulos, K., Bosch, R., Shikuma, C. and McComsey, G. (2010) 'Association Between Systemic Inflammation and Incident Diabetes in HIV-Infected Patients After Initiation of Antiretroviral Therapy', *Diabetes care*, 33(10), p. 2244–9. doi: 10.2337/dc10-0633.
- Car, B. D., Eng, V. M., Everds, N. E. and Bounous, D. I. (2006) 'Clinical Pathology of the Rat', in *The Laboratory Rat*. 2nd edn. Elsevier Inc., pp. 127–146. doi: 10.1016/B978-012074903-4/50008-X.
- Carbajo-Pescador, S., Martín-Renedo, J., García-Palomo, A., Tuñón, M. J., Mauriz, J. L. and

- González-Gallego, J. (2009) 'Changes in the expression of melatonin receptors induced by melatonin treatment in hepatocarcinoma HepG2 cells', *Journal of Pineal Research*, 47(4), pp. 330–338. doi: 10.1111/j.1600-079X.2009.00719.x.
- Casado, J., Marín, A., Romero, V., Bañón, S., Moreno, A., Perez-Elías, M., Moreno, S. and Rodríguez-Sagrado, M. (2015) 'The influence of patient beliefs and treatment satisfaction on the discontinuation of current first-line antiretroviral regimens', *HIV Medicine*, p. n/a-n/a. doi: 10.1111/hiv.12280.
- Cha, A., Besignano-Long, A. R., Rothberger, N. and Shah, B. (2016) 'Reversibility of renal dysfunction after discontinuation of tenofovir', *Journal of the American Pharmacists Association*. American Pharmacists Association, 56(3), pp. 280–283. doi: 10.1016/j.japh.2016.02.013.
- Chang, C. Y. and Schiano, T. D. (2007) 'Review article: Drug hepatotoxicity', *Alimentary Pharmacology and Therapeutics*, 25(10), pp. 1135–1151. doi: 10.1111/j.1365-2036.2007.03307.x.
- Chen, X., Cho, D.-B. and Yang, P.-C. (2010) 'Double staining immunohistochemistry.', *North American journal of medical sciences*. Wolters Kluwer -- Medknow Publications, 2(5), pp. 241–5. doi: 10.4297/najms.2010.2241.
- Cipolla-Neto, J., Amaral, F. G., Afeche, S. C., Tan, D. X. and Reiter, R. J. (2014) 'Melatonin, energy metabolism, and obesity: A review', *Journal of Pineal Research*, 56(4), pp. 371–381. doi: 10.1111/jpi.12137.
- Cuesta, S., Kireev, R., Forman, K., Garcia, C., Escames, G., Ariznavarreta, C., Vara, E. and Tresguerres, J. A. F. (2010) 'Melatonin improves inflammation processes in liver of senescence-accelerated prone male mice (SAMP8)', *Experimental Gerontology*. Elsevier Inc., 45(12), pp. 950–956. doi: 10.1016/j.exger.2010.08.016.
- Cuesta, S., Kireev, R., García, C., Rancan, L., Vara, E. and Tresguerres, J. A. F. (2013) 'Melatonin can improve insulin resistance and aging-induced pancreas alterations in senescence-accelerated prone male mice (SAMP8)', *Age*, 35(3), pp. 659–671. doi: 10.1007/s11357-012-9397-7.
- Deeks, E. D. and Perry, C. M. (2010) 'Efavirenz / Emtricitabine / Tenofovir Disoproxil Fumarate Single-Tablet Regimen ( Atripla Ò )', 70(17), pp. 2315–2338.

- Diger Hardeland, R., Cardinali, D. P., Srinivasan, V., Spence, D. W., Brown, G. M. and Pandi-Perumal, S. R. (2010) 'Melatonin - A pleiotropic, orchestrating regulator molecule', *Progress in Neurobiology journal*. doi: 10.1016/j.pneurobio.2010.12.004.
- Dolberg, O. T., Hirschmann, S. and Grunhaus, L. (1998) 'Melatonin for the treatment of sleep disturbances in major depressive disorder.', *The American Journal of Psychiatry*, 155(8), pp. 1119–1121. doi: 10.1176/ajp.155.8.1119.
- Dolensek, J., Rupnik, M. S. and Stozer, A. (2015) 'Structural similarities and differences between the human and the mouse pancreas', *Islets*, 7(1), pp. 2–9. doi: 10.1080/19382014.2015.1024405.
- Dossou-Yovo, F., Mamadou, G., Soudy, I. D., Limas-Nzouzi, N., Miantezila, J., Desjeux, J.-F. and Eto, B. (2014) 'Metronidazole or Cotrimoxazole therapy is associated with a decrease in intestinal bioavailability of common antiretroviral drugs.', *PloS one*, 9(2), p. e89943. doi: 10.1371/journal.pone.0089943.
- Elayat, A. A., el-Naggar, M. M. and Tahir, M. (1995) 'An immunocytochemical and morphometric study of the rat pancreatic islets.', *Journal of anatomy*, 186 ( Pt 3, pp. 629–37.
- Erlandsen, S. L., Hegre, O. D., Parsons, J. A., McEvoy, R. C. and Elde, R. P. (1976) 'Pancreatic islet cell hormones distribution of cell types in the islet and evidence of the presence of somatostatin and gastrin within the D cell', *The Journal of Histochemistry and Cytochemistry*, 24(7), pp. 883–897.
- Ersoz, N., Guven, A., Cayci, T., Uysal, B., Turk, E., Oztas, E., Akgul, E. O., Korkmaz, A. and Cetiner, S. (2009) 'Comparison of the efficacy of melatonin and 1400W on renal ischemia/reperfusion injury: a role for inhibiting iNOS.', *Renal failure*, 31(8), pp. 704–10. doi: 10.3109/08860220903085989.
- Eweka, A. O. (2009) 'Histological Studies Of The Teratogenic Effects Of Camphor On The Developing Kidney Of The Wistar Rats', *Annals of Biomedical Sciences*.
- Fabis, M., Pruszyńska, E. and Mackowiak, P. (2002) 'In vivo and in situ action of melatonin on insulin secretion and some metabolic implications in the rat', *Pancreas*, 25(2), pp. 166–169. doi: Doi 10.1097/01.Mpa.0000015382.94989.73.
- Farhadi, N., Doosti, A., Mohammadi, J. and Mohammadi, R. (2015) 'Effects of orally-administered melatonin and long-term exposure to light and dark on serum indices and gene expression

of insulin and glucagon in male Wistar rats', *Biological Rhythm Research*, 46(3), pp. 435–443. doi: 10.1080/09291016.2015.1020201.

Ferreira, F. M., Guercio, L., Santos, D., Guilherme, P., Miranda, D. A., Afonso, R. I., Marques, L. M., Bacci, M., Maria, A., Mader, A., Barbosa, A. G. and Chether, E. Z. (2015) 'HIV and Pancreas : Endocrinological Patterns of Pancreatic Morphology', *Journal of the Pancreas*, 16(4), pp. 369–372.

Fisher, S. D., Miller, T. L. and Lipshultz, S. E. (2006) 'Impact of HIV and highly active antiretroviral therapy on leukocyte adhesion molecules, arterial inflammation, dyslipidemia, and atherosclerosis', *Atherosclerosis*, 185(1), pp. 1–11. doi: 10.1016/j.atherosclerosis.2005.09.025.

la Fleur, S. E., Kalsbeek, A., Wortel, J., van der Vliet, J. and Buijs, R. M. (2001) 'Role for the pineal and melatonin in glucose homeostasis: pinealectomy increases night-time glucose concentrations.', *Journal of neuroendocrinology*, 13(12), pp. 1025–32.

Gallien, S., Flandre, P., Nguyen, N., De Castro, N., Molina, J.-M. and Delaugerre, C. (2015) 'Safety and efficacy of coformulated efavirenz/emtricitabine/tenofovir single-tablet regimen in treatment-naïve patients infected with HIV-1', *Journal of Medical Virology*, 87(2), pp. 187–191. doi: 10.1002/jmv.24023.

Giknis, M. L. . and Clifford, C. B. (2008) 'Clinical Laboratory Parameters For Rats'. Charles River, p. 14.

Gilad, E. and Zisapel, N. (1995) 'High-Affinity Binding of Melatonin to Hemoglobin', *Biochemical and Molecular Medicine*, 56(2), pp. 115–120. doi: <https://doi.org/10.1006/bmme.1995.1066>.

Giri, D. (2015) *Periodic Acid Schiff (PAS) Staining Technique For Carbohydrates*. Available at: <http://laboratoryinfo.com/periodic-acid-schiff-pas-staining-technique-for-carbohydrates/>.

Glick, M. R., Ryder, K. W. and Jackson, S. A. (1986) 'Graphical comparisons of interferences in clinical chemistry instrumentation', *Clinical Chemistry*, 32(3), pp. 470–475.

Gu, S.-Y., Yeh, T.-Y., Lin, S.-Y. and Peng, F.-C. (2016) 'Unfractionated bone marrow cells attenuate paraquat-induced glomerular injury and acute renal failure by modulating the inflammatory response', *Scientific Reports*. Nature Publishing Group, 6(November 2015), p. 23287. doi: 10.1038/srep23287.

- Guzik, T. J., Mangalat, D. and Korbut, R. (2006) ‘Adipocytokines - Novel link between inflammation and vascular function?’, *Journal of Physiology and Pharmacology*, 57, pp. 505–528. doi: 10.1111/j.1365-2036.2011.04905.x.
- Hara, C. D. C. P., Honorio-França, A. C., Fagundes, D. L. G., Guimarães, P. C. L. and França, E. L. (2013) ‘Melatonin nanoparticles adsorbed to polyethylene glycol microspheres as activators of human colostrum macrophages’, *Journal of Nanomaterials*, 2013. doi: 10.1155/2013/973179.
- Hara, M., Yoshida, M., Nishijima, H., Yokosuka, M., Iigo, M., Ohtani-Kaneko, R., Shimada, A., Hasegawa, T., Akama, Y. and Hirata, K. (2001) ‘Melatonin, a pineal secretory product with antioxidant properties, protects against cisplatin-induced nephrotoxicity in rats.’, *Journal of Pineal Research*, 30(3), pp. 129–138. doi: 10.1034/j.1600-079X.2001.300301.x.
- Haschek, W. M., Rousseaux, C. G. and Wallig, M. A. (2009a) ‘Cell injury’, in *Fundamentals of Toxicologic Pathology*. 2nd edn. Elsevier Inc., pp. 9–42. doi: 10.1016/B978-0-12-370469-6.00002-7.
- Haschek, W. M., Rousseaux, C. G. and Wallig, M. A. (2009b) ‘Clinical Pathology’, in *Fundamentals of Toxicologic Pathology*. 2nd edn. Academic Press, pp. 43–65.
- Haschek, W. M., Rousseaux, C. G. and Wallig, M. A. (2009c) ‘Kidney and Lower Urinary Tract’, in *Fundamentals of Toxicologic Pathology*. 2nd edn. Academic Press, p. 353. doi: 10.1016/B978-0-12-370469-6.00011-8.
- Haschek, W. M., Rousseaux, C. G. and Wallig, M. A. (2009d) ‘Pancreas’, in *Fundamentals of Toxicologic Pathology*. 2nd edn. Elsevier Inc, pp. 237–260.
- Haschek, W. M., Rousseaux, C. G. and Wallig, M. A. (2009e) ‘The Liver’, in Elsevier Inc (ed.) *Fundamentals of Toxicologic Pathology*. 2nd edn, pp. 197–233.
- Hassel, J. and Hand, A. R. (1974) ‘Tissue fixation with diimidoesters as an alternative to aldehydes. II. Cytochemical and biochemical studies of rat liver fixed with dimethylsuberimidate.’, *Journal of Histochemistry & Cytochemistry*, 22, pp. 229–239.
- Hickie, I. B. and Rogers, N. L. (2011) ‘Novel melatonin-based therapies: Potential advances in the treatment of major depression’, *The Lancet*. Elsevier Ltd, 378(9791), pp. 621–631. doi: 10.1016/S0140-6736(11)60095-0.
- Hlutkin, S. and Zinchuk, V. (2008) ‘Effect of melatonin on the blood oxygen transport during

- hypothermia and rewarming in rats.’, *Advances in medical sciences*, 53(2), pp. 234–9. doi: 10.2478/v10039-008-0035-7.
- Hofstetter, J., Suckow, M. A. and Hickman, D. L. (2006) ‘Chapter 4 Morphophysiology’.
- Howat, W. J. and Wilson, B. A. (2014) ‘Tissue fixation and the effect of molecular fixatives on downstream staining procedures’, *Methods*. Elsevier Inc., 70(1), pp. 12–19. doi: 10.1016/j.ymeth.2014.01.022.
- Hu, W., Ma, Z., Jiang, S., Fan, C., Deng, C., Yan, X., Di, S., Lv, J., Reiter, R. J. and Yang, Y. (2015) ‘Melatonin: the dawning of a treatment for fibrosis?’, *Journal of Pineal Research*. doi: 10.1111/jpi.12302.
- Hussein, M. R., Ahmed, O. G., Hassan, A. F. and Ahmed, M. A. (2007) ‘Intake of melatonin is associated with amelioration of physiological changes, both metabolic and morphological pathologies associated with obesity: An animal model’, *International Journal of Experimental Pathology*, 88(1), pp. 19–29. doi: 10.1111/j.1365-2613.2006.00512.x.
- Ibraheem, A. S., El-Sayed, M. F. and Ahmed, R. A. (2013) ‘Lymph node histopathological studies in a combined adjuvant–collagen induced arthritis model in albino rat *Rattus rattus*’, *The Journal of Basic & Applied Zoology*. The Egyptian German Society for Zoology, 66(4), pp. 195–205. doi: 10.1016/j.jobaz.2012.12.005.
- Ingiliz, P., Valantin, M. A., Duvivier, C., Medja, F., Dominguez, S., Charlotte, F., Tubiana, R., Poynard, T., Katlama, C., Lombes, A. and Benhamou, Y. (2009) ‘Liver damage underlying unexplained transaminase elevation in human immunodeficiency virus-1 mono-infected patients on antiretroviral therapy’, *Hepatology*, 49(2), pp. 436–442. doi: 10.1002/hep.22665.
- Izzedine, H., Launay-Vacher, V., Deray, G., al., et, Cadrobbi, P., Philipp, T. and Group, T. C. of H.-S.-S. C. S. (2005) ‘Antiviral Drug-Induced Nephrotoxicity’, *American Journal of Kidney Diseases*. Gilead Sciences Inc, Foster City, CA, 45(5), pp. 804–817. doi: 10.1053/j.ajkd.2005.02.010.
- Jao, J. and Wyatt, C. M. (2010) ‘Antiretroviral Medications: Adverse Effects on the Kidney’, *Advances in Chronic Kidney Disease*. Elsevier Ltd, 17(1), pp. 72–82. doi: 10.1053/j.ackd.2009.07.009.
- Jaworek, J., Brzozowski, T. and Konturek, S. J. (2005) ‘Melatonin as an organoprotector in the

stomach and the pancreas', *Journal of Pineal Research*, 38(2), pp. 73–83. doi: 10.1111/j.1600-079X.2004.00179.x.

Jaworek, J., Konturek, S. J., Nawrot, K., Bonior, J., Tomaszewska, R., Stachura, J. and Pawlik, W. W. (2002) 'Role of endogenous melatonin and its MT2 receptor in the modulation of caerulein-induced pancreatitis in the rat', *Journal of Physiology and Pharmacology*, 53(4), pp. 791–804.

Jaworek, J., Nawrot-Porabka, K., Leja-Szpak, A., Bonior, J., Szklarczyk, J., Kot, M., Konturek, S. J. and Pawlik, W. W. (2007) 'Melatonin as modulator of pancreatic enzyme secretion and pancreatoprotector', *Journal of Physiology and Pharmacology*, 58(SUPPL. 6), pp. 65–80.

Jaworek, J., Szklarczyk, J., Jaworek, A. K., Nawrot-Porabka, K., Leja-Szpak, A., Bonior, J. and Kot, M. (2012) 'Protective effect of melatonin on acute pancreatitis.', *International Journal of Inflammation*, pp. 1–8. doi: 10.1155/2012/173675.

Johannessen, A., Naman, E., Gundersen, S. G. and Bruun, J. N. (2011) 'Antiretroviral treatment reverses HIV-associated anemia in rural Tanzania.', *BMC infectious diseases*. BioMed Central, 11(1), p. 190. doi: 10.1186/1471-2334-11-190.

John, T. M., Viswanathan, M., George, J. C. and Scanes, C. G. (1990) 'Influence of chronic melatonin implantation on circulating levels of catecholamines, growth hormone, thyroid hormones, glucose, and free fatty acids in the pigeon', *General and Comparative Endocrinology*, 79(2), pp. 226–232. doi: 10.1016/0016-6480(90)90107-W.

Johnson, K. E. (1991) *Histology and Cell Biology*. 2nd edn. Mosby Elsevier.

Joly, A.-L., Wettstein, G., Mignot, G., Ghiringhelli, F. and Garrido, C. (2010) 'Dual role of heat shock proteins as regulators of apoptosis and innate immunity.', *Journal of innate immunity*, 2(3), pp. 238–247. doi: 10.1159/000296508.

Kabbara, W. K. and Ramadan, W. H. (2015) 'Emtricitabine/rilpivirine/tenofovir disoproxil fumarate for the treatment of HIV-1 infection in adults.', *Journal of infection and public health*. King Saud Bin Abdulaziz University for Health Sciences, 8(5), pp. 409–17. doi: 10.1016/j.jiph.2015.04.020.

Kannappan, S., Jayaraman, T., Rajasekar, P., Ravichandran, M. K. and Anuradha, C. V (2006) 'Cinnamon bark extract improves glucose metabolism and lipid profile in the fructose-fed rat', 47(November), pp. 2–8.

- Karras, A., Lafaurie, M., Furco, A., Bourgarit, A., Droz, D., Sereni, D., Legendre, C., Martinez, F. and Molina, J.-M. (2003) 'Tenofovir-related nephrotoxicity in human immunodeficiency virus-infected patients: three cases of renal failure, Fanconi syndrome, and nephrogenic diabetes insipidus.', *Clinical infectious diseases : an official publication of the Infectious Diseases Society of America*, 36(8), pp. 1070–1073. doi: 10.1086/368314.
- Kibaru, E. G., Nduati, R., Wamalwa, D. and Kariuki, N. (2015) 'Impact of highly active antiretroviral therapy on hematological indices among HIV-1 infected children at Kenyatta National Hospital-Kenya: retrospective study.', *AIDS research and therapy*, 12, p. 26. doi: 10.1186/s12981-015-0069-4.
- Kierszenbaum, A. L. (2007) *Histology and Cell Biology - An Introduction to Pathology*. 2nd edn. Philadelphia: Mosby Elsevier.
- Kierszenbaum, A. L. (2013) *HISTOLOGY AND CELL BIOLOGY - An Introduction to Pathology*. 2nd edn, *Journal of Chemical Information and Modeling*. 2nd edn. Philadelphia: Elsevier Ltd. doi: 10.1017/CBO9781107415324.004.
- Kim, R. J. and Rutstein, R. M. (2010) 'Impact of Antiretroviral Therapy on Growth, Body Composition and Metabolism in Pediatric HIV Patients', *Pediatric Drugs*, 12(3), pp. 187–199. doi: 10.2165/11532520-000000000-00000.
- King, A. J. F., Fernandes, J. R., Hollister-lock, J., Nienaber, C. E., Bonner-weir, S. and Weir, G. C. (2007) 'Normal relationship of beta and non-beta cells not needed for successful islet transplantation .', *Animals*, (February), pp. 1–23. doi: 10.2337/db07-0191.A.J.F.K.
- Kotyk, T., Dey, N., Ashour, A. S., Balas-Timar, D., Chakraborty, S., Ashour, A. S. and Tavares, J. M. R. S. (2016) 'Measurement of glomerulus diameter and Bowman's space width of renal albino rats', *Computer Methods and Programs in Biomedicine*, 126, pp. 143–153. doi: 10.1016/j.cmpb.2015.10.023.
- Labarga, P., Barreiro, P., Martin-Carbonero, L., Rodriguez-Novoa, S., Solera, C., Medrano, J., Rivas, P., Albalater, M., Blanco, F., Moreno, V., Vispo, E. and Soriano, V. (2009) 'Kidney tubular abnormalities in the absence of impaired glomerular function in HIV patients treated with tenofovir', *AIDS*, 23(6), pp. 689–696. doi: 10.1097/QAD.0b013e3283262a64.
- Lebrecht, D., Venhoff, A. C., Kirschner, J., Wiech, T., Venhoff, N. and Walker, U. a (2009) 'Mitochondrial tubulopathy in tenofovir disoproxil fumarate-treated rats.', *Journal of*



*acquired immune deficiency syndromes* (1999), 51(3), pp. 258–263. doi: 10.1097/QAI.0b013e3181a666eb.

- Leja-Szpak, A., Jaworek, J., Pierzchalski, P. and Reiter, R. J. (2010) ‘Melatonin induces pro-apoptotic signaling pathway in human pancreatic carcinoma cells (PANC-1)’, *Journal of Pineal Research*, 49(3), pp. 248–255. doi: 10.1111/j.1600-079X.2010.00789.x.
- Maldonado, M.-D., Murillo-Cabezas, F., Calvo, J.-R., Lardone, P.-J., Tan, D.-X., Guerrero, J.-M. and Reiter, R. J. (2007) ‘Melatonin as pharmacologic support in burn patients: a proposed solution to thermal injury-related lymphocytopenia and oxidative damage.’, *Critical care medicine*, 35(4), pp. 1177–85. doi: 10.1097/01.CCM.0000259380.52437.E9.
- Manfredi, R., Calza, L. and Chiodo, F. (2001) ‘Dual nucleoside analogue treatment in the era of highly active antiretroviral therapy (HAART): a single-centre cross-sectional survey.’, *The Journal of antimicrobial chemotherapy*, 48(2), pp. 299–302.
- Di Mascio, M., Srinivasula, S., Bhattacharjee, A., Cheng, L., Martiniova, L., Herscovitch, P., Lertora, J. and Kiesewetter, D. (2009) ‘Antiretroviral Tissue Kinetics: In Vivo Imaging Using Positron Emission Tomography’, *Antimicrobial Agents and Chemotherapy*, 53(10), pp. 4086–4095. doi: 10.1128/AAC.00419-09.
- Max, B. and Sherer, R. (2000) ‘Management of the adverse effects of antiretroviral therapy and medication adherence.’, *Clinical infectious diseases: an official publication of the Infectious Diseases Society of America*, 30 Suppl 2(Supplement\_2), pp. S96-116. doi: 10.1086/313859.
- Mazepa, R. C., Cuevas, M. J., Collado, P. S. and González-Gallego, J. (1999) ‘Melatonin increases muscle and liver glycogen content in nonexercised and exercised rats’, *Life Sciences*, 66(2), pp. 153–160. doi: 10.1016/S0024-3205(99)00573-1.
- Michels, J. E., Eric Bauer, G., Johnson, D. and Dixit, P. K. (1986) ‘Morphometric analysis of the endocrine cell composition of rat pancreas following treatment with streptozotocin and nicotinamide’, *Experimental and Molecular Pathology*, 44(3), pp. 247–258. doi: 10.1016/0014-4800(86)90039-0.
- Migrenne, S. (2011) *Birth and death of the  $\alpha$ -cell*, *International Group on Insulin Secretion*. Available at: [http://www.igis.com/igis-digest/xiith-igis-symposium/i-birth-and-death-of-the- \$\alpha\$ -cell/](http://www.igis.com/igis-digest/xiith-igis-symposium/i-birth-and-death-of-the-<math>\alpha</math>-cell/) (Accessed: 18 August 2017).

- Motta, P. M., Macchiarelli, G., Nottola, S. A. and Correr, S. (1997) 'Histology of the exocrine pancreas', *Microscopy Research and Technique*, 37(5–6), pp. 384–398. doi: 10.1002/(SICI)1097-0029(19970601)37:5/6<384::AID-JEMT3>3.0.CO;2-E.
- Mouly, S., Rizzo-Padoin, N., Simoneau, G., Verstuyft, C., Aymard, G., Salvat, C., Mahé, I. and Bergmann, J. F. (2006) 'Effect of widely used combinations of antiretroviral therapy on liver CYP3A4 activity in HIV-infected patients', *British Journal of Clinical Pharmacology*, 62(2), pp. 200–209. doi: 10.1111/j.1365-2125.2006.02637.x.
- Muñoz-Casares, F. C., Padillo, F. J., Briceño, J., Collado, J. A., Muñoz-Castañeda, J. R., Ortega, R., Cruz, A., Túnez, I., Montilla, P., Pera, C. and Muntané, J. (2006) 'Melatonin reduces apoptosis and necrosis induced by ischemia/reperfusion injury of the pancreas', *Journal of Pineal Research*, 40(3), pp. 195–203. doi: 10.1111/j.1600-079X.2005.00291.x.
- Mylonas, C. and Kouretas, D. (1999) 'Lipid peroxidation and tissue damage.', *In vivo (Athens, Greece)*, 13(3), pp. 295–309.
- Nava, M., Quiroz, Y., Vaziri, N. and Rodriguez-Iturbe, B. (2003) 'Melatonin reduces renal interstitial inflammation and improves hypertension in spontaneously hypertensive rats.', *American journal of physiology. Renal physiology*, 284(3), pp. F447-54. doi: 10.1152/ajprenal.00264.2002.
- Neuman, M. G., Schneider, M., Nanau, R. M. and Parry, C. (2013) 'HIV-Antiretroviral Therapy Induced Liver, Gastrointestinal, and Pancreatic Injury', *International Journal of Hepatology*, 2012, pp. 1–23. doi: 10.1155/2012/760706.
- Nikolac, N. (2014) 'Lipemia: Causes, interference mechanisms, detection and management', *Biochemia Medica*, 24(1), pp. 57–67. doi: 10.11613/BM.2014.008.
- Nsiah, K., Dzogbefia, V. P., Ansong, D., Akoto, A. O., Boateng, H. and Ocloo, D. (2011) 'Pattern of AST and ALT changes in relation to hemolysis in sickle cell disease', *Clinical Medicine Insights: Blood Disorders*, 4, pp. 1–9. doi: 10.4137/CMBD.S3969.
- Núñez, M. (2010) 'Clinical syndromes and consequences of antiretroviral-related hepatotoxicity', *Hepatology*, 52(3), pp. 1143–1155. doi: 10.1002/hep.23716.
- Nunez, M. and Soriano, V. (2005) 'Hepatotoxicity of Antiretrovirals', *Drug Safety*. Springer International Publishing, 28(1), pp. 53–66. doi: 10.2165/00002018-200528010-00004.
- Obirikorang, C. and Yeboah, F. A. (2009) 'Blood haemoglobin measurement as a predictive

- indicator for the progression of HIV/AIDS in resource-limited setting.’, *Journal of biomedical science*. BioMed Central, 16(1), p. 102. doi: 10.1186/1423-0127-16-102.
- Oliveira, N. M., Ferreira, F. A. Y., Yonamine, R. Y. and Chehter, E. Z. (2014) ‘Antiretroviral drugs and acute pancreatitis in HIV/AIDS patients: is there any association? A literature review.’, *Einstein (São Paulo, Brazil)*, 12(1), pp. 112–9. doi: 10.1590/S1679-45082014RW2561.
- Olivero-David, R., Schultz-Moreira, A., Vázquez-Velasco, M., González-Torres, L., Bastida, S., Benedí, J., Sanchez-Reus, M. I., González-Muñoz, M. J. and Sánchez-Muniz, F. J. (2011) ‘Effects of Nori- and Wakame-enriched meats with or without supplementary cholesterol on arylesterase activity, lipaemia and lipoproteinaemia in growing Wistar rats.’, *The British journal of nutrition*, 106(10), pp. 1476–86. doi: 10.1017/S000711451100198X.
- Ovalle, W. K. and Nahirney, P. C. (2013) ‘Liver, Gallbladder, and Exocrine Pancreas’, in *Netter’s Essential Histology*. 2nd edn. Saunders.
- Paik, I. J. and Kotler, D. P. (2011) ‘The prevalence and pathogenesis of diabetes mellitus in treated HIV-infection’, *Best Practice and Research: Clinical Endocrinology and Metabolism*. Elsevier Ltd, 25(3), pp. 469–478. doi: 10.1016/j.beem.2011.04.003.
- Parise, E. R., Oliveira, A. C., Figueiredo-Mendes, C., Lanzoni, V., Martins, J., Nader, H., Ferraz, M. L., Lanzoni, V., Martins, J. and Nader, H. (2006) ‘Noninvasive serum markers in the diagnosis of structural liver damage in chronic hepatitis C virus infection Ferraz ML. Noninvasive serum markers in the diagnosis of structural liver damage in chronic hepatitis C virus infection’, *Liver International Journal compilation r*. Blackwell Munksgaard, 26, pp. 1095–1099. doi: 10.1111/j.1478-3231.2006.01356.x.
- Peschke, E. (2008) ‘Melatonin, endocrine pancreas and diabetes’, *Journal of Pineal Research*, 44(1), pp. 26–40. doi: 10.1111/j.1600-079X.2007.00519.x.
- Peschke, E., Bach, A. G. and Mühlbauer, E. (2006) ‘Parallel signaling pathways of melatonin in the pancreatic  $\beta$ -cell’, *Journal of Pineal Research*, 40(2), pp. 184–191. doi: 10.1111/j.1600-079X.2005.00297.x.
- Peschke, E., Bähr, I. and Mühlbauer, E. (2013) ‘Melatonin and pancreatic islets: Interrelationships between melatonin, insulin and glucagon’, *International Journal of Molecular Sciences*, 14(4), pp. 6981–7015. doi: 10.3390/ijms14046981.
- Peschke, E. and Peschke, D. (1998) ‘Evidence for a circadian rhythm of insulin release from

- perifused rat pancreatic islets', *Diabetologia*, 41(9), pp. 1085–1092. doi: 10.1007/s001250051034.
- Peschke, E., Stumpf, I., Bazwinsky, I., Litvak, L., Dralle, H. and Mühlbauer, E. (2007) 'Melatonin and type 2 diabetes - A possible link?', *Journal of Pineal Research*, 42(4), pp. 350–358. doi: 10.1111/j.1600-079X.2007.00426.x.
- Picinato, M. C., Haber, E. P., Cipolla-Neto, J., Curi, R., de Oliveira Carvalho, C. R. and Carpinelli, A. R. (2002a) 'Melatonin inhibits insulin secretion and decreases PKA levels without interfering with glucose metabolism in rat pancreatic islets.', *Journal of pineal research*, 33(3), pp. 156–160. doi: 20903 [pii].
- Picinato, M. C., Haber, E. P., Cipolla-Neto, J., Curi, R., de Oliveira Carvalho, C. R. and Carpinelli, A. R. (2002b) 'Melatonin inhibits insulin secretion and decreases PKA levels without interfering with glucose metabolism in rat pancreatic islets.', *Journal of pineal research*, 33(3), pp. 156–60.
- Post, F. a, Moyle, G. J., Stellbrink, H. J., Domingo, P., Podzamczar, D., Fisher, M., Norden, A. G., Cavassini, M., Rieger, A., Khuong-Josses, M.-A., Branco, T., Pearce, H. C., Givens, N., Vavro, C. and Lim, M. L. (2010) 'Randomized comparison of renal effects, efficacy, and safety with once-daily abacavir/lamivudine versus tenofovir/emtricitabine, administered with efavirenz, in antiretroviral-naive, HIV-1-infected adults: 48-week results from the ASSERT study.', *Journal of acquired immune deficiency syndromes (1999)*, 55(1), pp. 49–57. doi: 10.1097/QAI.0b013e3181dd911e.
- Prescott, M. J. and Lidster, K. (2017) 'Improving quality of science through better animal welfare: the NC3Rs strategy', *Lab Animal*, 46(4), pp. 152–156. doi: 10.1038/labana.1217.
- Puchalski, S. S., Green, J. N. and Rasmussen, D. D. (2003) 'Melatonin Effect on Rat Body Weight Regulation in Response to High-Fat Diet at Middle Age', *Endocrine*. Humana Press, 21(2), pp. 163–168. doi: 10.1385/ENDO:21:2:163.
- Radogna, F., Diederich, M. and Ghibelli, L. (2010) 'Melatonin: A pleiotropic molecule regulating inflammation', *Biochemical Pharmacology*. Elsevier Inc., 80(12), pp. 1844–1852. doi: 10.1016/j.bcp.2010.07.041.
- Ramracheya, R. D., Muller, D. S., Squires, P. E., Brereton, H., Sugden, D., Huang, G. C., Amiel, S. A., Jones, P. M. and Persaud, S. J. (2008) 'Function and expression of melatonin receptors

- on human pancreatic islets', *Journal of Pineal Research*. Blackwell Publishing Ltd, 44(3), pp. 273–279. doi: 10.1111/j.1600-079X.2007.00523.x.
- Rector, R. S., Thyfault, J. P., Wei, Y. and Ibdah, J. A. (2008) 'Non-alcoholic fatty liver disease and the metabolic syndrome: an update.', *World journal of gastroenterology*. Baishideng Publishing Group Inc, 14(2), pp. 185–92. doi: 10.3748/wjg.14.185.
- Reiter, R. J., Tan, D. X., Terron, M. P., Flores, L. J. and Czarnocki, Z. (2007) 'Melatonin and its metabolites: New findings regarding their production and their radical scavenging actions', *Acta Biochimica Polonica*, 54(1), pp. 1–9. doi: 20071452 [pii].
- Ríos-Lugo, M. J., Cano, P., Jiménez-Ortega, V., Fernández-Mateos, M. P., Scacchi, P. A., Cardinali, D. P. and Esquifino, A. I. (2010) 'Melatonin effect on plasma adiponectin, leptin, insulin, glucose, triglycerides and cholesterol in normal and high fat-fed rats', *Journal of Pineal Research*, 49(4), pp. 342–348. doi: 10.1111/j.1600-079X.2010.00798.x.
- Rolls, G. (2017) *An Introduction to Specimen Processing*. Available at: <http://www.leicabiosystems.com/pathologyleaders/an-introduction-to-specimen-processing/>.
- Van Rompay, K. K. A., Brignolo, L. L., Meyer, D. J., Jerome, C., Tarara, R., Spinner, A., Hamilton, M., Hirst, L. L., Bennett, D. R., Canfield, D. R., Dearman, T. G., Von Morgenland, W., Allen, P. C., Valverde, C., Castillo, A. B., Martin, R. B., Samii, V. F., Bendele, R., Desjardins, J., Marthas, M. L., Pedersen, N. C. and Bischofberger, N. (2004) 'Biological Effects of Short-Term or Prolonged Administration of 9-[2-(Phosphonomethoxy) Propyl] Adenine (Tenofovir) to Newborn and Infant Rhesus Macaques', *Antimicrobial Agents and Chemotherapy*, 48(5), pp. 1469–1487. doi: 10.1128/AAC.48.5.1469.
- Roubenoff, R., Schmitz, H., Bairos, L., Layne, J., Potts, E., Cloutier, G. J. and Denry, F. (2002) 'Reduction of Abdominal Obesity in Lipodystrophy Associated with Human Immunodeficiency Virus Infection by Means of Diet and Exercise: Case Report and Proof of Principle', *Clinical Infectious Diseases*, 34(3), pp. 390–393. doi: 10.1086/338402.
- Rudel, L. L., Haines, J. L. and Sawyer, J. K. (1990) 'Effects on plasma lipoproteins of monounsaturated, saturated, and polyunsaturated fatty acids in the diet of African green monkeys.', *J Lipid Res*, 31(10), pp. 1873–1882.
- Ryom, L., Mocroft, A. and Lundgren, J. (2012) 'HIV therapies and the kidney: Some good, some

not so good?', *Current HIV/AIDS Reports*, 9(2), pp. 111–120. doi: 10.1007/s11904-012-0110-3.

Sands, J. M. and Veerlander, J. W. (2010) 'Functional Anatomy of the Kidney', in McQueen, C. A. (ed.) *Comprehensive Toxicology*. 2nd edn. Auburn, AL, USA: Elsevier.

Sener, G., Sehirli, a O., Altunbas, H. Z., Ersoy, Y., Paskaloglu, K., Arbak, S. and Ayanoglu-Dulger, G. (2002) 'Melatonin protects against gentamicin-induced nephrotoxicity in rats.', *Journal of pineal research*, 32(4), pp. 231–6. doi: 10858 [pii].

Sener, G., Sehirli, a O., Keyer-Uysal, M., Arbak, S., Ersoy, Y. and Yeğen, B. C. (2002) 'The protective effect of melatonin on renal ischemia-reperfusion injury in the rat.', *Journal of pineal research*, 32(2), pp. 120–6.

Shikuma, C. M., Zackin, R., Sattler, F., Mildvan, D., Nyangweso, P., Alston, B., Evans, S., Mulligan, K. and Team, A. C. T. G. 892 (2004) 'Changes in weight and lean body mass during highly active antiretroviral therapy', *Clinical Infectious Diseases*, 39(8), pp. 1223–1230. doi: 10.1086/424665.

Shima, T., Chun, S. J., Nijima, A., Bizot-Espiard, J. G., Guardiola-Lemaitre, B., Hosokawa, M. and Nagai, K. (1997) 'Melatonin suppresses hyperglycemia caused by intracerebroventricular injection of 2-deoxy-D-glucose in rats', *Neuroscience Letters*, 226(2), pp. 119–122. doi: 10.1016/S0304-3940(97)00257-7.

Sidhu, S., Pandhi, P., Malhotra, S., Vaiphei, K. and Khanduja, K. L. (2009) 'Melatonin treatment is beneficial in pancreatic repair process after experimental acute pancreatitis', *European Journal of Pharmacology*, 628, pp. 282–289. doi: 10.1016/j.ejphar.2009.11.058.

Sigala, F., Theocharis, S., Sigalas, K., Markantonis-Kyroudis, S., Papalabros, E., Triantafyllou, A., Kostopanagiotou, G. and Andreadou, I. (2006) 'Therapeutic value of melatonin in an experimental model of liver injury and regeneration', *Journal of Pineal Research*, 40(3), pp. 270–279. doi: 10.1111/j.1600-079X.2005.00310.x.

Souza, S. J., Luzia, L. A., Santos, S. S. and Rondó, P. H. C. (2013) 'Lipid profile of HIV-infected patients in relation to antiretroviral therapy: a review', *Revista da Associação Médica Brasileira*, 59(2), pp. 186–198. doi: 10.1016/j.ramb.2012.11.003.

Squillace, N., Ricci, E., Quirino, T., Gori, A., Bandera, A., Carezzi, L., De Socio, G. V., Orofino, G., Martinelli, C., Madeddu, G., Rusconi, S., Maggi, P., Celesia, B. M., Cordier, L., Vichi,

- F., Calza, L., Falasca, K., Di Biagio, A., Pellicanò, G. F. and Bonfanti, P. (2017) 'Safety and tolerability of Elvitegravir/ Cobicistat/Emtricitabine/Tenofovir Disoproxil fumarate in a real life setting: Data from surveillance cohort long-term toxicity antiretrovirals/antivirals (SCOLTA) project', *PLoS ONE*, 12(6), pp. 1–12. doi: 10.1371/journal.pone.0179254.
- Statistics South Africa (2014) 'Mid-year Population estimates', [www.statssa.gov.za/publications/.../P03022014.pdf](http://www.statssa.gov.za/publications/.../P03022014.pdf), (July), pp. 1–18. doi: Statistical release P0302.
- Sulkowski, M. S. (2004) 'Drug-induced liver injury associated with antiretroviral therapy that includes HIV-1 protease inhibitors.', *Clinical infectious diseases : an official publication of the Infectious Diseases Society of America*, 38 Suppl 2(Suppl 2), pp. S90–S97. doi: 10.1086/381444.
- Tan, D. X., Manchester, L. C., Esteban-Zubero, E., Zhou, Z. and Reiter, R. J. (2015) 'Melatonin as a potent and inducible endogenous antioxidant: Synthesis and metabolism', *Molecules*, 20(10), pp. 18886–18906. doi: 10.3390/molecules201018886.
- Tan, D. X., Manchester, L. C., Terron, M. P., Flores, L. J. and Reiter, R. J. (2007) 'One molecule, many derivatives: A never-ending interaction of melatonin with reactive oxygen and nitrogen species?', *Journal of Pineal Research*, 42(1), pp. 28–42. doi: 10.1111/j.1600-079X.2006.00407.x.
- Thapa, B. R. and Walia, A. (2007) 'Symposium : Newer Diagnostic Tests Liver Function Tests and their Interpretation', *Indian Journal of Pediatrics*, 74.
- Tseng, A., Seet, J. and Phillips, E. J. (2015) 'The evolution of three decades of antiretroviral therapy: Challenges, triumphs and the promise of the future', *British Journal of Clinical Pharmacology*, 79(2), pp. 182–194. doi: 10.1111/bcp.12403.
- UNAIDS (2016) *Fact sheet – Latest global and regional statistics on the status of the AIDS epidemic*.
- van Vonderen, M. G., Blumer, R. M., Hassink, E. A., Sutinen, J., Ackermans, M. T., van Agtmael, M. A., Yki-Jarvinen, H., Danner, S. A., Serlie, M. J., Sauerwein, H. P. and Reiss, P. (2010) 'Insulin sensitivity in multiple pathways is differently affected during zidovudine/lamivudine-containing compared with NRTI-sparing combination antiretroviral therapy', *Journal of Acquired Immune Deficiency Syndromes: JAIDS*, 53(1944–7884

(Electronic)), pp. 186–193. doi: 10.1097/QAI.0b013e3181c190f4.

- Wieczorek, G., Pospischil, A. and Perentes, E. (1998) ‘A comparative immunohistochemical study of pancreatic islets in laboratory animals (rats, dogs, minipigs, nonhuman primates)’, *Experimental and Toxicologic Pathology*. Gustav Fischer Verlag, 50(3), pp. 151–172. doi: 10.1016/S0940-2993(98)80078-X.
- Wilhelmsen, M., Amirian, I., Reiter, R. J., Rosenberg, J. and Gögenur, I. (2011) ‘Analgesic effects of melatonin: a review of current evidence from experimental and clinical studies.’, *Journal of pineal research*, 51(3), pp. 270–7. doi: 10.1111/j.1600-079X.2011.00895.x.
- Wolden-Hanson, T., Mitton, D. R., McCants, R. L., Yellon, S. M., Wilkinson, C. W., Matsumoto, A. M. and Rasmussen, D. D. (2000) ‘Daily Melatonin Administration to Middle-Aged Male Rats Suppresses Body Weight, Intraabdominal Adiposity, and Plasma Leptin and Insulin Independent of Food Intake and Total Body Fat <sup>1</sup>’, *Endocrinology*. San Diego, CA, 141(2), pp. 487–497. doi: 10.1210/endo.141.2.7311.
- Young, B. and O’Dowd, G. (2014) *Wheater’s Functional Histology*. 6th edn. Philadelphia: Elsevier Ltd.
- Yousaf, F., Seet, E., Venkatraghavan, L., Abrishami, A. and Chung, F. (2010) ‘Efficacy and Safety of Melatonin as an Anxiolytic and Analgesic in the Perioperative Period A Qualitative Systematic Review of Randomized Trials’, *Anesthesiology*, 113(4), pp. 968–76. doi: 10.1097/ALN.0b013e3181e7d626.



## APPENDIX 1 Haematoxylin and eosin protocol

The staining was done using an automated stainer (Leica Auto Stainer XL; Manufacturer & Model: Leica St 5010; Serial Number 1732/07.2007).

### **Procedure:**

1. Dewax sections through xylene and alcohol.
2. Stain in Haematoxylin for 4 minutes.
3. Wash in running tap water for 3 minutes.
4. Stain in Eosin for 2.30 seconds.
5. Wash in running tap water for 2 minutes.
6. Dehydrate and mount with DPX mounting medium.

### Results:

Nuclei----- Blue

Cytoplasm----- Pink

Red blood cells, eosinophilic granules, other tissue elements--- Varying shades of pink

## APPENDIX 2 Immunolabeling for anti-glucagon and anti-insulin protocol

Medical Research Council of South Africa SOP No: ICC\B7-V01

### **Reagents:**

- Distilled Water
- Hydrogen Peroxide
- 0.05M Tris Buffered Saline (TBS) pH7.2
- 0.1M Phosphate Buffered Saline (PBS) pH7.2
- Normal Goat Serum
- Normal Horse Serum
- Polyclonal Anti-Glucagon (Doka, North America)
- Monoclonal Anti-Insulin (Doka, North America)
- Biotinylated Rabbit Anti-IgG
- Biotinylated Mouse Anti-IgG
- Vectastain (Doka, North America)
- EnvisionG/2 System/AP Kit
- Liquid DAB+ Substrate Chromagen Solution (Doka, North America)
- Haematoxylin

### **Procedure:**

1. Dewax sections through xylene and alcohol.
2. Rinse slides in staining jar in distilled water.
3. Block for endogenous peroxidase with 3% hydrogen peroxide (H<sub>2</sub>O<sub>2</sub>) for five (5) minutes in staining jar. (6ml H<sub>2</sub>O<sub>2</sub>/194ml distilled water – left fridge).
4. Rinse slides with 0.05M TBS pH7.2 for five (5) minutes in staining jar.
5. Dry around section and add normal goat serum (NGS) 1:20 to slides in a moisture chamber (completely cover the section) for twenty (20) minutes at room temperature (18°C- 20°C).

6. Blot excess serum. (Do not rinse).
7. Add approximately 100µl anti-glucagon (P) (primary antibody) 1:100 to sections in moisture chamber and incubate at room temperature (18°C- 20°C) for thirty (30) minutes.
8. Jet wash with 0.05M TBS pH7.2 and rinse in staining jar in 0.05M TBS pH7.2 for five (5) minutes. (N.B. Make up Biotinylated Anti-Rabbit IgG and Vectastain).
9. Dry around sections and add Biotinylated Anti-Rabbit IgG 1:200 to slides in moisture chamber for (30) minutes at room temperature (18°C- 20°C).
10. Jet wash with 0.05M TBS pH7.2 and rinse in staining jar in 0.05M TBS pH7.2 for ten (10) minutes.
11. Dry around sections and add Vectastain to slides in moisture chamber for one (1) hour at room temperature (18°C- 20°C).
12. Jet wash slides with 0.05M TBS pH 7.2 and rinse for ten (10) minutes in 0.05M TBS pH7.2 in staining jar.
13. Dry around sections and add Liquid DAB+ Chromagen solution to slides on a rack over the sink for five (5) minutes. (Check progress under microscope).
14. Jet wash slides with distilled water and rinse with distilled water in a staining jar for five (5) minutes.
15. Rinse slides in 0.05M TBS pH7.2 in staining jar for five (5) minutes.
16. Dry around section and add normal horse serum (NHS) 1:20 to slides in a moisture chamber
17. (completely cover the section) for twenty (20) minutes at room temperature (R.T.) (18°C- 20°C).
18. Blot excess serum. (Do not rinse).
19. Add approximately 100µl anti-insulin (M) 1:10 000 to sections in moisture chamber and incubate at 4°C overnight.
20. Allow slides to reach room temperature.

21. Jet wash with 0.05M TBS pH7.2 and rinse in staining jar in 0.05M TBS pH7.2 for five (5) minutes.
22. Dry around sections and add 100µl Rabbit/Mouse (LINK) to slides in moisture chamber for thirty (30) minutes at room temperature (R.T.) (18°C- 20°C).
23. Jet wash with 0.05M TBS pH7.2 and rinse in staining jar in 0.05M TBS pH7.2 for ten (10) minutes.
24. Dry around sections and add 100ul AP Enzyme (ENHANCER) to slides in moisture chamber thirty (30) minutes at room temperature (R.T.) (18°C- 20°C).
25. Jet wash slides with 0.05M TBS pH 7.2 and rinse for ten (10) minutes in 0.05M TBS

## APPENDIX 3 Periodic acid Schiff protocol

### **Solutions and Reagents:**

#### 0.5% Periodic Acid Solution:

Periodic acid-----0.5g

Distilled water-----100ml

### **Schiff's reagent:**

Schiff's reagent with pararosaline

### **Procedure:**

1. Deparaffinize and hydrate to water.
2. Treat with periodic acid for 5 minutes.
3. Rinse well in distilled water.
4. Cover with Schiff's reagent for 15 minutes.
5. Wash in running lukewarm tap water for 5 minutes.
6. Counter stain with Mayer's haematoxylin for 1 minute.
7. Wash in tap water for 5 minutes.
8. Dehydrate and mount with DPX mounting medium.

### **Results:**

Glycogen, mucin and some basement membranes-----red/purple

Fungi-----red/purple

Background-----blue

**APPENDIX 4 Liver enzyme tests****Analyzer:** Roche/Hitachi cobas c 311, cobas c 501/502**Table A Materials needed for AST and ALT tests**

20764957 322	Alanine Aminotransferase acc. to IFCC 500 tests	System-ID 07 6495 7
20764949 322	Aspartate Aminotransferase acc. to IFCC 500 tests	System-ID 07 6494 9
10759350 190	Calibrator f.a.s. (12 x 3 mL)	Code 401
10759350 360	Calibrator f.a.s. (12 x 3 mL, for USA)	Code 401
12149435 122	Precinorm U plus (10 x 3 mL)	Code 300
12149435 160	Precinorm U plus (10 x 3 mL, for USA)	Code 300
12149443 122	Precipath U plus (10 x 3 mL)	Code 301
12149443 160	Precipath U plus (10 x 3 mL, for USA)	Code 301
10171743 122	Precinorm U (20 x 5 mL)	Code 300
10171778 122	Precipath U (20 x 5 mL)	Code 301
10171760 122	Precipath U (4 x 5 mL)	Code 301
05117003 190	PreciControl ClinChem Multi 1 (20 x 5 mL)	Code 391
05947626 190	PreciControl ClinChem Multi 1 (4 x 5 mL)	Code 391
05947626 160	PreciControl ClinChem Multi 1 (4 x 5 mL, for USA)	Code 391
05117216 190	PreciControl ClinChem Multi 2 (20 x 5 mL)	Code 392
05947774 190	PreciControl ClinChem Multi 2 (4 x 5 mL)	Code 392
05947774 160	PreciControl ClinChem Multi 2 (4 x 5 mL, for USA)	Code 392
04489357 190	Diluent NaCl 9 % (50 mL)	System-ID 07 6869 3

## Aspartate Aminotransferase (AST)

### Reagents:

1. TRIS buffer: 264 mmol/L, pH 7.8 (37 °C); L-aspartate: 792 mmol/L; MDH (microorganism): 24  $\mu$ kat/L; LDH (microorganisms):  $\geq$  48  $\mu$ kat/L; albumin (bovine): 0.25 %; preservative
2. NADH:  $\geq$  1.7 mmol/L; 2-oxoglutarate: 94 mmol/L; preservative

### Assay:

Assay type-----	Rate A
Reaction time / Assay points-----	10 / 12-31
Wavelength (sub/main) -----	700/340 nm
Reaction direction-----	Decrease
Units -----	U/L ( $\mu$ kat/L)
Reagent pipetting-----	Diluent (H <sub>2</sub> O)
Reagent 1-----	51 $\mu$ L
Reagent 2-----	20 $\mu$ L

**Alanine Aminotransferase (ALT)****Reagents:**

1. TRIS buffer: 224 mmol/L, pH 7.3 (37 °C); L-alanine: 1120 mmol/L; albumin (bovine): 0.25 %; LDH (microorganisms):  $\geq 45 \mu\text{kat/L}$ ; stabilizers; preservative
2. 2-Oxoglutarate: 94 mmol/L; NADH:  $\geq 1.7 \text{ mmol/L}$ ; additives; preservative

**Assay:**

Assay type-----	Rate A
Reaction time / Assay points-----	10 / 12-31
Wavelength (sub/main) -----	700/340 nm
Reaction direction-----	Decrease
Units -----	U/L ( $\mu\text{kat/L}$ )
Reagent pipetting-----	Diluent (H <sub>2</sub> O)
Reagent 1-----	32 $\mu\text{L}$
Reagent 2-----	20 $\mu\text{L}$



## APPENDIX 5 p-values obtained from pancreas measurements

**P-values for Table 4.1: Summary of the measurements on the pancreatic islets in the pancreas labelled with anti-insulin and anti-glucagon  $\pm$  SD of the four treatment groups.**

Cell No.	LSD test; variable Total Islet area (Breakdown Table of Descriptive Statistics (Spreadsheet in Corrected islet area.stw) in Corrected islet area.stw) Probabilities for Post Hoc Tests Error: Between MS = 2496E3, df = 36.000				
	Treatment	{1} 4755.7	{2} 4113.9	{3} 4928.8	{4} 5249.8
1	C/ART-		0.369736	0.807860	0.488799
2	ART	0.369736		0.256375	0.116628
3	ART+/M+	0.807860	0.256375		0.652261
4	C/M+	0.488799	0.116628	0.652261	

**P-values for Figure 0.1: The area of the  $\alpha$ - and  $\beta$ -cells did not differ between the four treatment groups.**

Cell No.	LSD test; variable A cell area (Breakdown Table of Descriptive Statistics (Spreadsheet in Corrected islet area.stw) in Corrected islet area.stw) Probabilities for Post Hoc Tests Error: Between MS = 48882., df = 36.000				
	Treatment	{1} 443.58	{2} 352.71	{3} 442.87	{4} 582.72
1	C/ART-		0.364205	0.994338	0.167934
2	ART	0.364205		0.367904	<b>0.025751</b>
3	ART+/M+	0.994338	0.367904		0.165842
4	C/M+	0.167934	<b>0.025751</b>	0.165842	

**P-values for Figure 0.2: The area of the  $\alpha$ - and  $\beta$ -cells did not differ between the four treatment groups.**

Cell No.	LSD test; variable B cell area (Breakdown Table of Descriptive Statistics (Spreadsheet in Corrected islet area.stw) in Corrected islet area.stw) Probabilities for Post Hoc Tests Error: Between MS = 7031E2, df = 36.000				
	Treatment	{1} 1902.8	{2} 1468.6	{3} 1880.7	{4} 1838.7
1	C/ART-		0.254550	0.953459	0.865417
2	ART	0.254550		0.279031	0.330158
3	ART+/M+	0.953459	0.279031		0.911503
4	C/M+	0.865417	0.330158	0.911503	

**P-values for Table 0-1: Percentage of  $\alpha$ -cell area and  $\beta$ -cell area in the pancreatic islets  $\pm$  SD of the four treatment groups**

Cell 1	LSD test; variable % A cells (Breakdown Table of Descriptive Statistics (Spreadsheet in Corrected islet area.stw) in Corrected islet area.stw) Probabilities for Post Hoc Tests Error: Between MS = 6.2989, df = 36.000				
	No.	Treatment	{1} 6.6474	{2} 5.8641	{3} 6.8949
1	C/ART-		0.489761	0.826722	0.853081
2	ART	0.489761		0.364550	0.382369
3	ART+/M+	0.826722	0.364550		0.973078
4	C/M+	0.853081	0.382369	0.973078	

**P-values for Table 0-2: Percentage of  $\alpha$ -cell area and  $\beta$ -cell area in the pancreatic islets  $\pm$  SD of the four treatment groups**

Cell 1	LSD test; variable % B cells (Breakdown Table of Descriptive Statistics (Spreadsheet in Corrected islet area.stw) in Corrected islet area.stw) Probabilities for Post Hoc Tests Error: Between MS = 55.416, df = 36.000				
	No.	Treatment	{1} 36.070	{2} 34.905	{3} 33.213
1	C/ART-		0.728255	0.396346	0.464460
2	ART	0.728255		0.614382	0.699397
3	ART+/M+	0.396346	0.614382		0.905927
4	C/M+	0.464460	0.699397	0.905927	

## APPENDIX 6 p-values obtained from body weight and liver enzyme tests

**P-values for the graphs of figure 4.1: Body mass of the rats did not differ significantly between the four treatment groups**

Comparisons Cell {#1}-{#2}	LSD test; variable Body weight (Body weights) Simultaneous confidence intervals Effect: Treatment						
	1st Mean	2nd Mean	Mean Differ.	Standard Error	P	-95,00% Cnf.Lmt	+95,00% Cnf.Lmt
{1}-{2}	C/ART-	C/ART+	10.9351	9.33022	0.247502	-7.8688	29.73888
{1}-{3}	C/ART-	C/M+	-3.7143	8.75252	0.673366	-21.3538	13.92526
{1}-{4}	C/ART-	ART+/M+	4.5714	9.89375	0.646320	-15.3681	24.51096
{2}-{3}	C/ART+	C/M+	-14.6494	9.33022	0.123557	-33.4532	4.15447
{2}-{4}	C/ART+	ART+/M+	-6.3636	10.40829	0.544081	-27.3402	14.61290
{3}-{4}	C/M+	ART+/M+	8.2857	9.89375	0.406855	-11.6538	28.22525

**P-values for Table 0-3: Summary of the values from liver function tests  $\pm$  SD of the four treatment groups**

Cell No.	Treatment	LSD test; variable Alanine transaminase (ALT) (Spreadsheet in Workbook18) Probabilities for Post Hoc Tests Error: Between MS = 946.30, df = 33.000			
		{1} 62.400	{2} 54.400	{3} 59.400	{4} 68.143
1	C/ART-		0.564846	0.828719	0.707245
2	C/ART+	0.564846		0.718590	0.371223
3	C/M+	0.828719	0.718590		0.568044
4	ART+/M+	0.707245	0.371223	0.568044	

**P-values for Table 0-4: Summary of the values from liver function tests  $\pm$  SD of the four treatment groups**

		LSD test; variable Aspartate transaminase (AST) (Spreadsheet in Workbook18) Probabilities for Post Hoc Tests Error: Between MS = 7374.8, df = 33.000			
Cell No.	Treatment	{1}	{2}	{3}	{4}
		181.50	160.80	188.60	217.71
1	C/ART-		0.593512	0.854462	0.398326
2	C/ART+	0.593512		0.474252	0.187847
3	C/M+	0.854462	0.474252		0.496293
4	ART+/M+	0.398326	0.187847	0.496293	

**P-values for Table 0-5: Summary of the values from liver function tests  $\pm$  SD of the four treatment groups**

		LSD test; variable AST/ALT Ratio (Spreadsheet in Workbook18) Probabilities for Post Hoc Tests Error: Between MS = .48465, df = 33.000			
Cell No.	Treatment	{1}	{2}	{3}	{4}
		2.9212	3.0161	3.3243	3.2985
1	C/ART-		0.762335	0.204371	0.279335
2	C/ART+	0.762335		0.329433	0.416314
3	C/M+	0.204371	0.329433		0.940569
4	ART+/M+	0.279335	0.416314	0.940569	

**P-values for Figure 0.3: Serum haemoglobin value differed significantly between the C/ART- group and C/ART+ group.**

		LSD test; variable Serum haemoglobin value (Spreadsheet in Workbook18) Probabilities for Post Hoc Tests Error: Between MS = 1849.0, df = 31.000			
Cell No.	Treatment	{1}	{2}	{3}	{4}
		50.900	98.000	66.200	92.167
1	C/ART-		0.023435	0.432302	0.072627
2	C/ART+	0.023435		0.117636	0.798576
3	C/M+	0.432302	0.117636		0.251157
4	ART+/M+	0.072627	0.798576	0.251157	

**P-values for Figure 0.4: Serum lipaemia value differed significantly between the C/ART- group and C/M+ group.**

		LSD test; variable Serum lipaemia value (Spreadsheet in Workbook18) Probabilities for Post Hoc Tests Error: Between MS = 18.782, df = 31.000			
Cell No.	Treatment	{1}	{2}	{3}	{4}
		12.000	8.3333	6.9000	9.6667
1	C/ART-		0.075150	0.013130	0.305189
2	C/ART+	0.075150		0.477028	0.563616
3	C/M+	0.013130	0.477028		0.225653
4	ART+/M+	0.305189	0.563616	0.225653	

### APPENDIX 7 p-values obtained from kidney measurements

**P-values for Figure 0.5: The area, diameter, perimeter and radius of the renal corpuscle differed significantly between the four treatment groups.**

Comparisons Cell {#1}- {#2}	LSD test; variable <b>Area</b> (Spreadsheet in Kidney data final.stw) Simultaneous confidence intervals Effect: Treatment Include condition: V4="Renal Corpuscle"						
	1st Mean	2nd Mean	Mean Differ.	Standard Error	p	-95.00% Cnf.Lmt	+95.00% Cnf.Lmt
{1}-{2}	C/ART-	C/ART+	1709.519	509.6210	0.001884	675.96	2743.078
{1}-{3}	C/ART-	C/M+	1142.314	509.6210	0.031251	108.75	2175.873
{1}-{4}	C/ART-	ART+/M+	991.141	509.6210	0.059636	-42.42	2024.701
{2}-{3}	C/ART+	C/M+	-567.205	509.6210	0.273088	-1600.76	466.355
{2}-{4}	C/ART+	ART+/M+	-718.377	509.6210	0.167230	-1751.94	315.182
{3}-{4}	C/M+	ART+/M+	-151.173	509.6210	0.768448	-1184.73	882.387

**P-values for Figure 0.6: The area, diameter, perimeter and radius of the renal corpuscle differed significantly between the four treatment groups.**

Comparisons Cell {#1}- {#2}	LSD test; variable <b>Diameter</b> (Spreadsheet in Kidney data final.stw) Simultaneous confidence intervals Effect: Treatment Include condition: V4="Renal Corpuscle"						
	1st Mean	2nd Mean	Mean Differ.	Standard Error	p	-95.00% Cnf.Lmt	+95.00% Cnf.Lmt
{1}-{2}	C/ART-	C/ART+	10.35700	3.058108	0.001724	4.1549	16.55913
{1}-{3}	C/ART-	C/M+	7.31875	3.058108	0.022039	1.1166	13.52088
{1}-{4}	C/ART-	ART+/M+	5.75510	3.058108	0.067952	-0.4470	11.95723
{2}-{3}	C/ART+	C/M+	-3.03824	3.058108	0.327096	-9.2404	3.16389
{2}-{4}	C/ART+	ART+/M+	-4.60190	3.058108	0.141095	-10.8040	1.60023
{3}-{4}	C/M+	ART+/M+	-1.56365	3.058108	0.612253	-7.7658	4.63848

**P-values for Figure 0.7: The area, diameter, perimeter and radius of the renal corpuscle differed significantly between the four treatment groups.**

Comparisons Cell {#1}- {#2}	LSD test; variable <b>Perimeter</b> (Spreadsheet in Kidney data final.stw) Simultaneous confidence intervals Effect: Treatment Include condition: V4="Renal Corpuscle"						
	1st Mean	2nd Mean	Mean Differ.	Standard Error	P	-95.00% Cnf.Lmt	+95.00% Cnf.Lmt
{1}-{2}	C/ART-	C/ART+	32.5329	9.476150	0.001516	13.3143	51.75139
{1}-{3}	C/ART-	C/M+	22.0288	9.476150	0.025846	2.8103	41.24734
{1}-{4}	C/ART-	ART+/M+	19.0597	9.476150	0.051823	-0.1589	38.27819
{2}-{3}	C/ART+	C/M+	-10.5041	9.476150	0.275008	-29.7226	8.71447
{2}-{4}	C/ART+	ART+/M+	-13.4732	9.476150	0.163690	-32.6917	5.74532
{3}-{4}	C/M+	ART+/M+	-2.9692	9.476150	0.755839	-22.1877	16.24937

**P-values for Figure 0.8: The area, diameter, perimeter and radius of the renal corpuscle differed significantly between the four treatment groups.**

Comparisons Cell {#1}- {#2}	LSD test; variable <b>Radius</b> (Spreadsheet in Kidney data final.stw) Simultaneous confidence intervals Effect: Treatment Include condition: V4="Renal Corpuscle"						
	1st Mean	2nd Mean	Mean Differ.	Standard Error	P	-95.00% Cnf.Lmt	+95.00% Cnf.Lmt
{1}-{2}	C/ART-	C/ART+	5.17850	1.515774	0.001588	2.10437	8.252630
{1}-{3}	C/ART-	C/M+	3.65938	1.515774	0.020980	0.58524	6.733509
{1}-{4}	C/ART-	ART+/M+	3.15234	1.515774	0.044735	0.07820	6.226470
{2}-{3}	C/ART+	C/M+	-1.51912	1.515774	0.322932	-4.59325	1.555012
{2}-{4}	C/ART+	ART+/M+	-2.02616	1.515774	0.189702	-5.10029	1.047972
{3}-{4}	C/M+	ART+/M+	-0.50704	1.515774	0.739937	-3.58117	2.567093

**P-values for Figure 0.9: The area, diameter, and radius of the glomerulus differed significantly between the four treatment groups.**

Comparisons Cell {#1}- {#2}	LSD test; variable <b>Area</b> (Spreadsheet in Kidney data final.stw) Simultaneous confidence intervals Effect: Treatment Include condition: V4="Glomerulus"						
	1st Mean	2nd Mean	Mean Differ.	Standard Error	p	-95.00% Cnf.Lmt	+95.00% Cnf.Lmt
{1}-{2}	<b>C/ART-</b>	<b>C/ART+</b>	<b>841.725</b>	<b>363.5612</b>	<b>0.026414</b>	<b>104.39</b>	<b>1579.061</b>
{1}-{3}	C/ART-	C/M+	-6.997	363.5612	0.984752	-744.33	730.340
{1}-{4}	C/ART-	ART+/M+	11.248	363.5612	0.975489	-726.09	748.585
{2}-{3}	<b>C/ART+</b>	<b>C/M+</b>	<b>-848.722</b>	<b>363.5612</b>	<b>0.025267</b>	<b>-1586.06</b>	<b>-111.385</b>
{2}-{4}	<b>C/ART+</b>	<b>ART+/M+</b>	<b>-830.477</b>	<b>363.5612</b>	<b>0.028355</b>	<b>-1567.81</b>	<b>-93.140</b>
{3}-{4}	C/M+	ART+/M+	18.245	363.5612	0.960253	-719.09	755.581

**P-values for Figure 0.10: The area, diameter and radius of the glomerulus differed significantly between the four treatment groups.**

Comparisons Cell {#1}- {#2}	LSD test; variable <b>Diameter</b> (Spreadsheet in Kidney data final.stw) Simultaneous confidence intervals Effect: Treatment Include condition: V4="Glomerulus"						
	1st Mean	2nd Mean	Mean Differ.	Standard Error	p	-95.00% Cnf.Lmt	+95.00% Cnf.Lmt
{1}-{2}	<b>C/ART-</b>	<b>C/ART+</b>	<b>6.16025</b>	<b>2.896538</b>	<b>0.040363</b>	<b>0.2858</b>	<b>12.03470</b>
{1}-{3}	C/ART-	C/M+	-0.34540	2.896538	0.905744	-6.2198	5.52905
{1}-{4}	C/ART-	ART+/M+	0.20879	2.896538	0.942935	-5.6657	6.08324
{2}-{3}	<b>C/ART+</b>	<b>C/M+</b>	<b>-6.50564</b>	<b>2.896538</b>	<b>0.030934</b>	<b>-12.3801</b>	<b>-0.63119</b>
{2}-{4}	<b>C/ART+</b>	<b>ART+/M+</b>	<b>-5.95146</b>	<b>2.896538</b>	<b>0.047223</b>	<b>-11.8259</b>	<b>-0.07700</b>
{3}-{4}	C/M+	ART+/M+	0.55419	2.896538	0.849344	-5.3203	6.42864



**P-values for Figure 0.11: The area, diameter and radius of the glomerulus differed significantly between the four treatment groups.**

Comparisons Cell {#1}- {#2}	LSD test; variable <b>Perimeter</b> (Spreadsheet in Kidney data final.stw) Simultaneous confidence intervals Effect: Treatment Include condition: V4="Glomerulus"						
	1st Mean	2nd Mean	Mean Differ.	Standard Error	p	-95.00% Cnf.Lmt	+95.00% Cnf.Lmt
{1}-{2}	C/ART-	C/ART+	16.8921	17.53998	0.341941	-18.6806	52.46481
{1}-{3}	C/ART-	C/M+	9.1842	17.53998	0.603753	-26.3885	44.75697
{1}-{4}	C/ART-	ART+/M+	5.6470	17.53998	0.749354	-29.9258	41.21970
{2}-{3}	C/ART+	C/M+	-7.7078	17.53998	0.662967	-43.2806	27.86489
{2}-{4}	C/ART+	ART+/M+	-11.2451	17.53998	0.525510	-46.8178	24.32762
{3}-{4}	C/M+	ART+/M+	-3.5373	17.53998	0.841311	-39.1100	32.03546

**P-values for Figure 0.12: The area, diameter and radius of the glomerulus differed significantly between the four treatment groups.**

Comparisons Cell {#1}- {#2}	LSD test; variable <b>Radius</b> (Spreadsheet in Kidney data final.stw) Simultaneous confidence intervals Effect: Treatment Include condition: V4="Glomerulus"						
	1st Mean	2nd Mean	Mean Differ.	Standard Error	p	-95.00% Cnf.Lmt	+95.00% Cnf.Lmt
{1}-{2}	C/ART-	C/ART+	3.08012	1.438921	0.039154	0.16186	5.998391
{1}-{3}	C/ART-	C/M+	-0.17270	1.438921	0.905135	-3.09097	2.745569
{1}-{4}	C/ART-	ART+/M+	-0.57846	1.438921	0.690055	-3.49673	2.339809
{2}-{3}	C/ART+	C/M+	-3.25282	1.438921	0.029927	-6.17109	-0.334554
{2}-{4}	C/ART+	ART+/M+	-3.65858	1.438921	0.015447	-6.57685	-0.740314
{3}-{4}	C/M+	ART+/M+	-0.40576	1.438921	0.779567	-3.32403	2.512508

**P-values for Figure 0.13: The area, diameter, perimeter and radius of the LPCT differed significantly between the four treatment groups.**

Comparisons Cell {#1}- {#2}	LSD test; variable <b>Area</b> (Spreadsheet in Kidney data final.stw) Simultaneous confidence intervals Effect: Treatment Include condition: V4="Tubule 1 & 2 & 3"						
	1st Mean	2nd Mean	Mean Differ.	Standard Error	P	-95.00% Cnf.Lmt	+95.00% Cnf.Lmt
{1}-{2}	C/ART-	C/ART+	408.849	137.5168	0.005232	129.952	687.7457
{1}-{3}	C/ART-	C/M+	254.706	137.5135	0.072208	-24.185	533.5959
{1}-{4}	C/ART-	ART+/M+	200.874	137.5135	0.152754	-78.016	479.7646
{2}-{3}	C/ART+	C/M+	-154.143	137.5168	0.269751	-433.040	124.7540
{2}-{4}	C/ART+	ART+/M+	-207.974	137.5168	0.139173	-486.871	70.9226
{3}-{4}	C/M+	ART+/M+	-53.831	137.5135	0.697763	-332.722	225.0589

**P-values for Figure 0.14: The area, diameter, perimeter and radius of the LPCT differed significantly between the four treatment groups.**

Comparisons Cell {#1}- {#2}	LSD test; variable <b>Diameter</b> (Spreadsheet in Kidney data final.stw) Simultaneous confidence intervals Effect: Treatment Include condition: V4="Tubule 1 & 2 & 3"						
	1st Mean	2nd Mean	Mean Differ.	Standard Error	P	-95.00% Cnf.Lmt	+95.00% Cnf.Lmt
{1}-{2}	C/ART-	C/ART+	4.98580	1.645109	0.004500	1.64937	8.322238
{1}-{3}	C/ART-	C/M+	2.98114	1.645073	0.078309	-0.35523	6.317499
{1}-{4}	C/ART-	ART+/M+	2.66504	1.645073	0.113958	-0.67132	6.001402
{2}-{3}	C/ART+	C/M+	-2.00467	1.645109	0.230936	-5.34110	1.331769
{2}-{4}	C/ART+	ART+/M+	-2.32076	1.645109	0.166915	-5.65720	1.015672
{3}-{4}	C/M+	ART+/M+	-0.31610	1.645073	0.848706	-3.65246	3.020266

**P-values for Figure 0.15: The area, diameter, perimeter and radius of the LPCT differed significantly between the four treatment groups.**

Comparisons Cell {#1}- {#2}	LSD test; variable <b>Perimeter</b> (Spreadsheet in Kidney data final.stw) Simultaneous confidence intervals Effect: Treatment Include condition: V4="Tubule 1 & 2 & 3"						
	1st Mean	2nd Mean	Mean Differ.	Standard Error	p	-95.00% Cnf.Lmt	+95.00% Cnf.Lmt
{1}-{2}	C/ART-	C/ART+	15.86502	5.364894	0.005453	4.9845	26.74553
{1}-{3}	C/ART-	C/M+	10.84465	5.364757	0.050715	-0.0356	21.72488
{1}-{4}	C/ART-	ART+/M+	8.46239	5.364757	0.123450	-2.4178	19.34262
{2}-{3}	C/ART+	C/M+	-5.02037	5.364894	0.355621	-15.9009	5.86014
{2}-{4}	C/ART+	ART+/M+	-7.40263	5.364894	0.176150	-18.2831	3.47788
{3}-{4}	C/M+	ART+/M+	-2.38226	5.364757	0.659659	-13.2625	8.49797

**P-values for Figure 0.16: The area, diameter, perimeter and radius of the LPCT differed significantly between the four treatment groups.**

Comparisons Cell {#1}- {#2}	LSD test; variable <b>Radius</b> (Spreadsheet in Kidney data final.stw) Simultaneous confidence intervals Effect: Treatment Include condition: V4="Tubule 1 & 2 & 3"						
	1st Mean	2nd Mean	Mean Differ.	Standard Error	p	-95.00% Cnf.Lmt	+95.00% Cnf.Lmt
{1}-{2}	C/ART-	C/ART+	2.49298	0.912873	0.009718	0.64159	4.344374
{1}-{3}	C/ART-	C/M+	1.49057	0.912839	0.111209	-0.36076	3.341892
{1}-{4}	C/ART-	ART+/M+	0.81550	0.912839	0.377593	-1.03582	2.666826
{2}-{3}	C/ART+	C/M+	-1.00241	0.912873	0.279457	-2.85381	0.848979
{2}-{4}	C/ART+	ART+/M+	-1.67748	0.912873	0.074389	-3.52887	0.173914
{3}-{4}	C/M+	ART+/M+	-0.67507	0.912839	0.464385	-2.52639	1.176259

**P-values for Figure 0.17: Proximal tubule area differed significantly between the four treatment groups.**

Comparisons Cell {#1}-{#2}	LSD test; variable <b>tubule thickness</b> (Spreadsheet395 in Kidney data final.stw) Simultaneous confidence intervals Effect: Treatment				
	1st Mean	2nd Mean	Mean Differ.	Standard Error	p
{1}-{2}	<b>C/ART-</b>	<b>C/ART+</b>	<b>283.87</b>	<b>96.64</b>	<b>0.01</b>
{1}-{3}	<b>C/ART-</b>	<b>C/M+</b>	<b>220.57</b>	<b>96.63</b>	<b>0.03</b>
{1}-{4}	C/ART-	ART+/M+	154.70	96.63	0.12
{2}-{3}	C/ART+	C/M+	-63.30	96.64	0.52
{2}-{4}	C/ART+	ART+/M+	-129.17	96.64	0.19
{3}-{4}	C/M+	ART+/M+	-65.87	96.64	0.50

**P-values for Figure 0.18: The renal space differed significantly between the four treatment groups**

Comparisons Cell {#1}-{#2}	LSD test; variable <b>Renal space</b> (Spreadsheet in Kidney data final.stw) Simultaneous confidence intervals Effect: Treatment				
	1st Mean	2nd Mean	Mean Differ.	Standard Error	p
{1}-{2}	<b>C/ART-</b>	<b>C/ART+</b>	<b>867.79</b>	<b>287.89</b>	<b>0.00</b>
{1}-{3}	<b>C/ART-</b>	<b>C/M+</b>	<b>1149.31</b>	<b>287.89</b>	<b>0.00</b>
{1}-{4}	<b>C/ART-</b>	<b>ART+/M+</b>	<b>979.89</b>	<b>287.89</b>	<b>0.00</b>
{2}-{3}	C/ART+	C/M+	281.52	287.89	0.33
{2}-{4}	C/ART+	ART+/M+	112.10	287.89	0.70
{3}-{4}	C/M+	ART+/M+	-169.42	287.89	0.56

**APPENDIX 8 Pathology observed in the pancreas**

Rat number	Treatment	Pancreas	
		Score	Proteinaceous material
94	C/ART-	0	0
112	C/ART+	0	0
130	C/ART+	0	0
154	C/ART-	0	0
160	C/ART+	0	0
166	C/ART+	0	0
172	C/ART-	0	0
190	ART+/M+	0	0
196	ART+/M+	0	0
202	ART+/M+	0	0
208	ART+/M+	0	0
214	ART+/M+	0	0
238	C/ART-	0	0
256	C/ART-	0	0
280	C/ART+	0	0
292	C/ART+	0	0
304	C/ART-	0	0
310	C/M+	0	0
316	C/M+	0	0
322	C/M+	0	0
328	C/M+	0	1
343	C/M+	0	0
349	C/M+	0	0
355	C/M+	0	0
361	C/M+	0	0
1573	C/ART-	0	0
1578	C/M+	0	1
1583	C/ART-	0	0
1593	C/ART-	0	0

1603	ART+/M+	0	0
1608	C/ART+	0	0
1621	C/ART+	0	0
1626	C/ART+	0	0
1636	C/ART+	0	0
1646	ART+/M+	0	0
1656	ART+/M+	0	0
1661	ART+/M+	0	0
1666	C/M+	0	0
1671	ART+/M+	0	0
1681	C/ART+	0	0
<b>Total</b>		<b>0</b>	<b>2</b>

**APPENDIX 9 Pathology observed in the liver**

Rat number	Treatment	Liver				
		Score	Granular appearance	Loss of hepatocyte architecture	Lymphocyte infiltration	Vacuolation
94	C/ART-	1	1	0	0	1
112	C/ART+	0	0	0	0	0
130	C/ART+	0	0	0	0	0
154	C/ART-	0	0	0	0	0
160	C/ART+	0	0	0	0	0
166	C/ART+	1	0	1	0	0
172	C/ART-	0	0	0	0	0
190	ART+/M+	0	0	0	0	0
196	ART+/M+	0	0	0	0	0
202	ART+/M+	0	0	0	0	0
208	ART+/M+	0	0	0	0	0
214	ART+/M+	0	0	0	0	0
238	C/ART-	0	0	0	0	1
256	C/ART-	0	0	0	0	1
280	C/ART+	0	0	0	0	0
292	C/ART+	0	0	0	0	0
304	C/ART-	0	0	0	0	0
310	C/M+	0	0	0	0	0
316	C/M+	0	0	0	0	0
322	C/M+	1	0	0	1	0
328	C/M+	1	1	0	0	0
343	C/M+	0	0	0	0	0
349	C/M+	0	0	0	0	0
355	C/M+	0	0	0	0	0
361	C/M+	0	0	0	0	0
1573	C/ART-	1	1	0	0	0

1578	C/M+	1	1	0	0	1
1583	C/ART-	1	1	0	0	0
1593	C/ART-	1	1	0	0	1
1603	ART+/M+	1	1	0	0	0
1608	C/ART+	0	0	0	0	0
1621	C/ART+	0	0	0	0	0
1626	C/ART+	1	1	0	0	1
1636	C/ART+	1	1	0	0	0
1646	ART+/M+	0	0	0	0	0
1656	ART+/M+	0	0	0	0	0
1661	ART+/M+	0	0	0	0	0
1666	C/M+	0	0	0	0	0
1671	ART+/M+	0	0	0	0	0
1681	C/ART+	0	0	0	0	0
<b>Total</b>		<b>11</b>	<b>9</b>	<b>1</b>	<b>1</b>	<b>6</b>



**APPENDIX 10 Pathology observed in the kidney**

Rat number	Treatment	Kidney		
		Score	Swelling	Vacuolation
94	C/ART-	0	0	0
112	C/ART+	0	0	0
130	C/ART+	1	1	0
154	C/ART-	0	0	0
160	C/ART+	0	0	0
166	C/ART+	0	0	0
172	C/ART-	0	0	0
190	ART+/M+	1	1	1
196	ART+/M+	1	1	1
202	ART+/M+	1	1	1
208	ART+/M+	1	1	1
214	ART+/M+	1	1	1
238	C/ART-	0	0	0
256	C/ART-	1	1	1
280	C/ART+	1	1	0
292	C/ART+	1	0	1
304	C/ART-	1	1	1
310	C/M+	1	1	1
316	C/M+	1	1	1
322	C/M+	1	1	1
328	C/M+	1	0	1
343	C/M+	0	0	0
349	C/M+	0	0	0
355	C/M+	1	1	1
361	C/M+	1	1	1
1573	C/ART-	1	0	2
1578	C/M+	1	1	1
1583	C/ART-	1	1	2
1593	C/ART-	0	0	0

1603	ART+/M+	0	0	0
1608	C/ART+	1	0	1
1621	C/ART+	1	1	1
1626	C/ART+	0	0	0
1636	C/ART+	0	0	0
1646	ART+/M+	1	0	1
1656	ART+/M+	0	0	0
1661	ART+/M+	1	1	1
1666	C/M+	0	0	0
1671	ART+/M+	0	0	0
1681	C/ART+	1	0	1
<b>Total</b>		<b>24</b>	<b>18</b>	<b>22</b>